Development of an adaptive variance reduction technique for Monte Carlo particle transport

Henri Louvin

NNT : 2017SACLS351

Thèse de doctorat de l'Université Paris-Saclay préparée à l'Université Paris-Sud

École doctorale n°576
Particules, Hadrons, Énergie, Noyau, Instrumentation, Image, Cosmos et Simulation (PHENIICS)
Spécialité de doctorat : Physique des particules

par

M. Henri Louvin

Development of an adaptive variance reduction technique for Monte Carlo particle transport

Thèse présentée et soutenue à Saclay, le 12 octobre 2017.

Composition du Jury :

M. Pierre Désesquelles	Professeur (CSNSM, Paris Sud)	**Président**
M. Kenneth Burn	Professeur (ENEA, Rome)	**Rapporteur**
M. Arnaud Guyader	Professeur (UPMC, Paris VI)	**Rapporteur**
M. Josselin Garnier	Professeur (École Polytechnique)	**Examinateur**
Mme Odile Petit	Ingénieure-Chercheure (CEA)	**Examinatrice**
M. Eric Dumonteil	Ingénieur-Chercheur, HDR (IRSN)	**Encadrant**
M. Tony Lelièvre	Professeur (CERMICS, ENPC)	**Directeur de thèse**
M. Cheikh M'Backé Diop	Directeur de recherche (CEA)	**Directeur de thèse**

Acknowledgements

This PhD thesis is the result of three years of research at the Laboratoire de Transport Stochastique et Deterministe (LTSD) of the Service d'Études de Reacteurs et de Mathematiques Appliquees (SERMA) at CEA Saclay. This work could not have succeeded without the support of the people who have shared this experience with me.

I would like to thank Cheikh Diop and Tony Lelièvre who assumed the direction of this thesis. The complementarity of their skills and their availability throughout this entire work have been crucial in this endeavour. I am very thankful to Kenneth Burn and Arnaud Guyader for taking on the important task of reviewing my thesis, to Josselin Garnier for accepting to be part of the examining committee, and to Pierre Désesquelles for assuming the presidency of the jury.

I wish to thank my advisor Eric Dumonteil, who gave me the opportunity to do my PhD under his supervision and battled to support my candidacy. Despite his departure from the laboratory halfway through the thesis, he always remained available and I am really grateful for it. I would also like to thank Odile Petit, who assumed the advisor position after Eric's departure and did a wonderful job.

I would like to give very special thanks to Andrea Zoia, who supervised my end of study internship at CEA back in 2013 and vouched for me when I applied for a PhD position in the laboratory.

The work presented here would not have been possible without the many talks I had with other researchers both at CEA and at CERMICS. I am very grateful to Mathias Rousset for his theoretical support, to Davide Mancusi for his guidance and endless knowledge, and to my office mate Michel Nowak who was the first user of my code and who made work so enjoyable.

Je souhaite également remercier mes parents, qui ont été et seront toujours mes premiers soutiens, mon frère Charles, ma sœur Sophie, ainsi que toutes celles et ceux dont l'amitié m'a accompagné durant ces trois dernières années. Un merci tout particulier aux docteurs Rohée et Montbarbon qui ont partagé ma condition de doctorant et qui m'ont montré la voie sur bien des points.

Enfin, je tiens à remercier du fond du cœur Clémence pour sa présence à mes côtés au quotidien et pour le sens qu'elle donne à ma vie. Merci d'avoir fait de notre mariage l'évènement le plus important de cette dernière année de thèse, loin devant l'obtention de mon doctorat.

H.L.

Table of Contents

Page

List of Figures

Figure **Page**

List of Tables

Table **Page**

Introduction

The behaviour of neutral particles travelling through matter can be described by a stochastic process. This process can be simulated using Monte Carlo particle transport codes. These codes can usually handle two types of simulations: either criticality or fixed-source calculations. While criticality simulations reproduce the nuclear chain reaction and make use of the power iteration technique to study core physics, fixed-source simulations are used in the context of radiation shielding, ageing and dismantling. The purpose of fixed-source simulations is to estimate a particle flux in an region of interest, or other quantities derived from the flux such as reaction rates or energy deposition. In a given Monte Carlo simulation, the estimated quantity is usually referred to as "score" or "tally". The configurations studied with radiation shielding calculations are often associated to deep penetration problems or other rare events estimations. In those cases, the number of particles to simulate in order to have enough contributions to the score is too large to hope getting a precise estimation in a reasonable computation time. Variance reduction methods are therefore used to alter the simulation process so as to increase the occurrence probability of the rare events at hand while keeping an unbiased estimation of the score. Hence, these methods allow for a variance reduction of the estimated score for a given computation time.

Multilevel splitting techniques are variance reduction methods that were introduced in the field of particle transport by Kahn and Harris [1]. The principle of these techniques is to increase the number of simulated particles when approaching areas of interest of the geometry. In practice, the simulated space is divided into regions of importance delimited by virtual frontiers called *splitting levels*. Whenever a particle goes from a less important to a more important region, it is duplicated. Each of the duplicated particles is given half the weight of the original particle to ensure that the simulation remains unbiased. Thus, more computation time is spent to simulate interesting particles, i.e. particle more likely to contribute to the score, rather than new particles emitted from the source. One of the advantages of these techniques over other types of variance reduction methods is that they do not alter the particle transport between splitting events. The particle transport in each importance region is left unchanged, keeping the underlying physics unperturbed. However, the inherent downside of these tech-

niques is that they require a fair knowledge of the system in order to accurately define the importance regions. One needs to ensure that enough particles are going from region to region, in order to have a noticeable effect on the variance of the estimated score. This requires to define close enough splitting levels. In the meantime, the levels must be sufficiently distant from one another to prevent an explosion of the particle population.

In order to cope with this issue, an adaptive method has been introduced in the field of applied mathematics by Cérou and Guyader [2]. The proposed algorithm, called Adaptive Multilevel Splitting (or AMS), was originally designed to help estimate rare events occurrence probabilities in Monte Carlo simulations of continuous Markov chains. It has then been extended to the simulation of discrete Markov chains by Bréhier et al. [3]. The AMS method aims at duplicating the interesting particles of the simulation, but does not use an a priori definition of importance regions. Instead, the positions of the splitting levels are determined on the fly, following a selection mechanism based on the classification of the simulated particle histories. To the best of our knowledge and rather surprisingly, this algorithm has never been applied to the field of particle transport.

In summary, the need for accurate simulation of rare events in Monte Carlo transport calculations led to the emergence of multiple variance reduction techniques over the years. Many of those methods are based on multilevel splitting techniques. However, multilevel splitting requires a precise positioning of the levels to efficiently reduce the variance. This sometimes requires extended insight on the system, which is not always available. In order to overcome this limitation, an adaptive method called Adaptive Multilevel Splitting has been proposed in the field of applied mathematics. Even if it has never been applied to particle transport simulation, it could be useful for configurations requiring a precise simulation of rare events.

This justifies the work presented in this thesis, which consists in studying the applicability of the Adaptive Multilevel Splitting algorithm as a variance reduction scheme for Monte Carlo particle transport.

After a presentation, in the opening chapters, of the physical context of this work, the main part of this manuscript is devoted to the description of the many steps required to implement the Adaptive Multilevel Splitting algorithm in the transport code TRIPOLI-4® and its applications to several practical examples.

To begin with, the AMS method had to be adapted to fit the specificities of particle transport. This is the subject of the third chapter. The original algorithm has been rewritten to be consistent with the context of particle transport, since it was created for variance reduction on generic Markov chains. In order to ensure the relevance of AMS for particle transport calculations, a Monte Carlo code simulating a simplified transport process in a trivial geometry was developed. It is able to perform Monte Carlo simulations in both AMS and analog mode (i.e.

without variance reduction), for a problem that is simple enough to be solved analytically. This allowed us to ensure that the AMS method yields unbiased results. Moreover, the obtained results were compared to those of analog simulations so as to evaluate the variance reduction efficiency of the adapted AMS method. This was the necessary first step towards an implementation of the AMS algorithm in a industrial Monte Carlo transport code.

Chapter 4 is dedicated to the implementation of the AMS algorithm in the neutral particle transport code TRIPOLI-4. An extended study of the code was necessary to determine the most efficient way to implement AMS in TRIPOLI-4. The idea was to find a way to implement the algorithm with the smallest impact on computational time. In the meantime, it was also necessary to minimize the intrusion of AMS in the code, in order to keep the existing modules unperturbed. The efficiency of the implemented AMS was then compared to analog simulations, and also to other variance reduction methods already available in TRIPOLI-4. The variance reduction scheme was exclusively tested for single-score simulations. Indeed, the original AMS algorithm was designed to reduce the variance on the estimation of a single probability. However, observation suggested that the information gathered during the simulation process with AMS could be used to reduce variance on multiple scores as well. This could be achieved through the implementation of an on-the-fly scoring technique.

In the fifth part, we introduce a method allowing for on-the-fly scoring during the AMS iterating process. To that end, multiple solutions were considered, and the most effective one was implemented in TRIPOLI-4. The updated version of the AMS algorithm was used to try and reduce the variance on multiple scores in two typical shielding configurations: a deep penetration problem and a three-dimensional streaming configuration. The obtained results were once again compared to those obtained via analog and non-analog calculations. In the work described up to this point, as well as in the literature, the AMS algorithm was exclusively applied to non-branching trajectories. However, this restriction is troublesome for particle transport Monte Carlo simulations, in which branching trajectories may occur. Indeed, a particle collision with a nuclei of the surrounding medium can induce the emission of one or more secondary particles, resulting in a branching trajectory.

The last chapter of this thesis addresses the extension of the AMS algorithm to branching processes. We propose an innovative way for the AMS algorithm to account for branching trajectories, and discuss its implementation in TRIPOLI-4. Allowing the AMS to handle branching trajectories in Monte Carlo transport simulations opens up new fields of applications for this variance reduction method, such as coupled neutron/photon simulations or gamma spectrometry. The last version of the AMS algorithm in TRIPOLI-4 has been used in both those fields of applications, for which two configurations have been especially chosen to test the suitability of AMS as a variance reduction technique in cases that require explicit treatment of branching trajectories.

Part I

Background

Chapter 1

Monte Carlo particle transport

Neutral particle transport is the study of the behaviour of neutral particles travelling through matter. It is theoretically described by the linear Boltzmann equation, which is therefore referred to as *transport equation*. The methods used to solve this equation fall into two categories: deterministic methods, and stochastic methods also known as Monte Carlo methods [4]. Deterministic methods solve the transport equation by numerical integration, which requires to discretize the phase space and sometimes even to reduce the number of dimensions involved in the problem. Even though these methods are very time-efficient, they are built on approximations which lead to uncertainties on the calculated responses. On the other hand, Monte Carlo methods use few approximations in the transport model. In the context of particle transport, Monte Carlo methods simulate the trajectory of each particle individually, from emission to absorption, while the interactions of particles with matter are modelled as close to the physics as possible, thus eliminating the need for phase space discretization. Furthermore, the Monte Carlo approach, as a statistical method, provides results with associated confidence intervals, which can be reduced by simulating more and more particles. Despite their large computational time, the specificities of Monte Carlo methods make them reference methods both for the validation of deterministic calculations and for industrial calculations.

As neutral particle transport by the Monte Carlo method is the basis of this work, the first chapter is devoted to the presentation of this method. First, the theoretical formulation of the transport equation is introduced, then we describe the Monte Carlo approach for solving the Boltzmann equation.

1.1 Transport equation

1.1.1 Definitions and notations

Neutral particle transport theory describes the mathematical framework required to model the behaviour of neutral particles (e.g. neutrons, photons) travel-

ling through matter. The fundamental assumptions in transport theory are that particles can be treated as point-like, and that all interactions between transported particles can be ignored. Before going any further, let us introduce some definitions and notations which will be used throughout this thesis.

We define the position of a particle in the 6-dimensional *phase space* $\mathcal{S}$ as the set of coordinates $(\vec{X}, \vec{\Omega}, E)$, where

- $\vec{X}$ denotes the particle position in the 3-dimensional space,
- $\vec{\Omega}$ is the unit vector giving the direction of displacement of the particle,
- E stands for the particle energy, which is the norm of the particle velocity (except for massless particles).

The laws governing the interactions between particle and matter are represented by macroscopic cross sections $\Sigma(\vec{X}, E)$, which basically represent the probability of interaction per unit length for a particle at point $\vec{X}$ travelling along a straight line at energy E [5]. The unit of macroscopic cross sections is the inverse of a length, and the term macroscopic refers to the fact that cross sections are weighted over the material density $\rho(\vec{X})$ of the medium. The so-called microscopic cross sections $\sigma(\vec{X}, \vec{\Omega}, E)$ are related to $\Sigma(\vec{X}, \vec{\Omega}, E)$ by $\Sigma(\vec{X}, \vec{\Omega}, E) = \rho(\vec{X})\sigma(\vec{X}, \vec{\Omega}, E)$, and are expressed in area units called barns ($1\,\mathrm{b}{=}1\mathrm{E}{-}24\,\mathrm{cm}^2$). Throughout the remaining of this thesis, the following macroscopic cross sections will be used:

- $\Sigma_a(\vec{X}, E)$, the macroscopic absorption cross section, related to the probability of absorption at point $(\vec{X}, E)$,
- $\Sigma_s\big(\vec{X}, \vec{\Omega} \to \vec{\Omega}', E \to E'\big)d\vec{\Omega}'dE'$, the probability for a particle colliding with the medium at point $(\vec{X}, \vec{\Omega}, E)$ to come out of the collision with a direction inside the elementary solid angle $d\vec{\Omega}'$ around $\vec{\Omega}'$ and an energy inside the elementary energy interval dE' around E'.
- $\Sigma_t(\vec{X}, E)$, the total macroscopic cross section such that

$$\Sigma_t(\vec{X}, E) = \Sigma_a(\vec{X}, E) + \iiint \Sigma_s\big(\vec{X}, \vec{\Omega} \to \vec{\Omega}', E \to E'\big)d\vec{\Omega}d\vec{\Omega}'dE'. \quad (1.1)$$

Cross sections, multiplicities and distribution functions of outgoing and secondary particles, which are the necessary ingredients to perform Monte Carlo particle transport, depend on a series of parameters such as the temperature of the medium, the nuclear properties of the target nucleus, the type and energy of incident particle, etc. For each combination of such parameters, the displacement and collision kernels have different shapes and thus modify the particles propagation through matter. Accurate simulation results clearly depend on the quality of the nuclear data available for the Monte Carlo code. Nuclear data are usually evaluated combining experimental and theoretical studies, thus depending on the available experimental data and on the chosen physical models.

The mainly used libraries are the European Joint Evaluated Fission and Fusion data (JEFF-3.1.1 [6]) and the American Evaluated Nuclear Data File (ENDF/B-VII [7]). The calculations presented in this work has been carried out using the JEFF-3.1.1 library.

1.1.2 Integro-differential formulation

Under the assumption that the system has reached equilibrium, which is always the case in radiation shielding problems, the particle flows in and out of any volume element $d\vec{X}d\vec{\Omega}dE$ are equal. The modelling of such systems is achieved using the steady-state linear Boltzmann equation. Written in its integro-differential form, it establishes a balance of the particle flux ϕ at a given point of the phase space $(\vec{X}, \vec{\Omega}, E)$.

$$\begin{gathered}\vec{\Omega}.\vec{\nabla}\phi\big(\vec{X},\vec{\Omega},E\big)+\Sigma_t\big(\vec{X},E\big)\phi\big(\vec{X},\vec{\Omega},E\big)= \\ \iint \Sigma_s\big(\vec{X},\vec{\Omega}'\rightarrow\vec{\Omega},E'\rightarrow E\big)\phi\big(\vec{X},\vec{\Omega}',E'\big)d\vec{\Omega}'dE'+Q\big(\vec{X},\vec{\Omega},E\big).\end{gathered} \tag{1.2}$$

The left-hand side of the equation describes the particles leaving the volume element $d\vec{X}d\vec{\Omega}dE$ around $(\vec{X}, \vec{\Omega}, E)$:

- $\vec{\Omega}.\vec{\nabla}\phi(\vec{X},\vec{\Omega},E)$ represents the particles leaking out of the three-dimensional volume element $d\vec{X}$ around $\vec{X}$,

- $\Sigma_t(\vec{X},E)\phi(\vec{X},\vec{\Omega},E)$ represents the particles entering a collision, thus being absorbed or changing their direction and/or energy,

while the right-hand side of the equation gathers the terms describing the particles arriving in $d\vec{X}d\vec{\Omega}dE$:

- $\iint \Sigma_s\big(\vec{X},\vec{\Omega}'\rightarrow\vec{\Omega},E'\rightarrow,E\big)\phi\big(\vec{X},\vec{\Omega}',E'\big)d\vec{\Omega}'dE'$ represents those emerging from of a collision at point $\vec{X}$ with direction $\vec{\Omega}$ and energy E

- $Q(\vec{X},\vec{\Omega},E)$ represents the external sources of particles.

In order to have a transport equation suitable for Monte Carlo resolution, the Boltzmann equation has to be cast into integral form [4].

1.1.3 Integral formulation

The flux at point $(\vec{X}, \vec{\Omega}, E)$ can be expressed as the sum of two integrals. The first corresponds to the contribution of particles coming directly from the source point, and the second to the contribution of particles having undergone one or

several collision(s) [8]:

$$\phi\big(\vec{X},\vec{\Omega},E\big) = \int e^{-\int_0^x \Sigma_t(\vec{X}-s\vec{\Omega},E)ds} Q\big(\vec{X}-x\vec{\Omega},\vec{\Omega},E\big)dx + \iiint e^{-\int_0^x \Sigma_t(\vec{X}-s\vec{\Omega},E)ds} \Sigma_s\big(\vec{X}-x\vec{\Omega}',\vec{\Omega}'\to\vec{\Omega},E'\to E\big)\phi\big(\vec{X}-x\vec{\Omega}',\vec{\Omega}',E'\big)dx d\vec{\Omega}' dE' \tag{1.3}$$

In order to simplify the above formula, let us introduce the so-called collision density $\psi(\vec{X},\vec{\Omega},E)$ of particles entering a collision in $(\vec{X},\vec{\Omega},E)$, defined as

$$\psi\big(\vec{X},\vec{\Omega},E\big) = \Sigma_t\big(\vec{X},E\big)\phi\big(\vec{X},\vec{\Omega},E\big), \tag{1.4}$$

as well as the following operators:

- the displacement operator, whose kernel is $D(\vec{X}'\to\vec{X},\vec{\Omega},E)$, describing a flight from point $\vec{X}'$ to point $\vec{X}=\vec{X}'+x\vec{\Omega}$, where $x>0$ and such that

$$D\left(\vec{X}'\to\vec{X},\vec{\Omega},E\right) = \Sigma_t\big(\vec{X},E'\big)e^{-\int_0^x \Sigma_t(\vec{X}-s\vec{\Omega},E)ds}. \tag{1.5}$$

- the collision operator whose kernel is $C(\vec{X},\vec{\Omega}'\to\vec{\Omega},E'\to E)$, describing a collision at point $\vec{X}$ resulting in a change of direction and energy from $(\vec{\Omega}',E')$ to $(\vec{\Omega},E)$ and such that

$$C\left(\vec{X},\vec{\Omega}'\to\vec{\Omega},E'\to E\right) = \frac{1}{\Sigma_t\big(\vec{X},E'\big)}\Sigma_s\big(\vec{X},\vec{\Omega}'\to\vec{\Omega},E'\to E\big). \tag{1.6}$$

- $\mathcal{T}(P'\to P)$ the transport kernel giving the density of particles passing through point $P'=(\vec{X}',\vec{\Omega}',E')$ that will emerge from their next collision at point $P=(\vec{X},\vec{\Omega},E)$. It is the product of the displacement and collision operator's kernels:

$$\mathcal{T}(P'\to P) = D(\vec{X}'\to\vec{X},\vec{\Omega}',E')C(\vec{X},\vec{\Omega}'\to\vec{\Omega},E'\to E). \tag{1.7}$$

The transport kernel $\mathcal{T}$ is sometimes denoted by $\mathcal{K}$ in the literature. We can now derive from Equation (1.3) the integral equation satisfied by $\psi(P)$:

$$\psi(P) = \int \psi(P')\mathcal{T}(P'\to P)dP' + \int Q(P')D(\vec{X}'\to\vec{X},\vec{\Omega},E)dP', \tag{1.8}$$

which is an inhomogeneous Fredholm equation of the second kind [9].

1.1.4 Neumann series expansion

It can be shown that Equation (1.8) admits a unique solution ψ, which may be expanded as a Neumann series [10]:

$$\psi(P) = \sum_{n=0}^{\infty} \psi_n(P), \tag{1.9}$$

where

$$\psi_0(P) = \int D(P' \to P) Q(P') dP' \tag{1.10}$$

and for any $n \geq 1$

$$\psi_n(P) = \int \mathcal{T}(P' \to P) \psi_{n-1}(P') dP'. \tag{1.11}$$

In the Neumann expansion, each of the terms $\psi_n(P)$ in Equation (1.9) can be interpreted as the contribution to $\psi(P)$ of particles having undergone n collisions between the source and the point P. Therefore, the reconstruction of every event taking part in the particles propagation allows for a numerical estimation of the particle flux.

1.2 Monte Carlo resolution

Let us consider a subset $\mathcal{D}$ of the phase space, which we will refer to as the *detector*. The purpose of the simulation is to estimate a response $R(\mathcal{D})$ associated to the detector, which is the measurement of a physical quantity of interest inside $\mathcal{D}$ and is defined as

$$R(\mathcal{D}) = \int_{P \in \mathcal{D}} g_R(P) \phi(P) dP, \tag{1.12}$$

where g_R is the response function associated to the response R. For example, if R is the flux, $g_R = 1$. For a reaction rate, $g_R(P) = \Sigma_t(P)$. Substituting the collision density into this equation, we obtain for any response R:

$$R(\mathcal{D}) = \int_{P \in \mathcal{D}} \frac{g_R(P)}{\Sigma_t P} \psi(P) dP. \tag{1.13}$$

In practice, the Monte Carlo method for particle transport consists in :

- determining the source point(s) of the simulation

- defining the rules for the statistical process of displacement and collision for the simulated particles, according to the displacement and collision operators used in Equation (1.8)

- realizing n distinct runs of the process: n independent particle histories are simulated

- defining a random variable $\hat{R}(\mathcal{D})$ such that $\mathbb{E}(\hat{R}(\mathcal{D})) = R(\mathcal{D})$. $\hat{R}(\mathcal{D})$ is called *score* and is an unbiased estimator of the response $R(\mathcal{D})$. It is computed using all parts of particle trajectory that are in $\mathcal{D}$.

In order to compute the expected value of $\hat{R}(\mathcal{D})$, n distinct runs of the statistical process are performed, so that the Central Limit Theorem provides an average score associated with a confidence interval.

1.2.1 Particle tracking process

The statistical process governing the construction of particle histories is composed of two parts: the displacement sampling and the collision sampling. If the displacement does not result in the particle leaking out of the simulated space, a collision is sampled according to the properties of the medium. If the particle is not absorbed, a new displacement is sampled, and then another collision, etc. This process is shown in Figure 1.1.

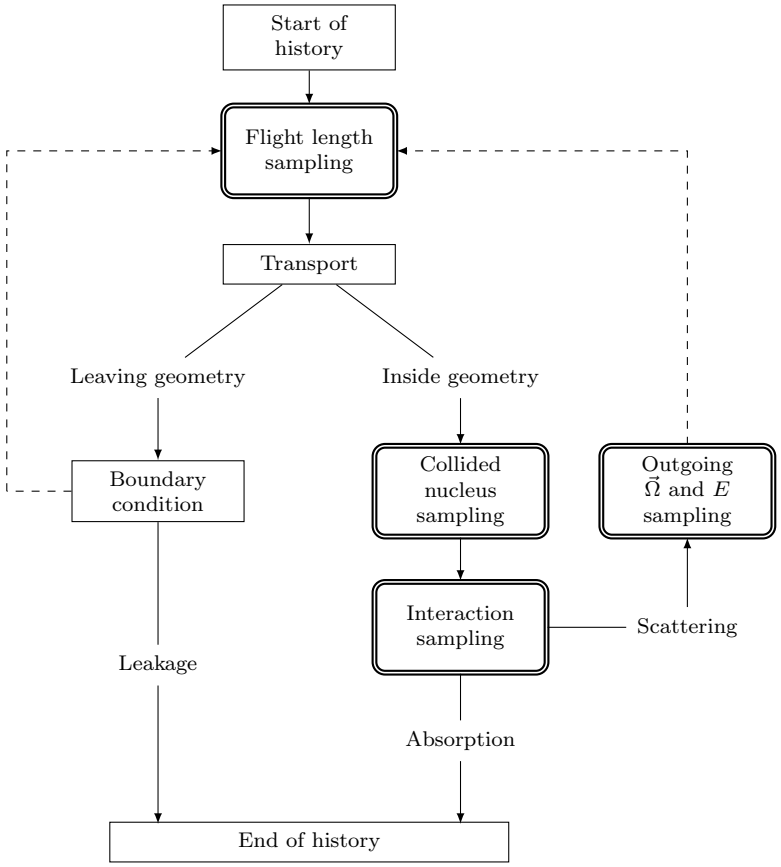

Figure 1.1. Schematic representation of the simulation of a particle history using the Monte Carlo approach in a homogeneous medium.

The probability density functions for displacement and collision are derived from the corresponding expressions of the displacement and collision kernels (Equation (1.5) and (1.6)). We present in the following the sampling laws obtained for a particle travelling in a homogeneous medium. As most of the simulated problems implies the simulation of heterogeneous geometries, the standard procedure for Monte Carlo particle transport simulations is to divide the simulated three-dimensional space into multiple volumes, each of which is assumed to be homogeneous. The process for particles that crosses boundaries between those volumes will be discussed at the end of this section.

Flight length sampling

Under the assumption that the transport is bounded to a single volume, the cross section at any point $(\vec{X}, \vec{\Omega}, E)$, with $\vec{X}$ inside the volume, depends only on the energy. Consequently, we have for the displacement kernel from point $\vec{X}'$ to point $\vec{X} = \vec{X}' + x\vec{\Omega}$:

$$D\big(\vec{X}' \to \vec{X}, \vec{\Omega}, E\big) = \Sigma_t(E) e^{-x\Sigma_t(E)}, \tag{1.14}$$

meaning that the distance x travelled by a particle between two interactions with the medium is exponentially distributed with a probability density function:

$$f(x, E) = \Sigma_t(E) e^{-x\Sigma_t(E)} \mathbb{1}_{x>0}, \tag{1.15}$$

whose associated repartition function is:

$$F(x, E) = \int_0^x f(x', E) dx' = [1 - e^{-x\Sigma_t(E)}] \mathbb{1}_{x>0}. \tag{1.16}$$

Therefore, a particle displacement length can be sampled by sampling an uniformly distributed random variable ξ on the unit interval and using the inverse of F:

$$x = F^{-1}(\xi, E) = -\frac{1}{\Sigma_t(E)} \ln(1 - \xi). \tag{1.17}$$

Collision sampling

Once the particle has been moved a distance x in the direction Ω, a collision has to be sampled. The collision kernel from Equation (1.6) can be rewritten

$$C(\vec{\Omega}' \to \vec{\Omega}, E' \to E) = \frac{1}{\Sigma_t(E')} \Sigma_s\big(\vec{\Omega}' \to \vec{\Omega}, E' \to E\big). \tag{1.18}$$

A homogeneous medium is actually a homogeneous mixture of nuclides. The collision kernel can be expressed in terms of the total macroscopic cross sections

$\Sigma_{j,t}$ of each nuclide j, and of the cross section of each interaction i, denoted for nuclide j by $\Sigma_{j,i}$:

$$C\big(\vec{\Omega}' \to \vec{\Omega}, E' \to E\big) = \sum_j \frac{\Sigma_{j,t}(E)}{\Sigma_t(E)} \sum_i \frac{\Sigma_{j,i}(E)}{\Sigma_{j,t}(E)} f_{j,i}\big(\vec{\Omega}' \to \vec{\Omega}, E' \to E\big), \quad (1.19)$$

where $f_{j,i}\big(\vec{\Omega}' \to \vec{\Omega}, E' \to E\big)$ is the probability density function of going from $(\vec{\Omega}', E')$ to $(\vec{\Omega}, E)$ during a collision of type i on nuclide j. From this last formulation, we derive the sampling procedure for the particle collision:

- sampling of the nuclide which the particle collides with: the nuclide j is chosen with probability
$$P_j = \frac{\Sigma_{j,t}(E)}{\Sigma_t(E)}. \quad (1.20)$$

- sampling of the reaction type: the reaction i is selected from all reactions available for nuclide j with probability
$$P_{j,i} = \frac{\Sigma_{j,i}(E)}{\Sigma_{j,t}(E)} = \frac{\sigma_{j,i}(E)}{\sigma_{j,t}(E)}. \quad (1.21)$$

- sampling of the direction $\vec{\Omega}$ and energy E of the particle after the collision: those parameters depend on the direction $\vec{\Omega}'$ and energy E' of the particle before the collision, and are distributed with the probability density function available in the nuclear data:
$$f_{j,i}\big(\vec{\Omega}' \to \vec{\Omega}, E' \to E\big). \quad (1.22)$$

1.2.2 Case of geometry with multiple volumes

As discussed above, the geometry is most of the time divided into multiple volumes, each of which is assumed to be homogeneous. Various procedures for handling geometries consisting of multiple volumes can be found in [11]. The process described in the following has been selected because it presents some advantages for the further use of the Adaptive Multilevel Splitting technique, which will be discussed in Chapter 3.

As long as the particles travel and interact inside a single volume, the transport process remains unchanged. However, it may also happen that a flight length sampled for a displacement causes the particle to change volume. In that case, the particle is placed at the boundary between the volumes, and a new flight length is sampled from this point, using the characteristics and cross sections

of the new volume. The corresponding adapted transport scheme is shown in Figure 1.2.

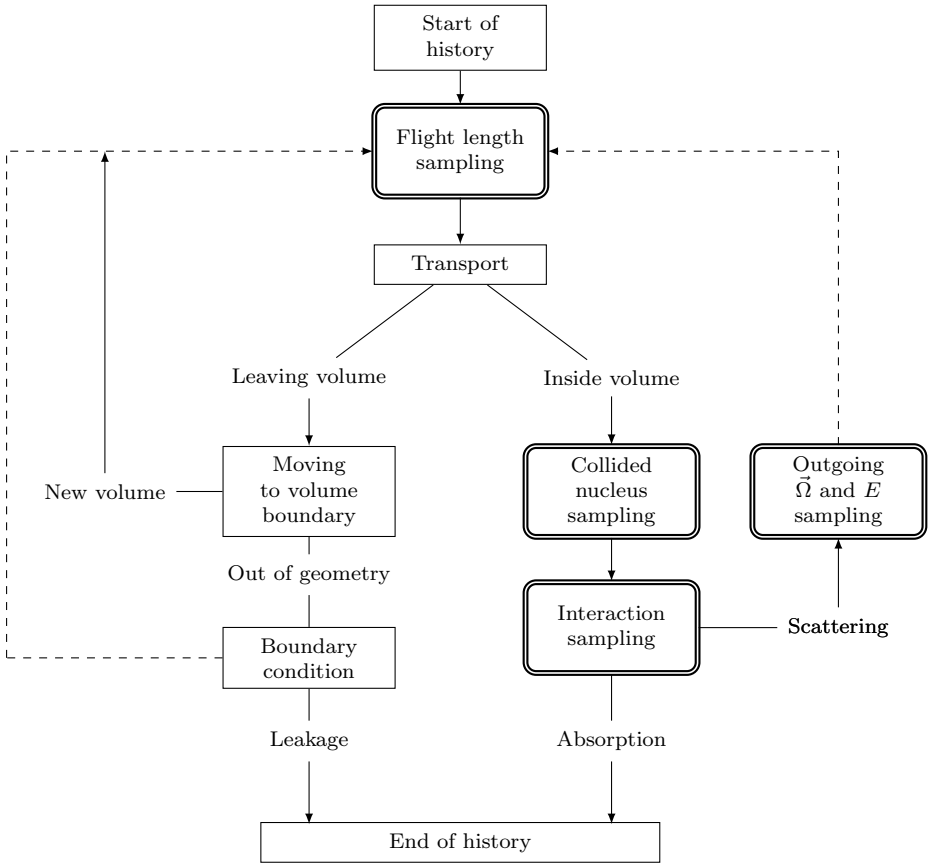

Figure 1.2. Schematic representation of the simulation of a particle history using the Monte Carlo approach in multiple volumes.

1.2.3 Score definitions

The purpose of a fixed-point Monte Carlo simulation is to compute an estimate of a response function within an area of interest. This estimate is computed by counting particle-related events occurring in the area of interest, such as collisions or displacement lengths, to which we refer as "contributions" to the estimation. We refer to the couple estimator/area of interest as a "score". There are many different scores that can be evaluated in Monte Carlo simulations. In the following, we present the most common responses and the associated estimators: the particle flux either in a volume or at a surface, the particle current and the reaction rates.

One can compute multiple scores in a single Monte Carlo simulation: either various responses in the same area of interest (for example a particle flux in a detector and particle current at the detector's boundary), or the same response in various locations (like a reaction rate estimated in multiple volumes).

Particle flux in a volume

A particle flux is defined as the number of particles travelling through a unit area per unit time. It is therefore expressed in $\mathrm{cm}^{-2}\mathrm{s}^{-1}$. In fixed-point Monte Carlo simulations, it is common to disregard the time dependency of the problem. Most of the time, we assume that the particle sources emit one particle per second, and that the particle transport is instantaneous, thus obviating the time dependence in the simulation as well as in the result.

There are two standard estimators that can be used to estimate the particle flux in a volume. The first one is the track-length estimator, which computes the score as the total distance travelled by the particles in the volume of interest (in cm), divided by the number of simulated particles and the volume of the detector area (in cm^3):

$$\hat{\phi}_{\mathrm{TRACK}} = \frac{1}{nV} \sum_{i=0}^{n} l_i, \tag{1.23}$$

where n is the number of source particles, V the volume of the detector area and l_i the distance travelled by particle i in the volume of interest (which is therefore the "contribution" of particle i to the score).

The second estimator of the flux in a volume is the *collision* estimator, which estimates the particle flux by counting the number of collisions in the detector area and multiplying this value by the mean distance travelled by a particle between two collision points in the volume of interest, which is the multiplicative inverse of the total cross section in the detector. We have therefore

$$\hat{\phi}_{\mathrm{COLL}} = \frac{1}{nV} \sum_{i=0}^{n} \frac{c_i}{\Sigma_t}, \tag{1.24}$$

where c_i is the number of collisions undergone by particle i in the volume of interest, and Σ_t is the total cross section in the detector.

The collision estimator is a priori less precise that the track-length estimator, especially in low-density media in which the collision probability is low. However, it is slightly simpler to compute, as it does not require to evaluate travelled distances between collisions and interfaces of volumes. This property can for example be interesting to estimate a flux in the cells of a mesh covering part of the geometry.

Particle current and surface flux

The estimator used to evaluate the particle current at a surface is simply the number of particles crossing the surface divided by the number of source particle

and the surface area.

$$\hat{J}_{\text{SURF}} = \frac{1}{nA} \sum_{i=0}^{n} \mathbb{1}_S(i), \tag{1.25}$$

where $\mathbb{1}_S(i)$ is 1 if particle i crossed the surface, and zero otherwise.

It is also possible to evaluate the particle flux through a surface, in which case the contribution of each particle crossing the surface is computed as the cosine of the angle between the particle direction and the normal vector of the surface:

$$\hat{\phi}_{\text{SURF}} = \frac{1}{nA} \sum_{i=0}^{n} \frac{\mathbb{1}_S(i)}{\vec{\Omega}_i \vec{n}_S}, \tag{1.26}$$

where $\vec{\Omega}_i$ denotes the direction of particle i at the crossing point and $\vec{n}_S$ is the unit normal vector of the surface.

Reaction rates

The reaction rate is estimated in a volume as the average number of interactions taking place per cubic centimeter per second. It is computed as the product between the particle flux in the volume and the cross section of the reaction of interest. For reaction j (total, absorption, etc.), we have

$$R_j = \Sigma_j \phi, \tag{1.27}$$

and the associated Monte Carlo estimator:

$$\hat{R}_j = \Sigma_j \hat{\phi}, \tag{1.28}$$

where $\hat{\phi}$ can be either the track-length or collision estimator of the flux.

Chapter 2

Variance reduction techniques

This chapter is devoted to the presentation of several variance reduction techniques. This description is not meant to be exhaustive, but rather focused on the methods implemented in the transport code TRIPOLI-4, around which this thesis work revolved. The purpose of this chapter is to introduce the state of the art, as a frame to help the reader understand the starting point of this Ph.D. work. To that end, the last section of this chapter consists in the presentation of the Adaptive Multilevel Splitting algorithm, in a formalism adapted to the simulation of discrete Markov chains. It should be noted however that the theoretical description made in this section is not a mandatory step to understand how the method works when applied to particle transport, which will be the main objective of Chapter 3.

2.1 Motivation

In a Monte Carlo particle transport simulation, the limiting factor is the number of histories that need to be simulated in order to get a result with a reasonably small confidence interval. In the case of radiation shielding simulations, we are interested in the simulation of rare events, whose occurrence probabilities are typically between 10^{-5} and 10^{-20}. Only a few simulated histories will therefore contribute to the response associated to such events, resulting in either a large statistical error on the result, or a very long computation time.

Variance reduction methods were introduced in order to tackle this issue. They aim to alter the simulation process, in order to reduce the variance on the estimated score for a given computation time. In the following, we will refer to simulations without variance reduction as *analog*. There are three ways for a variance reduction technique to modify the simulation:

- To control the particle population, by increasing/decreasing it in areas of high/low interest

- To modify the occurrence probability of certain physical processes in order to increase the probability for a particle history to contribute to the score

- To replace parts of the Monte Carlo simulation by deterministic calculations to improve the overall computation time

Obviously, the modifications induced by the methods of the first two categories must be balanced in order to keep an unbiased estimation of the response. Indeed, a non-analog Monte Carlo simulation will hopefully provide many more contributions to the score than an analog simulation. This problem is addressed by assigning a so-called *weight* to the altered trajectories. The contribution of any weighted particle to the score will then be multiplied by the particle's weight, thus ensuring that the simulation result remains unbiased.

2.2 Figure of merit

The efficiency of a variance reduction method is based on two quantities: the variance on the estimated result σ^2, and the computation time t (CPU time).

The variance, as the square of the standard deviation σ, varies with the inverse of the number of simulated histories n:

$$\sigma^2 \sim \frac{1}{n}. \tag{2.1}$$

On the other hand, the computation time is directly proportional to n, provided that the number of simulated particles is large enough to smooth out the differences of computation time between two distinct particle trajectories. As a result, the product $\sigma^2 \times t$ is independent of the number of simulated particles, and can be used to compare the efficiency of two simulations. To this end, the figure of merit (or FOM) is defined as

$$FOM = \frac{1}{\sigma^2 t}, \tag{2.2}$$

as a measurement of the simulation efficiency. The higher the FOM, the greater the performances of the simulation.

2.3 Exponential Transform

The Exponential Transform [12], derived from the *Exponential Biasing* (or *Importance Sampling*), is the reference variance reduction method of the transport code TRIPOLI-4 [13]. It is based on the use of a so-called *importance function*, which is an arbitrary function associating any point of the phase space to an importance value $I(\vec{X}, \vec{\Omega}, E) \in \mathbb{R}$, quantifying whether or not a particle located at point $(\vec{X}, \vec{\Omega}, E)$ is of interest to the simulation. The purpose of exponential transform is to build a biased game, which means a stochastic process that has the same global behaviour as an analog simulation, but with different operators.

We recall the linear Boltzmann equation satisfied by ϕ, in its integro-differen-

tial formulation (see Section 1.1.2):

$$\begin{aligned}\vec{\Omega}.\vec{\nabla}\phi\big(\vec{X},\vec{\Omega},E\big)+\Sigma_t\big(\vec{X},E\big)\phi\big(\vec{X},\vec{\Omega},E\big)=\\ \iint\Sigma_s\big(\vec{X},\vec{\Omega}'\to\vec{\Omega},E'\to E\big)\phi\big(\vec{X},\vec{\Omega}',E'\big)d\vec{\Omega}'dE'+Q\big(\vec{X},\vec{\Omega},E\big).\end{aligned}\tag{2.3}$$

We define the *biased flux* $\phi^\star$ such that for any point of the phase space, $\phi^\star(\vec{X},\vec{\Omega},E)=I(\vec{X},\vec{\Omega},E)\phi(\vec{X},\vec{\Omega},E)$. We can rewrite Equation (2.3) to get an equation on $\phi^\star$:

$$\begin{aligned}\vec{\Omega}.\vec{\nabla}\phi^\star\big(\vec{X},\vec{\Omega},E\big)+\left(\Sigma_t\big(\vec{X},E\big)-\vec{\Omega}.\frac{\vec{\nabla}I(\vec{X},\vec{\Omega},E)}{I(\vec{X},\vec{\Omega},E)}\right)\phi^\star\big(\vec{X},\vec{\Omega},E\big)=\\ \iint\Sigma_s\big(\vec{X},\vec{\Omega}'\to\vec{\Omega},E'\to E\big)\frac{I(\vec{X},\vec{\Omega},E)}{I(\vec{X},\vec{\Omega}',E')}\phi\big(\vec{X},\vec{\Omega}',E'\big)d\vec{\Omega}'dE'\\ +Q\big(\vec{X},\vec{\Omega},E\big)I(\vec{X},\vec{\Omega},E).\end{aligned}\tag{2.4}$$

We now introduce for any point $(\vec{X},\vec{\Omega},E)$ of the phase space the following quantities:

- $\vec{\Omega}_0=\frac{\vec{\nabla}I(\vec{X},E)}{\left\|\vec{\nabla}I(\vec{X},E)\right\|}$,
- $\kappa(\vec{X},E)=\frac{|\vec{\nabla}I(\vec{X},E)|}{I(\vec{X},E)}$,
- $\Sigma_t^\star(\vec{X},\vec{\Omega},E)=\Sigma_t(\vec{X},\vec{\Omega},E)-\kappa(\vec{X},E)\vec{\Omega}.\vec{\Omega}_0$,
- $\Sigma_s^\star(\vec{X},\vec{\Omega}'\to\vec{\Omega},E'\to E)=\frac{I(\vec{X},E)}{I(\vec{X},E')}\Sigma_s(\vec{X},\vec{\Omega}'\to\vec{\Omega},E'\to E)$,

which we then substitute in Equation (2.4) in order to obtain

$$\begin{aligned}\vec{\Omega}.\vec{\nabla}\phi^\star\big(\vec{X},\vec{\Omega},E\big)+\Sigma_t^\star\big(\vec{X},\vec{\Omega},E\big)\phi^\star\big(\vec{X},\vec{\Omega},E\big)=\\ \iint\Sigma_s^\star\big(\vec{X},\vec{\Omega}'\to\vec{\Omega},E'\to E\big)\phi^\star\big(\vec{X},\vec{\Omega}',E'\big)d\vec{\Omega}'dE'+I\big(\vec{X},\vec{\Omega},E\big)Q\big(\vec{X},\vec{\Omega},E\big).\end{aligned}\tag{2.5}$$

Equation (2.9) written in this manner has the same form as Equation (1.2). It is simply the linear Boltzmann equation, but with biased operators: $\Sigma_t^\star$ instead of Σ_t, $\Sigma_s^\star$ instead of Σ_s and $I\times Q$ instead of Q.

The Exponential Transform method is restrained to the biasing of the displacement operator, while the collision sampling remains unchanged. This is obviously not optimal, but the collision biasing requires heavy implementation, while the

displacement biasing simply consists in tampering with the displacement sampling procedure by substituting the biased cross section $\Sigma_t^\star = \Sigma_t - \kappa\vec{\Omega}.\vec{\Omega_0}$ for the total cross section Σ_t. Since the parameter κ is always positive, $\Sigma_t^\star$ is smaller than Σ_t when the particles have a direction oriented towards $\vec{\Omega}_0$, and greater when they go in the opposite direction. Therefore, the flight lengths are stretched for the particles going in the direction of the importance gradient, and shortened for those directed the way opposite. Consequently, the particles are drawn towards the areas of greater importance, thus helping the simulated particles to reach areas of interest if the importance function I is well-defined.

The response associated to the biased flux is, according to Equation (1.12),

$$\begin{aligned} R^\star(\mathcal{D}) &= \int_{(\vec{X},\vec{\Omega},E)\in\mathcal{D}} g_R^\star\big(\vec{X},\vec{\Omega},E\big)\phi^\star\big(\vec{X},\vec{\Omega},E\big)d\vec{X}d\vec{\Omega}dE \\ &= \int_{(\vec{X},\vec{\Omega},E)\in\mathcal{D}} g_R^\star\big(\vec{X},\vec{\Omega},E\big)\phi\big(\vec{X},\vec{\Omega},E\big)I\big(\vec{X},E\big)d\vec{X}d\vec{\Omega}dE. \end{aligned} \tag{2.6}$$

Since the response estimated using the biased game should be the same as the response estimated with an analog simulation, we have

$$g_R^\star\big(\vec{X},\vec{\Omega},E\big) = \frac{g_R\big(\vec{X},\vec{\Omega},E\big)}{I\big(\vec{X},E\big)}. \tag{2.7}$$

In other terms, every contribution to the score obtained during the biased simulation should be weighted by a factor

$$w_{ET} = \frac{1}{I\big(\vec{X},E\big)}, \tag{2.8}$$

which is handled in practice by the corrective weights of the particles.

The choice of an appropriate importance function lies at the heart of the exponential transform method. There are multiple ways to obtain an importance function. The most interesting candidate however is the solution of the adjoint equation [4, 10]:

$$\begin{aligned} -\vec{\Omega}.\vec{\nabla}\phi^\dagger\big(\vec{X},\vec{\Omega},E\big) + \Sigma_t\big(\vec{X},E\big)\phi^\dagger\big(\vec{X},\vec{\Omega},E\big) = \\ \iint \Sigma_s\big(\vec{X},\vec{\Omega}\to\vec{\Omega}',E\to E'\big)\phi^\dagger\big(\vec{X},\vec{\Omega}',E'\big)d\vec{\Omega}'dE' + Q^\dagger\big(\vec{X},\vec{\Omega},E\big). \end{aligned} \tag{2.9}$$

where $Q^\dagger$ is the adjoint source of the problem (related to the detector response). The solution $\phi^\dagger$ of this equation is called the *adjoint flux*, which is for any given

point of the phase space the average flux that would be generated by a particle placed at this location.

It can be shown that if the adjoint flux is used as importance function, the variance on the associated flux estimate is zero or nearly zero whatever the number of simulated particles. In any case, the computation of the adjoint flux is a problem at least as complex as the resolution of the direct equation.

However, using an approximation of the adjoint flux as importance function for the Exponential Transport method may be sufficient to efficiently reduce the variance without requiring the simulation of too large a number of particle histories. In this view, TRIPOLI-4 has a module called INIPOND that automatically pre-computes an importance map to be used during the biased simulation [14]. INIPOND approximates the adjoint flux on a discretized space and energy mesh, by using an analogy with a one-dimensional problem. This module and the importance map it generates will be used and discussed in Chapter 3.

2.4 Implicit capture

One of the possible causes of rare events is the presence of a highly absorbing material in the simulated space. Indeed, a simulated particle entering such a material has a low probability of ever coming out. It can therefore be interesting to reduce the probability for a simulated trajectory to end in a capture, and rather let the associated particle explore the geometry further. This can be done using *implicit capture*.

Implicit capture simply consists in replacing capture events (and more generally absorption events) by scattering events. The corrective weight associated to the implicit capture is the non-absorption probability associated to the collided nucleus. The weight of a particle entering a collision on a nucleus j at point P has to be multiplied by a factor

$$w_{IC} = 1 - \frac{\sigma_{j,a}}{\sigma_{j,t}} = \frac{\sigma_{j,s}}{\sigma_{j,t}}, \tag{2.10}$$

where $\sigma_{j,a}$ is the microscopic absorption cross section for nucleus j, and $\sigma_{j,s}$ its microscopic scattering cross section.

The removal of all the absorption processes allows for longer particle trajectories, but then no event can be sampled to stop the particles transport except for the leakage out of the geometry or of the energetic domain of simulation. Therefore, the implicit capture has to be associated with another method capable of ending the particle histories. This can be done using weight control methods [15].

2.5 Weight control

The purpose of weight control is to limit the discrepancies in the weight distribution among the particles. Whenever weights are introduced in a Monte Carlo

simulation, the danger of having big discrepancies in the particle weight values arises. If the weight of a particle becomes insignificant compared to the average contribution to the score, the computational resources spent to simulate the transport of this particle may be considered as a waste. On the other hand, if a particle happens to contribute to the score with a far greater weight than any other, the estimation of the score and its variance becomes unstable, due to a single contribution carrying most of the score.

The splitting and Russian roulette mechanisms are the most commonly used tools to address these issues [10, 16]. Splitting is used to reduce the weight of particles, while Russian roulette prevents them from dropping too low.

2.5.1 Splitting

The principle of the splitting technique [1] is to split a particle of weight w into n distinct particles, each carrying a weight $w_j, j \in [1, n]$ such that

$$\sum_{j=1}^{n} w_j = w, \tag{2.11}$$

in order to have a better exploration of the geometry while keeping the global simulated weight constant.

In practice, the use of splitting in Monte Carlo transport simulation is not restrained to weight control. However, as the particles generated by splitting carry only a fraction of their precursor's weight, splitting can be used to prevent the particles weights from diverging. In that case, a threshold weight w_{max} is defined, as well as a splitting number n. Whenever a particle weight w becomes greater than w_{max}, the corresponding particle is instantaneously split into n particles, each carrying one n-th of the initial weight w.

A wider exploration of the phase space should help reduce the variance, but the multiplication of the particles implies an increase in computation time. Nonetheless, a wise choice of the splitting parameters should allow for a significant increase of the FOM.

2.5.2 Russian roulette

The Russian roulette [10, 16] aims at limiting the lifespan of particles that are unlikely to yield a relevant contribution to the final score. It can therefore be used as a weight control technique to stop the transport of particles carrying a small weight.

Similarly as for the splitting technique, a threshold weight w_{min} has to be defined. When the weight of a particle becomes lower than w_{min}, a random game

is played to decide whether or not the particle is killed. Any particle of weight $w \leq w_{min}$ is killed by the Russian roulette with probability

$$P_{kill} = 1 - w. \tag{2.12}$$

If the particle does survive the roulette, its weight is set to 1 in order to keep the average particle weight equal to the particle weight before the triggering of Russian roulette. In a more general setting, a survival weight $w_s > w_{min}$ can be defined for the roulette, in which case the probability P_{kill} becomes

$$P_{kill} = 1 - \frac{w}{w_s}, \tag{2.13}$$

the weight of the surviving particles being set to w_s instead of 1.

2.6 Adaptive Multilevel Splitting

A new variance reduction method has recently been proposed in the literature of applied mathematics [2]. Originally designed to help the simulation of rare events associated to continuous Markov chains, it has been extended to discrete Markov chains [3]. Consequently, there will be no mention of particles in this section, whose purpose is to present a general theoretical setting of the AMS algorithm. We present in this section the mathematical setting of the AMS algorithm applied to discrete Markov chains, which is the most suitable version of the AMS algorithm in view of a transposition to the field of particle transport. This choice will be justified in Chapter 3 alongside the description of the practical implementation of AMS as a variance reduction method for Monte Carlo particle transport.

It should however be kept in mind that the version of the AMS presented in this section fits perfectly the theoretical framework of [3], so that the estimator of the rare event occurrence probability introduced in the following is unbiased.

The following description is extracted from an article written as part of this Ph.D. and presented at the joint conference International Conference on Radiation Shielding / Topical Meeting of the Radiation Protection and Shielding Division of the American Nuclear Society (ICRS-13 & RPSD-2016) [17].

2.6.1 Objective and setup

Let $X = (X_t)_{t\in\mathbb{N}}$ be a discrete-time Markov chain with values in $\mathbb{R}^d$, $d \in \mathbb{N}^*$. We define $\mathcal{P}$ as the path space, containing all possible realisations of the Markov chain X. Given D a subset of $\mathbb{R}^d$, we define the entrance time of the Markov chain X in D:

$$\tau_D = \inf\{t \in [0; \tau_f] : X_t \in D\}, \tag{2.14}$$

where τ_f is the final stopping time of the Markov chain X, which we suppose almost surely finite.

Given an observable $\phi_D : \mathcal{P} \to \mathbb{R}$ such that $\phi_D(X) = 0$ on the event $\tau_f < \tau_D$, we would like to estimate the average $\mathbb{E}(\phi_D(X))$ of ϕ_D. Let us suppose now that the probability for (X_t) to enter D before τ_f is very small, i.e. $\mathbb{P}(\tau_D < \tau_f) \ll 1$. Estimating $\mathbb{E}(\phi_D(X))$ requires to sample the rare event $\tau_D < \tau_f$. In such a case of rare event simulation, the AMS algorithm proposes to reduce the variance of the estimation of $\mathbb{E}(\phi_D(X))$ by increasing the number of Markov chains reaching the subset D. AMS is an iterative algorithm that consists of several steps. The first step is a basic Monte Carlo simulation of multiple replicas of the Markov chain X with a given initial condition. Each of the following steps consists in the resampling of some Markov chains among the replicas, with an initial condition getting closer to D at each iteration of the algorithm.

2.6.2 The AMS algorithm

Importance function

We define a so-called *importance function*, mapping $\mathbb{R}^d$ to $\mathbb{R}$:

$$\xi : \mathbb{R}^d \to \mathbb{R},$$

which is used to quantify the proximity of a point in $\mathbb{R}^d$ to the subset of interest D. The only requirement on ξ is that there exists a constant $Z_{max} \in \mathbb{R}$ such that

$$\xi(x) \geq Z_{max} \quad \text{if} \quad x \in D. \tag{2.15}$$

We further define the *importance* of a realization $X = (X_t)_{t\in\mathbb{N}}$ of the Markov chain as the supremum of ξ along the chain:

$$I(X) = \sup_{t\in[0;\tau_f]} \xi(X_t). \tag{2.16}$$

The ξ function is probably the most important ingredient of the AMS algorithm, since it is used to quantify the proximity of a path to the subset D. It is therefore important to choose a good function ξ with regards to the rare event we are trying to simulate. Even if the AMS algorithm is proven to yield an unbiased result *regardless of* ξ, the choice of an optimized importance function is expected to improve the variance reduction efficiency.

Initialization

The AMS algorithm consists in an evolving interacting system of weighted replicas. Given $n > 0$, we simulate n i.i.d. replicas of the Markov chain X, denoted by $X_0^j = (X_{0,t}^j)_{t\in\mathbb{N}}$, $j \in \{1, \ldots, n\}$. For all j, the initial state $X_{0,0}^j$ is a point x_0 located outside D. We define Z_0 as

$$Z_0 = \xi(x_0). \tag{2.17}$$

Let us denote by $q \in \mathbb{N}$ the current iteration number, and by k the number of replicas to be resampled at each iteration.Within an iteration of the AMS algorithm, every replica has *the same weight*. The common weight at iteration q will be denoted w_q, with w_0 set to 1.

For the sake of simplicity, we assume in the following that distinct paths cannot have the same importance. The general case is discussed in Section 2.6.3. Now we can start iterating on $q \geq 0$.

Iterations

1. For each $j \in \{1, \ldots, n\}$, denote by $\tau_{q,f}^j$ the stopping time of the Markov chain X_q^j, and by S_q^j its importance (See Equation (2.16)):

$$S_q^j = I(X_q^j). \tag{2.18}$$

2. Sort the sample $(S_q^1, \ldots, S_q^n)$ in increasing order:

$$S_q^{(1)} < \ldots < S_q^{(k)} < \ldots < S_q^{(n)}.$$

3. Denote by Z_{q+1} the k-th order statistics $S_q^{(k)}$:

$$Z_{q+1} := S_q^{(k)}. \tag{2.19}$$

4. If $Z_{q+1} \geq Z_{max}$, stop iterating, set $Q = q$ and go to the final step

5. For all $j \in \{1, \ldots, k\}$, resample replica $X_q^{(j)}$ according to the resampling kernel described in the following, and denote it by X_{q+1}^j

6. For all $j \in \{k+1, \ldots, n\}$, define $X_{q+1}^j = X_q^{(j)}$

7. Update the common weight:

$$w_{q+1} = \frac{n-k}{n} w_q. \tag{2.20}$$

8. Increment q and go to step 1.

Resampling process

At each iteration of the AMS algorithm, k replicas are resampled. Let us denote the current iteration number by q and the associated resampling level by Z_{q+1}.

For each of the k replicas $X^{(j)}, j \in \{1, \dots, k\}$ to be resampled, one of the remaining replica $X^{(i)}, i > k$ is *randomly* selected for duplication. We know for sure that the Markov chain $(X_t^{(i)})_{t\in[0;\tau_f^{(i)}]}$ contains at least one state whose importance is greater than Z_{q+1} (otherwise it would have been resampled). We can therefore define

$$\tau_q^{(i)} = \inf\left\{t \in [0; \tau_{q,f}^{(i)}] : \xi(X_{q,t}^{(i)}) > Z_{q+1}\right\} \tag{2.21}$$

as the first time at which the replica $X^{(i)}$ has an importance greater than Z_{q+1}. The resampled Markov chain $(Y_t)_{t\geq 0}$ is defined as a copy of $X_{q,t}^{(i)}$ for all $t \in [0, \tau_q^{(i)}]$, and is then completed independently using the original Markov kernel, up to the stopping time τ_f. This resampled Markov chain replaces the original one $X^{(j)}$ for the next iteration of AMS.

Final step

Once the algorithm stops iterating, Q is the number of completed iterations. Given the bounded observable ϕ_D introduced in Section 2.6.1, we define $\hat{\phi}_D$ such as

$$\hat{\phi}_D = \frac{w_Q}{n} \sum_{j=1}^{n} \phi_D(X_N^j). \tag{2.22}$$

Since the algorithm described in this section and the construction of $\hat{\phi}$ fit the theoretical framework of a Generalized Adaptive Multilevel Splitting algorithm, we can apply Theorem 4.1 of [3] (the "unbiasedness theorem"), which states that

$$\mathbb{E}(\hat{\phi}_D) = \mathbb{E}(\phi_D(X)), \tag{2.23}$$

so that $\hat{\phi}_D$ is an *unbiased* estimator of $\mathbb{E}(\phi_D(X))$.

2.6.3 Interpretation of the replicas weights

In this section we provide a practical interpretation of the AMS weights to give an intuition on the estimator Equation (6.6). The mathematical proofs of the unbiasedness and consistency of the AMS estimator are not presented here. We refer the reader to [2] and [3] for theoretical support.
At each iteration $q \geq 0$, the level Z_{q+1} is chosen in such a way that the probability for a path X_q^j to have an importance greater than Z_{q+1} (i.e. $\mathbb{P}(S_q^j \geq Z_{q+1} | S_q^j \geq$

$Z_q)$) is estimated by

$$\hat{p}_q = 1 - \frac{k}{n}. \tag{2.24}$$

Keeping that in mind, we can see that the weights of the replicas at iteration $q+1$ are nothing more than an estimate of the probability $\mathbb{P}(S_{q+1}^j \geq Z_{q+1})$.
In other words, the AMS algorithm provides us at each iteration q with a set of paths X_q^j, $j \in \{1, \ldots, n\}$, carrying a common weight, which can be interpreted as an estimate of the probability to have this particular set of paths instead of the paths sampled at iteration 0.

2.6.4 About the number of resampled replicas

The algorithm presented in Section 2.6.2 is an ideal case. In reality, it may occur that multiple replicas have the same importance. In that case, k should not be seen as the number of resampled replicas, but rather as the parameter which defines the splitting levels.

Indeed, the number of replicas having an importance less or equal to the k-th lowest importance may very well be greater than k. When such a situation arises, **every** path whose importance is less or equal to the level has to be resampled [3].

This modification has to be taken into account in the replicas weights. If the current iteration is the q-th and the number of particles to be resampled is $K_q \geq k$, then the weight update at step 7 of the algorithm has to be changed to:

$$w_{q+1} = \frac{n - K_q}{n} w_q. \tag{2.25}$$

In some pathological configurations, all the replicas may happen to have the same importance, which leads to extinction at the next iteration. In such a case, the iterating process is interrupted and the algorithm goes straight to the final step (See Section 2.6.2), eventually yielding a null contribution.

Part II

Adaptive Multilevel Splitting for Monte Carlo particle transport

Chapter 3

Adaptation of the AMS algorithm to particle transport

Every Monte Carlo transport code relies on the particle tracking routine, which simulates the random trajectories of the particles by transporting them from one interaction to another, until they are absorbed or leak out of the geometry.

The purpose of this chapter is to introduce AMS to the field of particle transport, and show that it can be used as an effective variance reduction technique in this new context. To do so, we first present a practical reformulation of the AMS algorithm that takes the notions of particles and particle tracks into account. In a second part, we introduce the MENHIR prototype, a simplified Monte Carlo simulation code that was specifically designed to test the AMS implementation in the context of particle transport. The last section of this chapter is devoted to the presentation and analysis of some of the results obtained with MENHIR.

3.1 Applicability of AMS to particle transport

As described in Section 1.2, the simulation process of particle transport is such that at any given time in the particle life, the position and characteristics of the next interaction can be determined using only the particles coordinates (position, direction, energy) and the medium properties. This implies that the random process of particle transport can be seen as a discrete-time markovian process. Let us refer to the sequence of the phase-space coordinates of a particle (namely position, direction and energy) at each interaction with the medium as the particle's *track*. During the transport, the track of each transported particle is built step by step, one interaction after the other, using only the knowledge available from the last point of the track. The particle tracks are therefore Markov chains, so that the AMS algorithm described in Section 2.6.2 can be implemented.

We mentioned in Section 2.6 the existence of several versions of the AMS algorithm. Indeed, the AMS algorithm we presented in Section 2.6.2 can be adapted to handle continuous Markov chains (which is actually its original framework). Particle trajectories can very well be considered as continuous Markov processes, since a particle transport can be stopped and resumed even between collision points. However, the use of the continuous version of AMS is troublesome in our case for two reasons: on the one hand, it requires to evaluate particle importances *continuously* between collision points, which complicates the computation process if the importance function is nonlinear. On the other hand, the collision sampling process implies brutal changes of direction and energy at collision points, which may induces discontinuities in the importance along the particle trajectory for angular and/or energy dependent importance functions.

Using the discrete formulation of AMS however, the importance of a particle trajectory can easily be computed by evaluating the particle importance at each collision point.

3.2 Practical AMS formulation

In the context of particle transport, the initialization step of the AMS algorithm consists in the analog simulation of a set of independent particles. Then, the AMS algorithm starts iterating until the stopping criterion is met. Each AMS iteration consists in two steps: first, the set of particles is sorted with regard to the particle importances (See Section 3.2.1). Then, the lowest-rated particles are resampled by splitting the other tracks as described in Section 3.2.2. The parameter k that is used to define the splitting level is defined before the first iteration and remains constant throughout the simulation.

In Monte-Carlo particle transport simulations, the particles are usually gathered into *batches*, which are simulated one after the other. The mean score is computed as the empirical mean of the scores of each batch, and the associated standard error σ as the standard deviation of the batch scores divided by the square root of the number of batches minus 1. By analogy to other simulations, we will refer to an entire AMS simulation (initialization+iterations+final step) as a *batch*, so that the mean score is computed as the empirical mean of the AMS estimations of each batch.

3.2.1 The sorting step

Importance functions

In order to use the AMS algorithm, one has to be able to determine which regions of the geometry are of interest to the simulation. Therefore, an importance function has to be associated to the geometry. This function maps any point of the phase space to an importance value, related to the probability for a particle

located at a given point P to contribute to the final score. We denote it by

$$I(P) = I(\vec{X}, \vec{\Omega}, E), \tag{3.1}$$

where $\vec{X}$, $\vec{\Omega}$ and E are the position, direction and energy of the point P, respectively.

It has to be noted that within AMS, this function is only used to rank the particles *with respect to one another*, so that the value of the importance at a given point does not need to be meaningful on its own. This property is one of the strengths of the AMS algorithm, as it allows for the use of trivial importance functions for any problem, such as the inverse of the distance to the area of interest.

It is believed (although up to now without any theoretical proof), that the *adjoint score* of the problem is the most efficient importance function for AMS. The adjoint score at a given point of the phase space is defined as the average score generated in the area of interest by a particle emitted from this point. Therefore, it gives the most precise indication concerning the interest of a particle located at a given point with regards to the score.

However, the determination of the adjoint score is a problem at least as complex as the estimation of the direct score. Furthermore, if one has access to the adjoint score, the solution of the direct problem is directly available as the value of the adjoint score at the source point, obviating the need to perform the simulation in the first place. As the AMS is robust with regards to the imperfections of the importance map, an approximation of the adjoint score seems to be a good importance function candidate for the AMS algorithm.

Particle tracks importance

In order to sort the particles, a value of importance has to be attached to each of the particle tracks. When a new particle is simulated, a track is created. We denote by $P_0 = (\vec{X}_0, \vec{\Omega}_0, E_0)$ the emission point of a particle, and the first point of its track. This particle travels along straight lines between collisions with the medium, each collision resulting either in the absorption of the particle or in a scattering event resulting in a random change of the particle direction and energy. If the particle undergoes N collisions before being absorbed or leaking out of the geometry, we define its track T as follows:

$$T = (P_0, \ldots, P_N), \tag{3.2}$$

where $P_i = (\vec{X}_i, \vec{\Omega}_i, E_i)$ represents the properties of the particle outgoing its i-th collision with the medium. Using these notations, we introduce the importance

of a particle track as:

$$I(T) = \max_{i \in [0,N]} I(P_i). \tag{3.3}$$

We show in Figure 3.1 a particle track T. In this example, we assume that the importance of a point is given by its abscissa x. Therefore, the track importance $I(T)$ is that of the rightmost point.

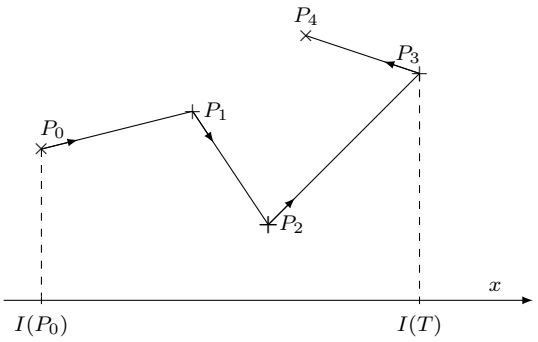

Figure 3.1. Illustration of a particle track and associated importance.

Importance function requirement

Theoretically, there is only one requirement on the importance function (Equation (2.15)). We designed a trick to ensure that this requirement is always met whatever the importance function: any point within the area of interest is given a *numerical infinite importance*. Furthermore, when a particle enters the area of interest, the entry point is retrieved and appended to the particle track, also with infinite importance). Thus, if a particle goes through the area of interest without colliding in it, it would still have an infinite importance and would never be resampled.

With this technique, if a particle that reached the area of interest is selected for duplication, the splitting takes place at the boundary and not inside the area of interest, which means that the contribution of the selected track has not to be duplicated (since the particles outside the area of interest do not contribute to the score).

Definition of the splitting level

Let n be the number of simulated particles, k the minimum number of tracks to be resampled per iteration and q the index of the current iteration.

After the n particles have been absorbed or have leaked out of the geometry, the AMS algorithm computes the importance $I(T_j),\ j \in [1, n]$ of each particle track (see Equation (3.3)). The splitting level Z_q is then defined as the k-th smallest value in the sample $(I(T_1), \ldots, I(T_n))$. Each particle track having an importance less or equal to Z_q is deleted, and the number K_q of suppressed

particles at this iteration is kept in memory. K_q is by construction larger than k, and could be strictly larger if multiple tracks have the same importance.

3.2.2 The splitting step

Resampling process

Once the sorting step of iteration q is over, the AMS proceeds to the resampling of the K_q particle tracks that have been deleted from the simulation, so that n distinct tracks are available for the next iteration of the algorithm.

For each of the particles to be resampled, one of the $n - K_q$ remaining tracks is selected. The probability distribution for the choice of the track to duplicate is uniform and with replacement. Let us denote by $T_j = (P_i),\ i \in [0, N_j]$ one of the selected tracks. The emission point P_{split} of the new particle is then defined as:

$$P_{split} = \inf \{i \in [0, N_j] : I(P_i) > Z_q\}, \tag{3.4}$$

which is the first point of the track T_j having an importance strictly greater than Z_q. The resampled particle is simulated from the point P_{split}, and a new track is filled with its collision points.

AMS global weight

The resampling process splits K_q particle tracks among a set of $n - K_q$ tracks, therefore all particles weights have to be weighted at the end of iteration q by a factor

$$W_q = 1 - \frac{K_q}{n} \tag{3.5}$$

to ensure unbiasedness [2, 3].

In practice, the cumulated weight factor due to the AMS process from iterations 1 to q is the same for each particle, and can be stored in a global weight

$$\begin{aligned} w_q &= \prod_{i=1}^{q} W_i \\ &= \prod_{i=1}^{q} (1 - \frac{K_i}{n}). \end{aligned} \tag{3.6}$$

3.2.3 Scoring step

The AMS algorithm stops at the end of iteration q if $n - K_q + 1$ particles have reach the area of interest (i.e. Z_{q+1} is equal to numerical infinite). An estimator can be constructed for any score ϕ in the area of interest. If we denote by $\hat{\phi}_{MC}$

the value estimated using a standard Monte Carlo estimator, then

$$\hat{\phi}_{AMS} = w_q \times \hat{\phi}_{MC} \tag{3.7}$$

is an unbiased estimator of the quantity $\mathbb{E}(\phi(X))$ [3].

3.2.4 Optimization

Crossing points

Most of the time, the geometries considered are composed of many regions, each of these regions having specific properties that impact the particle transport (travel length, collision probabilities,...). When a particle passes from one region to another during a flight, it can be stopped as it crosses the interface between the regions, and a new flight length is resampled from this crossing point, taking into account the properties of the entered region.

In that case, the characteristics of the particle at the crossing point depend only on the coordinates of the particle at the last collision point and on the physical properties of the first region. Similarly, the next collision point can be determined based solely on the coordinates of the particle at the crossing point and the physical properties of the second region.

Consequently, if the crossing points are added to the particle track in the same manner as real collision points, the enriched track remains a Markov chain. The AMS can thus be used on the enriched tracks [3]. This allows for a more precise estimation of tracks importances, as it adds an importance estimation between some collision points without any additional computing. This property can also be used to improve the knowledge of the track importance within a single volume by adding virtual surfaces in it (or simply by dividing it in sub-volumes).

Track storage

One of the downsides of the AMS algorithm is that it requires a priori to keep the particle tracks accessible in memory at all times. However, it is not mandatory for the algorithm to store every point of the tracks.

The points composing the tracks are used in two ways during the AMS iterations:

- To compute the importance of the track

- To define the splitting points during the resampling process

In order to avoid going through the importances of all points composing a track to find the maximum value and define the importance of the track, an

importance value can be assigned to each particle before their transport. Each time a point is added to the particle's track, the previous particle importance is compared to the new point importance, and updated if necessary. By means of the particle importance, there is no more need to keep every collision points in the track in order to compute the track importance.

Furthermore, we can see that according to Equation (3.4), the splitting point on a given track is defined as the first point of the track which importance is greater than the current AMS splitting level. This means that the only points that may be chosen for splitting are those having an importance greater than any preceding point on the track. There is consequently no need to store a point in the track if the point importance is less than the importance the particle had when reaching it.

In the following implementations of the AMS algorithm, the tracks will only contain points of increasing importance, and the importance of the tracks will be computed on the fly.

Parallelization

Since a Monte Carlo particle transport simulation is made of a large number of independent batch simulations, the standard parallelization of such codes is simply performed by running batches in parallel while a collector thread manages the gathering of each thread's results. This procedure can be optimized by sharing data concerning the geometry, materials, and other global variables.

Concerning AMS for particle transport, a straightforward way of parallelizing the calculations is to run independent AMS simulations on distinct threads, each handling alone the initialization, iterations and final step. One may consider other options to parallelize AMS calculations, like using multiple threads at each resampling step to transport simultaneously all new replicas. However, since simulations using the AMS algorithm still require to perform multiple independent batch simulations, no options appears to be more efficient than to run the batches on distinct threads and collect the estimations of each batch afterwards to compute the average result.

3.3 The MENHIR prototype

In order to test the feasibility of implementing the AMS algorithm in a particle transport code, we decided to use a toy model depicting a geometry in which analytical reference results can easily be computed. The problem consists in an isotropic source of monoenergetic particles within an infinite homogeneous medium. The source is placed at the centre of a spherical shell in which the particle flux is estimated. A simplified Monte Carlo transport prototype, called MENHIR, has been developed to simulate this problem. MENHIR has been specifically designed for AMS testing, allowing for an easy implementation and validation of the algorithm.

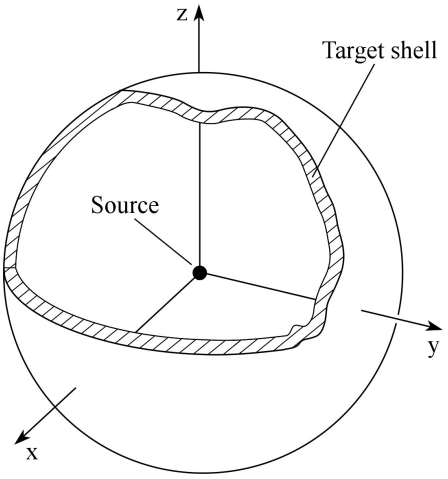

Figure 3.2. MENHIR geometry.

3.3.1 Physics

The physics simulated in MENHIR is very simplified.The transported particles are monoenergetic. They travel at constant speed and undergo only two types of collision: absorption and isotropic scattering. As the medium composing the geometry is homogeneous, the absorption and scattering events occur with constant probability rates. The associated cross sections are denoted Σ_a and Σ_s, such that

$$\Sigma_t = \Sigma_a + \Sigma_s. \tag{3.8}$$

When a particle is absorbed, transport is over and the particle's history is terminated. On the other hand, a particle undergoing a scattering event remains alive but changes direction at random. The angular distribution of particles outgoing a scatter is isotropic.

These assumptions allow for an easy prototyping of the AMS algorithm. Furthermore, the flux in the target shell can be analytically computed, which provides a reference value to validate the AMS implementation. Details concerning the computation of the analytical solution can be found in Appendix A.

3.3.2 Code structure

MENHIR is written in C++. It is composed of 6 files, accounting for roughly 1100 lines of code. MENHIR is object oriented and divided into 4 classes: Point, Vector, Geometry and Particle.

- The Point and Vector classes are basic classes containing three-dimensional coordinates, as well as methods returning for example the distance of a given point to the source, the norm of a vector, sampling methods to generate isotropic vectors, etc.

- The Geometry class handles cross sections, sampling procedures for the

flight length and collision type as well as methods computing importance values.

- The Particle class holds everything relevant to a given particle: coordinates, track, as well as the method that determines the position of splitting points.

MENHIR is capable of performing both analog and AMS simulations. The code is executed using a simple command line, in which the simulation parameters can be modified. The particle source point is fixed and always located at the origin of the coordinate system $(0, 0, 0)$. The free parameters of the simulation are:

- The simulation type (AMS or ANALOG)
- The total cross section Σ_t (in cm^{-1})
- The scattering probability $\frac{\Sigma_s}{\Sigma_t} \in [0; 1[$
- The distance between the source point and the target shell
- The thickness of the target shell
- The number of batches
- The number of particles per batch
- The minimum proportion of deleted particles by iteration (AMS only)
- The importance function to be used for tracks classification (AMS only)

3.3.3 Transport process

Before presenting and discussing the results obtained using MENHIR with various parametrizations, we describe here the particle transport and the AMS process within MENHIR. The pseudo-code for the analog transport process can be found in Algorithm 1.

A particle is emitted at point $(0, 0, 0)$ with an isotropically sampled direction $\vec{\Omega}$. A flight length d is sampled from the exponential distribution of parameter Σ_t. If this flight length is long enough for the particle to cross the boundary of the target shell, the particle is moved to the shell's boundary and a new flight length is sampled. Otherwise, the particle is moved of distance d in the direction $\vec{\Omega}$, to the location of its first collision site. The particle is absorbed with probability $\frac{\Sigma_a}{\Sigma_t}$. If it is not absorbed, the particle is scattered towards a new isotropically sampled direction. The process is repeated until the particle is absorbed.

In a similar way as for the particles entering the target shell, if the flight length of a particle within the shell is long enough for the particle to exit the shell, the particle is moved to the exterior boundary, and a new flight length is sampled from here. The consideration of such interface crossing points allows for an easy scoring of the track estimator: the particle tracks that contribute to the

flux are actually already divided into parts that are either completely within the shell or completely out of it.

Algorithm 1: Pseudo-code for analog particle transport in MENHIR.

```
1  while particle is alive do
2  |  sample flight length;
3  |  if entering or leaving target shell then
4  |  |  move particle to target boundary ;
5  |  |  if leaving then  update track length estimator ;
6  |  else
7  |  |  move particle to collision site ;
8  |  |  if collision in target shell then
9  |  |  |  update track length estimator ;
10 |  |  |  update collision estimator ;
11 |  |  end
12 |  |  solve collision;
13 |  end
14 end
```

The particle transport process in the case of an AMS simulation is only altered by the storing of the particle tracks and the computation of the track importances, and remains otherwise unchanged. The entry points of particles in the target shell are given a *numerically infinite* importance so as to ensure that the requirement on the importance function is met (see Equation (2.15) and Section 3.2.1). In practice, MENHIR sets this importance to `DBL_MAX`, which is in C and C++ the value of maximum representable finite floating-point number and depends on the system and compiler used. On our system, `DBL_MAX`= 1.797 69E308.

MENHIR takes into account the considerations described in Section 3.2.4: the importance of each track is computed on the fly, and only the points of increasing importance are added to the particle track. The pseudo-code describing the particle transport for AMS simulations in MENHIR is shown in Algorithm 2.

3.3.4 AMS iteration process

When MENHIR uses the AMS algorithm, the code starts iterating after the initial simulation of n particles. The pseudo-code of the AMS iteration process is shown in Algorithm 3.

At the end of the initial simulation, the importances of the n generated tracks are ordered, so as to find the k-th smallest value which will be our first splitting level Z. In order to be efficient in the particle classification, the vector containing the track importances is only partially sorted, making use of the C++ *nth_element* function with parameter k, which rearranges the elements of the

Algorithm 2: Pseudo-code for AMS particle transport in MENHIR.

```
1  I_track := 0 ;
2  while particle is alive do
3  |  sample flight length;
4  |  if entering target shell then
5  |  |  move particle to target boundary ;
6  |  |  set I_point ←DBL_MAX ;
7  |  if leaving target shell then
8  |  |  move particle to target boundary ;
9  |  |  update track length estimator ;
10 |  else
11 |  |  move particle to collision site ;
12 |  |  if collision in target shell then
13 |  |  |  update track length estimator ;
14 |  |  |  update collision estimator ;
15 |  |  end
16 |  |  solve collision;
17 |  |  get I_point as the importance after collision;
18 |  end
19 |  if I_point > I_track then
20 |  |  add point to particle track;
21 |  |  update I_track ← I_point;
22 |  end
23 end
```

vector in such a way that the element at the k-th position is the element that would be in that position if the vector was entirely sorted [18].

Once the splitting level Z is obtained, the tracks are separated into two vectors: the *rejected* and the *survivors* vectors, according to whether or not the importance of the track is greater than the splitting level. The global weight W, which is set to 1 before the first AMS iteration, is multiplied by $(1 - \frac{K}{n})$, where K is the size of the rejected vector. Each of the tracks within the rejected vector is then resampled according to the resampling process described in Section 3.2.2, by randomly selecting and duplicating a track from the survivors vector, and sampling a new track using the transport process presented in Section 3.3.3.

When the K rejected tracks have been resampled, the new splitting level Z is computed, and if Z is less than `DBL_MAX`, another iteration begins. Otherwise, the AMS algorithm stops iterating, and the cumulated estimators of the flux are weighted by W before the simulation ends.

Algorithm 3: Pseudo-code for AMS iterations in MENHIR.

```
1  q := 1 ;
2  W := 1 ;
3  Z := kth_element(I(T_1), ..., I(T_n)) ;
4  while Z ≤ DBL_MAX do
5  |  K := 0 ;
6  |  empty rejected and survivors vectors ;
7  |  for i ∈ [1, n] do
8  |  |  if I(T_i) ≤ Z then
9  |  |  |  add i to rejected vector;
10 |  |  |  K ← K + 1
11 |  |  else
12 |  |  |  add i to survivors vector;
13 |  |  end
14 |  end
15 |  W ← W × (1 − K/n) ;
16 |  for j in rejected vector do
17 |  |  randomly select a track l from the survivors vector ;
18 |  |  determine the splitting point on T_l ;
19 |  |  sample a new track T_j from the splitting point ;
20 |  end
21 |  q ← q + 1 ;
22 |  Z ← kth_element(I(T_1), ..., I(T_n)) ;
23 end
```

3.3.5 Importance functions

Within MENHIR, three importance functions are available for AMS use. We denote them I_d, I_a and I_x. They are described in the following, and shown in Figure 3.3.

Distance importance function I_d

In our geometry, a straightforward way of defining an importance is to use a function that increases as the distance to the target shell decreases. This can be achieved for example by using the distance to the source point. For a spatial point $\vec{X} = (x, y, z)$, the distance to the source point $(0, 0, 0)$ is:

$$d_{source} = \sqrt{x^2 + y^2 + z^2}. \tag{3.9}$$

As it has already been stressed before, the AMS uses the importance function only to classify particles, therefore the simulation remains unchanged if the importance is replaced by any function having the same level sets. This is why we can get rid of the square root without impacting the AMS behaviour. We then

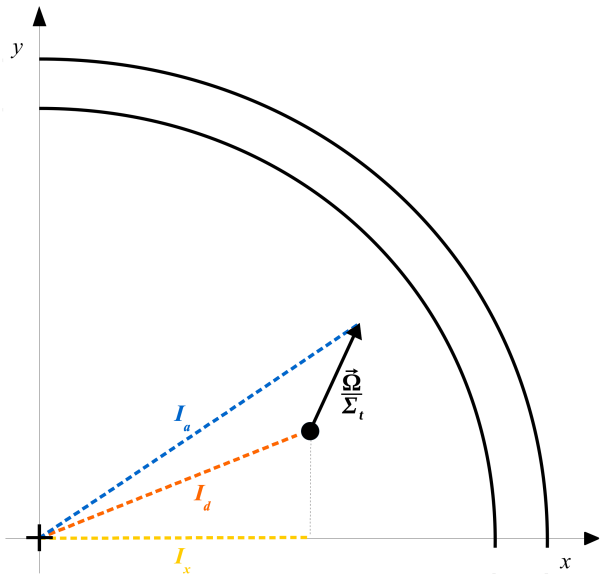

Figure 3.3. Illustration of importance functions in MENHIR.

define I_d by

$$I_d(\vec{X}) = x^2 + y^2 + z^2. \tag{3.10}$$

Angular importance I_a

The importance function I_d, as defined in Equation (3.10), does not take into account the direction of the particles. However, it seems natural that two particles located at equal distance to the target shell should have different importances if one is going straight towards the target, and the other one in the opposite direction. In order to have a more precise definition of the importance, we try and build an importance function that depends on the angular coordinates. Due to the homogeneity of the medium and also the fact that all scattering events are isotropic, a pertinent classification can be obtained using I_d for two particles *before collision*.

Keeping that in mind, an angular importance function can be derived for a particle after collision by estimating the position of the next collision from the current position and direction of the particle. As the flight lengths are exponentially distributed with parameter Σ_t, the mean free path of a particle in the geometry is $1/\Sigma_t$. Therefore, we define the angular importance of any point $(\vec{X}, \vec{\Omega})$ as

$$I_a(\vec{X}, \vec{\Omega}) = I_d\left(\vec{X} + \frac{1}{\Sigma_t}\vec{\Omega}\right). \tag{3.11}$$

X-Importance I_x

In order to test the robustness of the AMS algorithm, which should be able to provide an unbiased estimation of the flux whatever the importance function,

we also test a "bad" importance function, i.e. a function that does not accurately represent the problem at hand. In this view, MENHIR can use the coordinate x as an importance function:

$$I_x(\vec{X}) = x. \tag{3.12}$$

The use of I_x as importance function for the AMS algorithm is obviously not optimal, as it prevents the duplication of particle tracks having points with negative x coordinates. The contributions of such particles can therefore only be taken into account if they reach the detector directly from the source in the initialization phase of the AMS algorithm.

3.4 Validation of AMS for particle transport with MENHIR

Now that the MENHIR prototype has been introduced, we present in this section various results obtained with MENHIR simulations. In a first part, we will present results obtained at *short distance*, meaning that the position of the shell will be chosen in order to be able to get an analog estimation of the flux. After testing the impact of each AMS parameter on the efficiency of the algorithm, which we will compare both to analog MENHIR results and analytical values, we will move the shell away from the source, to repeat some of the comparisons in a more severe configuration.

Throughout this section, every simulation result presented was obtained with 10^4 independent batches each of $n = 10^4$ initial particles (even for the analog simulations). The same analysis was performed during this PhD for various initial particles numbers, showing no difference in the resulting Figure Of Merit.

3.4.1 Flux estimation in a shell near the source point

In this configuration, the target shell has a width of 1 cm, and its inner boundary is placed at 10 cm of the source point. Under these conditions, we are going to investigate the impact of the parameter k on AMS efficiency.

Mean flux analysis

In order to investigate the impact of k on the AMS algorithm, we set the scattering probability to 90%, and the mean free path of the particles to 1 cm. The corresponding cross sections in MENHIR are

$$\Sigma_t = 1\,\mathrm{cm}^{-1} \qquad \text{and} \qquad \Sigma_s = 0.9\,\mathrm{cm}^{-1},$$

and under these conditions the reference flux in a 1-cm-width shell located at 10 cm from the source point is:

$$\phi_{ref} = 1.072 \times 10^{-1} \mathrm{particles/cm^2/s},$$

for a unitary source emitting 1 particle/s.

For each of the three AMS importances I_d, I_a and I_x (defined in Equations (3.10),(3.11) and (3.12)), multiple simulations were run with various k values, ranging from $k = 1$ (0.01% of the initial particles) to $k = 9900$ (99% of the number of initial particles). The obtained results are gathered in Figure 3.4. In this figure, the upper plot shows the empirical mean of the estimated flux as a function of k, with associated 68% confidence intervals. The middle part of the figure shows the relative standard error $\sigma_{\%}$, expressed in percentage of the mean flux, and the bottom one the Figure Of Merit, which is computed as:

$$FOM = \frac{1}{\sigma_{\%}^2 \times t}, \tag{3.13}$$

where $\sigma_{\%}^2$ is the variance of the mean flux, and t is the simulation time (CPU time between the first particle instantiation and the end of the 10^4 batches).

The main observation is that the AMS estimation of the flux is in perfect agreement with the reference for every combination of k and I, confirming that the AMS adaptation to a particle transport process is successful. The reference value of the flux is never seen out of the three-sigma interval around the estimated flux, which is remarkable considering that the standard error, which is also shown in Figure 3.4, is never greater than 0.07% of the mean.

Relative standard error comparison

As all simulations presented in this section were run for 10^4 batches, it is relevant to compare the relative standard error on the mean flux for different AMS parametrization and for the analog computation. The middle graph of Figure 3.4 shows the relative standard error at the end of the 10^4 batches as a function of k for each importance function, as well as the analog result (which does not depend on k).

First of all, we observe that the standard errors obtained with the AMS simulations are always lower than for the analog simulation *for the same number of batches and of initial particles*. In the AMS results we observe that $\sigma_{\%}$ does not depend on k as long as $\frac{k}{n} < 50\%$, whatever the importance function is. However, the variance grows rapidly when more than half of the particles are resampled at each iteration of the algorithm. This is a side-effect of the correlations between particles. When too many particles are resampled per AMS iteration, the risk of selecting several times the same track for duplication increases drastically. In the meantime, the distance between the splitting levels in terms of importance grows ever bigger. Consequently, reaching a given importance level requires fewer iterations, leading to loss of precision in the associated global weight estimation.

Concerning the impact of the importance function, we can see that the errors on the results obtained with I_a and I_d are comparable, even if the use of the

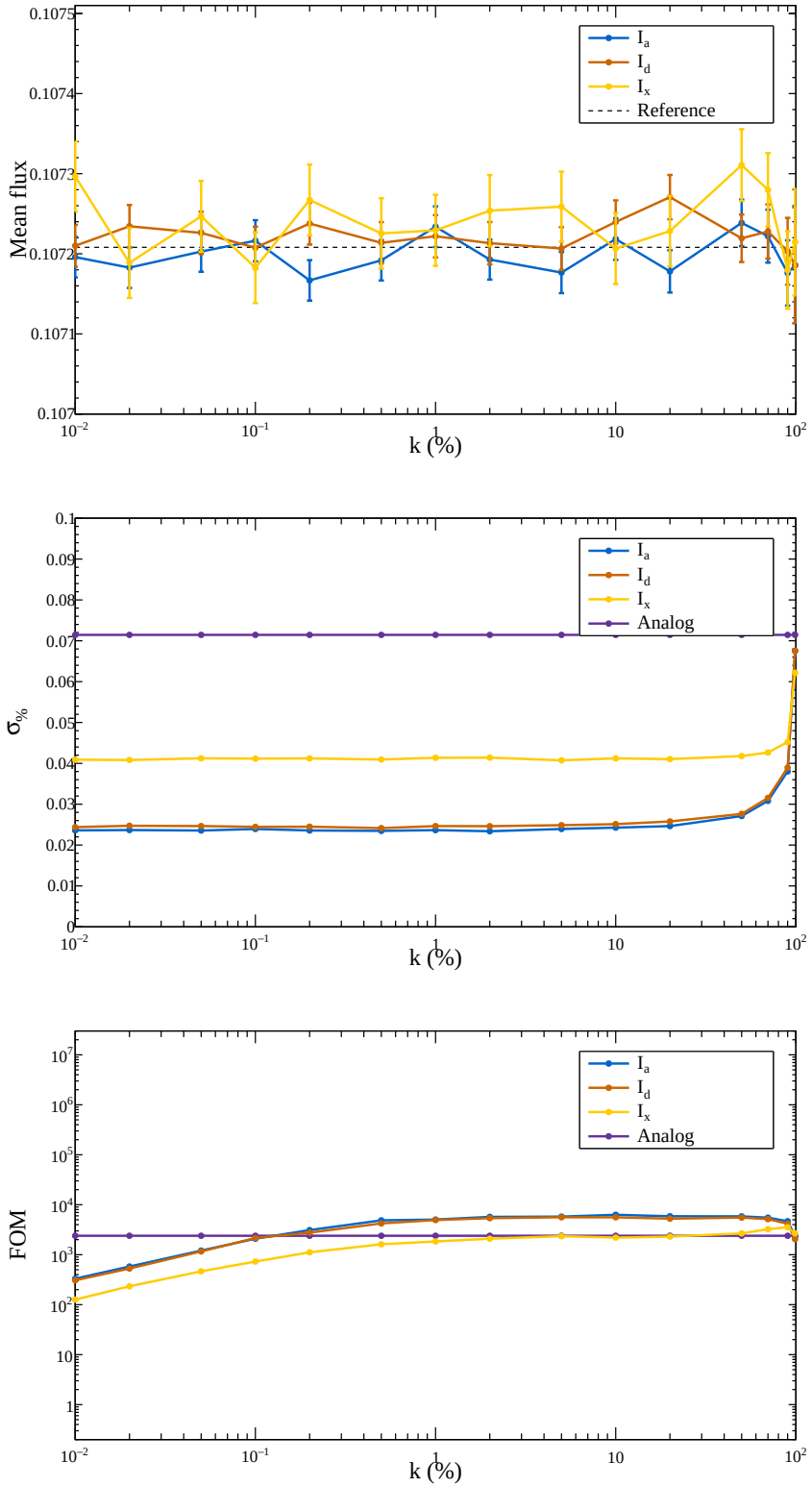

Figure 3.4. Influence of the parameter k on AMS efficiency in MENHIR. Upper to lower: mean flux with 68% confidence intervals, relative standard error, and FOM.

angular function I_a seems to slightly improve the convergence. As expected, the use of I_x is less effective.

Figures Of Merit

In the bottom plot of Figure 3.4, the FOM is represented for each AMS simulation as a function of k. For reference purposes, the FOM obtained with an analog simulation in the same configuration is also shown. As it obviously does not depend on k, the analog value remains constant over the figure. We can see that, although the errors are independent of k for values of the parameter below 50%, the figure of merit rises with k up to a plateau value around $\frac{k}{n} = 10\%$. This result is not predictable by the theory, and is most likely dependent on the simulation code and the problem geometry. However, it seems to be a systematic behaviour regardless of the importance function.

In the current setting, the I_x importance always yields less interesting results in terms of FOM than the analog simulation. This is understandable, as I_x does not accurately describe the system, preferably selecting for duplication particles that are further in the x direction. The AMS process does not help to estimate more precisely the importance of particles going in other directions. In this particular case, the result obtained is still unbiased, because particles are always close enough to the target shell to be able to reach it without requiring variance reduction techniques, and the symmetry of the problems allows even I_x to reduce the variance on the result for a given computation time. However, the error reduction does not compensate for the AMS computational cost, so that the results obtained using I_x are less interesting than the analog ones.

In the end, the computational cost of the AMS classification and resampling process is penalizing for the AMS using I_x. We can see that it is also the case for the other importance maps when k is smaller than 0.1% of the number of initial particles. Above this threshold value however, AMS is more efficient than the analog simulation, gaining up to a factor 2 in efficiency when the 10%-plateau is reached.

On the far right side of the k axis, we can see that the effect of large k on the standard error described previously seems to be somewhat smoothed on the FOM plot. The impact of information loss due to multiple replicas being resampled at once is balanced by the corresponding reduction of computation time. Indeed, large k values imply that less iterations are required to reach the detector, which saves a lot of computing time. On the other hand, each iteration requires more time to complete, as there are at least k particles to be transported per iteration, an effect that is strengthened by the partial sorting process (see Section 3.3.4), whose complexity is on average linear in k [18]. Figure 3.5 shows the mean number of iterations at which the AMS stopped, the mean duration of a single iteration as well as the computation time of batch as functions of k. We can see that the drop in the number of iterations takes precedence over the computation time per iteration, so that the simulation time is decreasing with increasing k. However,

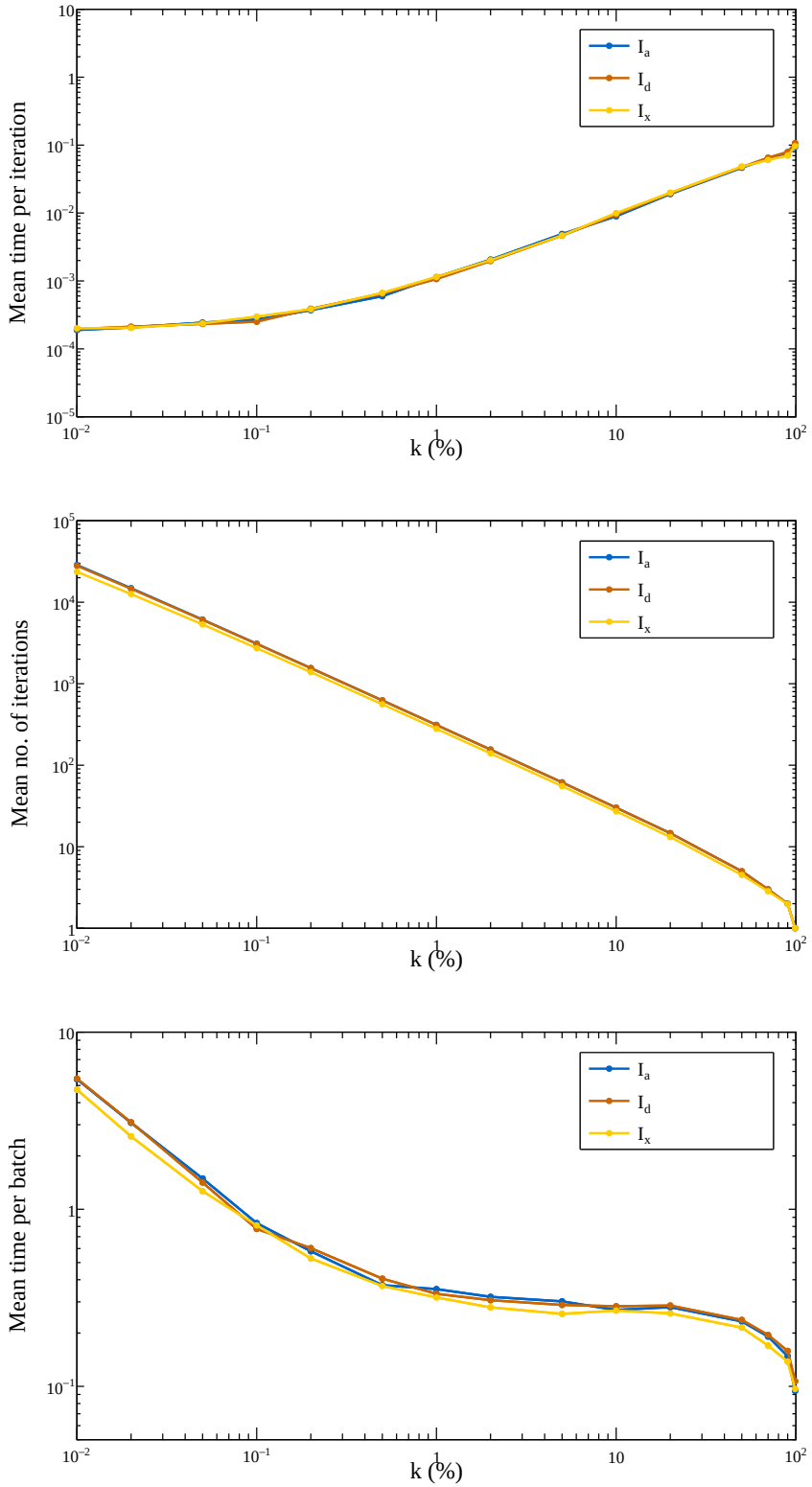

Figure 3.5. Computation time analysis in function of k. Upper to lower: mean computation time per iteration, mean number of iterations and batch simulation time.

this is not enough to counteract the increase in variance observed in Figure 3.4, so that the FOM ultimately drops when k is too high.

Summary

The main result of this analysis is that, under some conditions regarding its parametrization, the use of the AMS algorithm results in an improved estimation efficiency over the analog calculation. The AMS seems therefore to be a good variance reduction scheme for Monte Carlo particle transport simulations. As expected, the algorithm is always able to reduce the variance on the result *for a given number of batches*. However, we exhibited some cases in which the impact of AMS on the computation time makes it too slow to be able to reduce the variance for a given computation time. This might be explained by the fact that the geometry considered in this section was small enough for the analog simulation to yield converged results in a short computation time. Let us now investigate the AMS behaviour when the target shell is moved far away from the source, to the point where no analog result can be obtained in a reasonable amount of computation time.

3.4.2 Flux estimation in a shell far from the source point

In this second setting, the width of the target shell is 10 cm, and its inner boundary is placed 1 m from the source point (that is, 10 times farther than in the first case). Under these new conditions, we are going to repeat the simulations and results analysis performed previously.

Setting

We take the same properties for the medium as in the 10-cm-shell case:

$$\Sigma_t = 1\,\mathrm{cm}^{-1} \qquad \text{and} \qquad \Sigma_s = 0.9\,\mathrm{cm}^{-1},$$

which results this time in a theoretical flux

$$\phi_{ref} = 7.377 \times 10^{-21} \mathrm{particles/cm^2/s},$$

for a unitary source emitting 1 particle/s.

Analysis

The results obtained with each of the three AMS importances I_d, I_a and I_x and various k values are displayed in Figure 3.6 and 3.7. The upper frame of Figure 3.6 shows the empirical mean of the estimated flux as a function of k, with associated 68% confidence intervals. On the middle part of the figure, the relative standard error $\sigma_{\%}$ is represented, expressed in percentage of the mean flux. The corresponding Figures Of Merit are shown in the bottom frame. Figure 3.7 shows

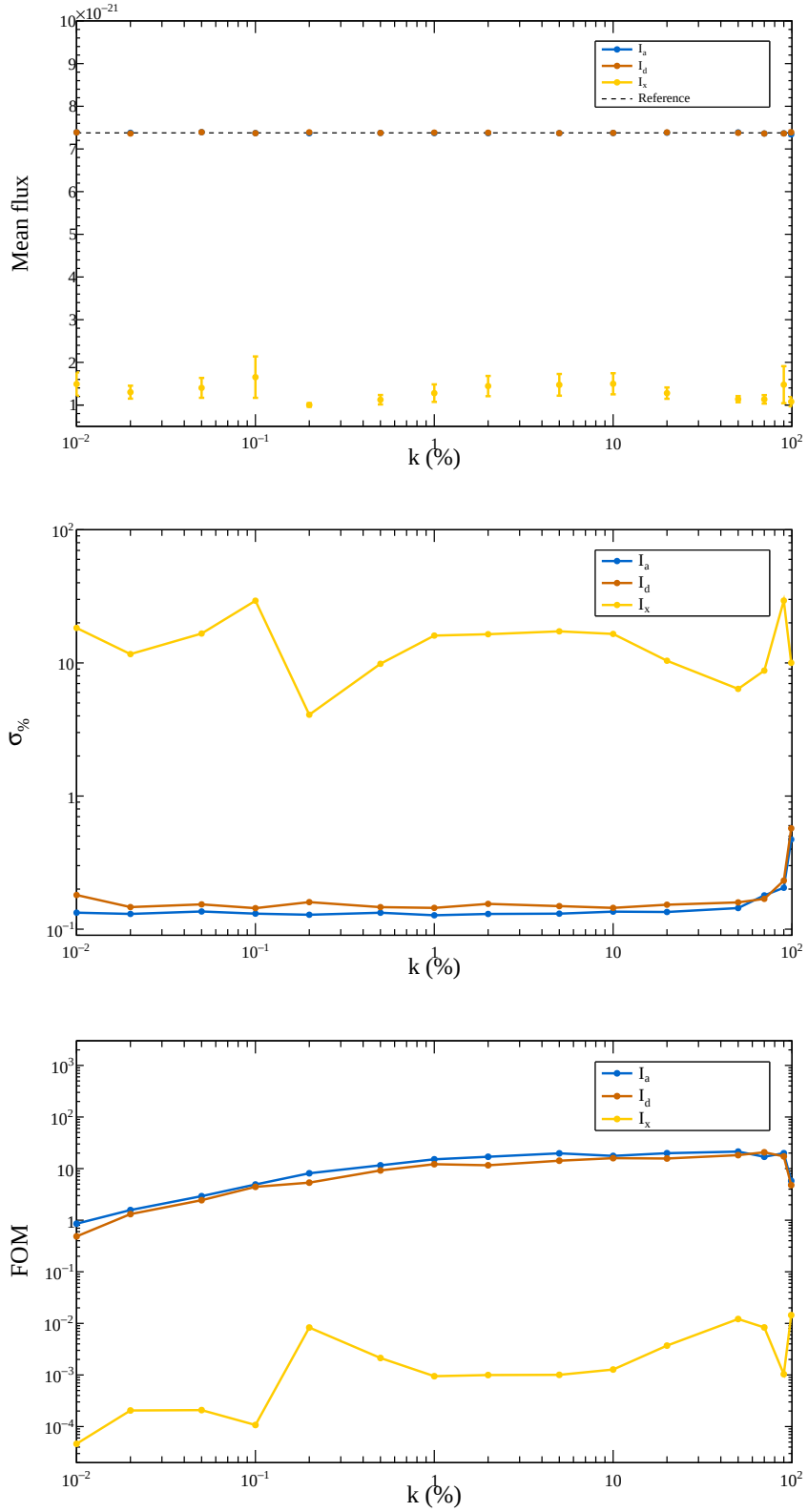

Figure 3.6. Influence of the parameter k on AMS efficiency in the 1-m-shell. Upper to lower: mean flux with 68% confidence intervals, relative standard error, and FOM.

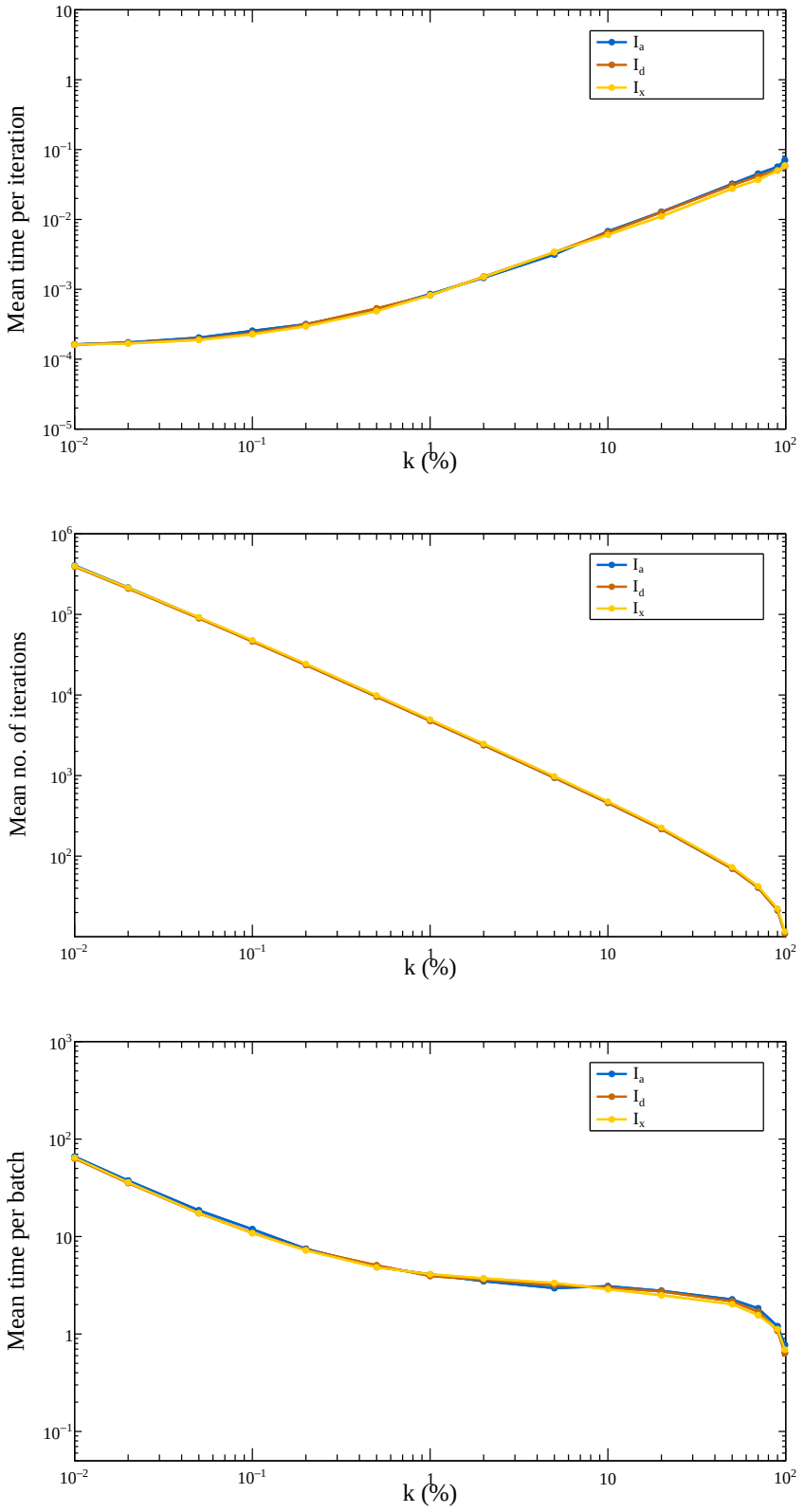

Figure 3.7. Computation time analysis in function of k for the 1-m-shell configuration. Upper to lower: mean computation time per iteration, mean number of iterations and batch simulation time.

the mean number of iterations at which the AMS stopped, the mean duration of a single iteration as well as the computation time for a batch as functions of k.

The first point to notice is that there are no analog results available for this setting. Despite simulating 10^{10} particles, not a single one reached the shell. On the other hand, two out of three AMS simulation managed to give an estimation of the flux in agreement with the reference value. Each AMS simulation consisted of 10^4 batches of 10^4 initial particles.

The importances I_d and I_a yielded both a result in good agreement with the reference value, with similar performances. The estimates obtained with those importance functions are superimposed on the top graph of Figure 3.6, so that the I_a results are behind the I_d points. On the middle graph, we can see that taking the direction into account in the importance function (I_a) tends to slightly improve the efficiency of the AMS algorithm. The shapes of the standard error (middle frame) and the FOM (bottom frame) are comparable to those obtained in the 10-cm-shell situation, and the drawn conclusions are therefore identical. Once again, a plateau can be observed for the FOM, and the value of $\frac{k}{n} = 10\%$ seems to be the more interesting parametrization of the k value. The interpretation of the Figure 3.7 is also the same as for the 10-cm-shell.

Apparent bias using I_x

The I_x importance function seems to yield biased results. In reality, the problem encountered here is a well-known phenomenon for splitting algorithms, called *apparent bias* [3, 19]. The mean flux is actually not biased, but the empirical variance dramatically underestimates the real variance. This is due to the use of an importance function that helps estimating the contribution to the flux of particles going far in the x direction, but not in the others. Therefore, in order to have a correct estimation of both the mean flux and the associated standard error, one has to wait for contributions in other directions to happen "naturally", i.e. directly from the source point at iteration zero of the AMS algorithm, as is the case for analog simulations.

In the previous situation, the target shell was close enough to the source point for particles to reach it and contribute to the estimated values. As a matter of fact, we even had analog results in that configuration. With the target shell located farther however, the probability for a particle to reach the shell from the source is so low that it would take many more particle simulations to get analog contributions to the flux. The same applies a fortiori for the AMS simulation using I_x as importance.

3.5 Conclusion

In this chapter we introduced a formulation of the AMS algorithm adapted to particle transport simulations. The MENHIR prototype has been presented, and the results obtained using this simplified transport code led to multiple observations.

First of all, we observed that the AMS algorithm can be used as a variance reduction scheme for Monte Carlo particle transport. It yields unbiased results, and in certain conditions improves the efficiency of the transport simulation.

The AMS particle transport simulations have only two more free parameters than an analog simulation:

- the number of tracks resampled at each AMS iteration (k)
- the importance function used to classify the tracks (I).

After analysing the performance of AMS for multiple choices of k and I, in two distinct configurations, we observed that the AMS efficiency increases with k up to a plateau when k reaches 10 % of the initial particles. This value seems to be the most interesting choice for k, but it is not predicted by the theory, and is most likely dependent on the problem, and on the AMS implementation in the transport code.

Concerning the importance function, we saw in this chapter that the use of an angular importance function slightly improved the AMS efficiency, however the problem that we considered is simplistic and symmetrical, so that the angular dependence of the importance function may have greater impact in other configurations. We also exhibited in Section 3.4.2 the penalizing effect of a strongly inaccurate importance function on AMS simulations. The apparent bias issue can be a source of real imprecision in the simulation results. However, we saw that it can be made visible by running multiple AMS simulations using distinct importance functions, and checking the confidence intervals overlapping.

As it has been repeatedly stressed, the geometry and physics simulated in MENHIR are very simple. Therefore, the conclusions drawn in this chapter cannot be extended to more realistic particle transport problems. However, the development of MENHIR paves the way for the AMS implementation in a real-life particle transport code.

Chapter 4

AMS in TRIPOLI-4®

The Monte Carlo particle transport code TRIPOLI-4 is currently developed in the Laboratory of Stochastic and Deterministic Transport (LTSD). The TRIPOLI family has been developed at CEA since the 60's. It is able to simulate neutron, photon, positron and electron transport in three-dimensional geometries, with a continuous energy treatment [20]. TRIPOLI-4 can be used for core physics, criticality, shielding and nuclear instrumentation applications, and already encompasses variance reduction techniques, such as Exponential Transform and Implicit Capture.

The implementation of the AMS algorithm as a new variance reduction scheme in TRIPOLI-4 represents the most important part of the work carried out during this Ph.D. This is the reason why the remainder of this thesis is devoted to presenting the implementation and characteristics of the AMS algorithm in TRIPOLI-4. We will discuss the structure and interactions of the algorithm within the transport code and then highlight the innovative alterations of the method, that allows for a wider range of applications. All along, the AMS efficiency will be tested against analog simulations and pre-existing variance reduction schemes.

In this chapter, we present the implementation of AMS in the TRIPOLI-4 code. As an industrial transport code which has various applications, the code structure is much more complex in TRIPOLI-4 than in the MENHIR prototype introduced in Section 3.3. In a first part, some details will be provided concerning the structure of the code. Then, the implementation of AMS will be described, from the iteration routine to the anchor points of the algorithm in the code and the description of the interactions between AMS and TRIPOLI-4. The final part of the chapter is devoted to the validation of the AMS implementation in TRIPOLI-4, to which end we will present the results obtained in a simple geometry and compare them to both analog simulations and pre-existing variance reduction methods.

4.1 Overview of the TRIPOLI-4 code

TRIPOLI-4 is mostly written in C++ and makes heavy use of object-oriented programming. AMS in TRIPOLI-4 interacts with three main classes of the code:

- the geometry class
- the particle class
- the response class

In the following, we will use the 'particle' term to refer to an instantiation of the corresponding TRIPOLI-4 particle class and 'geometry' to an instantiation of the geometry class.

Particle class

The particle class contains the particle type (neutron, photon, positron or electron) and the associated properties, its position, direction, energy and statistical weight, the volume and/or mesh cell in which the particle is, the status of the particle ("at source point", "entering a collision", "emerging from a collision" or "killed"), as well as a structure storing information about the last free flight of the particle: length, number of volumes crossed, corresponding cross sections, etc.

Geometry class

The geometry class stores instantiations of all volume classes composing the problem, as well as information regarding the positions of those volumes.

Response class

The response class is designed to store the contributions of particles to a score in a given volume or sum of volumes. The particle contributions are computed by a method of the response class which is directly called by the particles at various moments in the transport process. The response class is also in charge of computing mean values and associated relative standard errors on the score at the end of each batch. This step is referred to as "collecting".

4.1.1 TRIPOLI-4 simulation process

The user interaction with TRIPOLI-4 is carried out through an input file. It is a basic text file using commands in a dedicated language in order to define the geometry, the compositions of the materials present in the geometry, the characteristics of the sources, the scores and all the parameters of the simulation (number of batches, number of particles per batch, variance reduction schemes, etc.). Once the input file has been read, the simulation begins.

The purpose of this section is to introduce the context for the implementation of AMS in TRIPOLI-4. The description carried out here is therefore restricted to the analog simulation process of neutrons for shielding applications. Furthermore,

the AMS algorithm introduced earlier is unable to take branching processes into account. This particular issue will be discussed in the last chapter of this thesis. For pure-neutron simulations though, TRIPOLI-4 can handle multiplying collisions by taking into account neutron multiplicity in the particle weights.

Batch simulation

At the beginning of each batch, a vector holding all the source neutrons for the entire batch is created. Particles are extracted one after the other from this vector, and transported until it is absorbed or leak out of the geometry. During the neutron transport, the response class is called after each neutron flight and after each collision, storing the contributions associated to those events if there are any.

Once the source vector has been emptied, the response class collects the value associated to the whole batch, updates the average score and the associated standard error over all completed batches, and dumps the current result to the output file. The simulation stops when the number of simulated batches meets the number of batches asked by the user in the input file.

Analog neutron transport process

Once a neutron is extracted from the source vector, its transport is simulated as a succession of free flights and collisions in the medium until the neutron is absorbed or leaks out of the geometry. Let us now describe the standard transport process for the analog simulations of neutrons.

The free flights are sampled according to the following displacement kernel [20]:

$$T(\vec{X} \rightarrow \vec{X}', \vec{\Omega}, E) = \Sigma_t(\vec{X}', E) e^{-\int_0^{|\vec{X}'-\vec{X}|} \Sigma_t(\vec{X}+s\vec{\Omega},E)ds}, \tag{4.1}$$

where $\Sigma_t(\vec{X}, E)$ is the macroscopic total cross section at position $\vec{X}$ and energy E, which is given by the geometry class.

If the sampled flight length is short enough for the neutron to remain inside the geometry boundaries, the neutron is moved to the collision site. After the particle displacement, the response class is called to compute and memorize any contributions to the score, if the last flight went through the target volume. Then the collided nuclide is sampled and the collision type selected. If the neutron is not absorbed, the energy and direction of the neutron emerging from the collision are computed. For reactions with multiple outgoing neutrons, *only one* neutron is simulated, the multiplicity of the reaction is taken into account in the outgoing-neutron weight.

4.1.2 Importance map generation

As briefly discussed in Section 2.3, TRIPOLI-4 has a built-in module called INIPOND that automatically pre-computes importance maps for the Exponential Transform variance reduction technique. The importance maps provided by

this module can be of interest for AMS use as importance function.

The INIPOND module has been specifically developed for TRIPOLI as early as 1990 [14]. It has been optimized for the use of the Exponential Transform technique, and extensively discussed in [13] and [21]. Its purpose is to quickly compute an approximate solution of the adjoint problem on a spatial and energy mesh defined by the user. Given a spatial detector $\mathcal{D}$, the importance function is assumed to be factorized in spatial, angular and energy parts:

$$I(\mathbf{X}, \mathbf{\Omega}, E) = I_s(\mathbf{X}, g) \times I_a(\mathbf{X}, \mathbf{\Omega}, g) \times I_e(g), \tag{4.2}$$

where g denotes the energy group containing E.

The three parts of the importance are evaluated as follows:

$$I_s(\mathbf{X}, g) = \exp\left(- \int_0^{dist(\mathbf{X},\mathcal{D})} K(\mathbf{X} + r.\mathbf{\Omega_0}, g) dr \right), \tag{4.3}$$

$$I_a(\mathbf{X}, \mathbf{\Omega}, g) = \frac{\Sigma_t(\mathbf{X}, g)}{\Sigma_t(\mathbf{X}, g) - K(\mathbf{X}, g)\mathbf{\Omega}.\mathbf{\Omega_0}}, \tag{4.4}$$

$$I_e(g) = \frac{1}{\beta + 1} \frac{(E^g_{sup})^{\beta+1} - (E^g_{inf})^{\beta+1}}{E^g_{sup} - E^g_{inf}}, \tag{4.5}$$

where Σ_t is the total macroscopic cross section and $\mathbf{\Omega_0}$ the direction of interest (related to the slope of the importance map). The values of K are assumed constant for each material and each energy group, and are either derived from a Placzek-like equation as described in [14], or set by the user. E^g_{inf} and E^g_{sup} denote the bounding values for energy group g, and the β parameter is set by the user in order to adjust the global strength of the biasing and define the energy profile of the importance map at the detector.

The INIPOND module can also compute the importance for a problem figuring multiple detectors, in which case a weight is associated to each detector and the importance at a given point is defined as the weighted sum of the importance for each detector. More details concerning the construction of the importance map by the INIPOND module can be found in Appendix B.

4.2 AMS implementation

This section is devoted to the description of the AMS implementation in TRIPOLI-4 for neutron shielding simulations. The purpose is to describe how the AMS algorithm is integrated in TRIPOLI-4: the interactions between the AMS algorithm and the rest of the code, as well as the anchor points of the method in TRIPOLI-4. The use of AMS is activated through the use of dedicated

commands in the input file, which toggles a control flag in the code. The syntax of the AMS commands in the TRIPOLI-4 input file are detailed in Appendix C.

The implementation of AMS in TRIPOLI-4 was intended to optimize the algorithm efficiency while remaining as non-intrusive as possible.

4.2.1 The AMS Manager

In order for the AMS-related methods to remain as independent as possible from the rest of the code, a new class has been implemented. The AMS Manager handles all AMS parameters, variables, and methods, so that each interaction of TRIPOLI-4 with the AMS algorithm is carried out by a simple call of an AMS Manager method.

Tracks and points

The main ingredient for AMS is the track structure needed to store neutron histories. The AMS Manager holds a vector of tracks, each of which consists of a vector of points and an importance value. The data structure of the track class is represented in Figure 4.1.

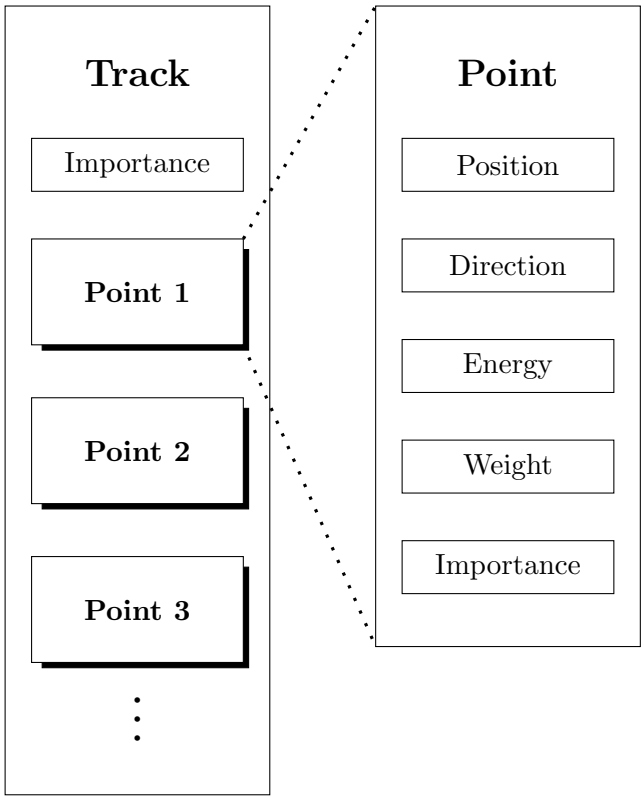

Figure 4.1. Data structure of the track class.

The track points contain all the information required for the particle class to be able to restart the transport process. This is mandatory for the AMS resam-

pling step, in which splitting points are used as starting points of new neutron histories. Keeping the resampling process in mind, each point should also carry an importance value that will be used to define the splitting point. The minimum content of the point class is therefore:

- the position in space (three floating-point numbers)
- the direction (three floating-point numbers)
- the energy
- the statistical weight
- the importance value

Building neutron tracks

Assuming that the AMS is activated, the AMS Manager empties the tracks vector at the beginning of each batch. The Manager is then called by the particle class once *before* each free flight displacement. The Manager computes the local importance I_S of the neutron, which depends on the importance function and the neutron's position, direction and energy. Then the Manager checks the neutron's status. If the status is "at source point", a point holding every information about the source point is created, added to a new track whose importance is set to I_S and the track is appended to the tracks vector.

If the neutron status is "about to fly", the neutron's track already exists (it is the last track of the tracks vector). In that case, the last free flight of the neutron is examined in order to determine whether or not it crossed the target boundary. If so, a crossing point is created with the coordinate the neutron had when it crossed the target boundary, and appended to the track with importance `DBL_MAX` ($\sim 1.797\,69\text{E}308$).

If the neutron's importance is less than `DBL_MAX`, the importance I_P of the point emerging from the collision is computed. If I_P is strictly greater than the track importance, a new point is created and added to the last track of the tracks vector, whose importance is then set to I_P.

The set of tracks obtained with this procedure is consistent with the description of "tracks of increasing importance" made in Section 3.2.4. In addition to the attributes of the point class, all the information required by the AMS algorithm is available.

End of the analog simulation

The AMS algorithm does not interfere in any way with the transport and scoring process. Therefore, the only difference between an AMS and a regular TRIPOLI-4 simulation at the end of the last neutron transport of each batch is the state of the AMS Manager and of its tracks vector.

Once the analog batch simulation of n neutrons is complete, TRIPOLI-4 usually calls the response class to collect the score. If the AMS is used however, this step is bypassed, the score remains as-is and the AMS Manager is called to launch the iteration process. Before the iteration process begins, the global weight W of the AMS algorithm is set to 1.

AMS iterations

The AMS Manager builds a vector holding only the importances of the n simulated tracks, and determine the splitting level using the C++ *nth_element* function on this vector(see Section 3.3.4). If the splitting level value is less than `DBL_MAX`, the Manager cycles through the tracks vector and erases every track whose importance is less than *or equal to* the level. The purpose here is to keep an array containing only the survivor tracks in order to simplify the sampling procedure for the duplication process later on.

The removal of elements from the tracks vector is performed using a swap-and-pop technique: the element to erase is swapped with the last element of the vector and then popped out. Swap-and-pop prevents the costly moving of elements resulting from a standard erasing function that preserves the sequence order, which is of no interest in our case. The number of erased tracks K_{pop} is used to update the AMS global weight:

$$W \leftarrow W \times \left(1 - \frac{K_{pop}}{n}\right). \tag{4.6}$$

Once the tracks vector has been purged of tracks having an importance less than the splitting level, K_{pop} new neutrons are simulated by duplicating some of the survivor tracks.

Neutron resampling

For each of the deleted neutrons, a new track has to be created and appended to the tracks vector. Therefore, each of the tracks selected for duplication have to be sampled among the first $n - K_{pop}$ tracks of the vector. Each selected track is then navigated through to find the first point whose importance is strictly larger than the splitting level. The AMS Manager creates a new track containing the splitting point, appends it to the tracks vector and instantiates a new neutron which properties are given by the splitting point's attributes. The new neutron status is set to "about to fly", and the standard TRIPOLI-4 transport method for analog neutrons is called.

Throughout the transport process, the new neutron tracks are built in the exact same way as the analog tracks at iteration 0, by adding the points of increasing importance to the last track of the tracks vector. Any neutron passing through the target area generates a contribution to the score, which is computed and stored by the response class with a weight of 1 as usual, since the final AMS

global weight remains unknown until the end of the iterating process.

Scores collect

Once the AMS algorithm stops iterating, the response class is directly called by the AMS Manager to collect the score, i.e. to add up the contributions stored during all iterations, and multiply the result by the final global AMS weight W. The computation of the average score value over past batches and the associated standard error is then performed.

4.2.2 Pre-collision AMS algorithm

Up to this point, we always considered particle tracks that were composed of the particles coordinates coming out of the collisions. Yet, the sequences of pre-collision coordinates are also discrete Markov chains, on which the AMS algorithm could be used. The AMS implementation has however to be slightly altered, and the use of importance maps taking the particle directions into account becomes irrelevant.

This option is toggled by a designated command in the TRIPOLI-4 input file. The importance of points are estimated before each collisions and appended to the particle tracks if their importance exceeds the track's one. When a particle is duplicated, the resampled particle starts its transport by a collision instead of a flight. Otherwise nothing changes in the simulation process.

When splitting a particle track, the regular AMS algorithm duplicates the splitting point and samples a new flight length, whereas the pre-collision algorithm does not duplicate the particle direction, and resamples the collision. The use of a pre-collision algorithm can be either advantageous or disadvantageous, depending on whether or not a given particle importance is correlated with its direction.

The efficiency of the pre-collision AMS is therefore highly dependent on the importance function definition. If the importance correctly takes into account the particles directions, it will presumably be more suitable for the regular AMS algorithm. This option of the AMS algorithm in TRIPOLI-4 will therefore be tested in several cases in the following.

4.2.3 Importance functions

Spatial importance functions

The AMS implementation in TRIPOLI-4 allows for the use of purely spatial importance functions, which do not take angle and energy coordinates into account. The geometry is provided with a spatial object S, which can be a point, a line, a ring or a simple 3D-surface (plane, cylinder or sphere). The chosen object is defined in the TRIPOLI-4 input file as follows:

- Points are defined by three spatial coordinates.

- Lines are defined by a point and a direction vector.

- Rings are defined by a radius, a point (position of the ring center) and a vector (direction of the ring axis)

- Planes are defined by a point of the plane and a normal vector

- Spheres are defined by a point (position of the sphere center) and a radius

- Cylinders are defined by a line (axis of the cylinder) and radius

Once the object of interest S has been defined, the importance can be computed at any point of the geometry as a function of the distance to S. The computation of the spatial importance is carried out on-the-fly by the AMS Manager whenever the importance of a particle is requested. Two distinct importance functions are available: either the importance decreases with the distance to S, so that particles are "attracted towards" S, or the importance increases with the distance to S, so that particles are "pushed away" from S. The desired importance is defined by a dedicated command in the input file.

If we denote by I_S and $I_{\bar{S}}$ the attractive and repulsive importance functions, their values at any point $(\mathbf{X}, \mathbf{\Omega}, E)$ within the geometry are given by:

$$I_S(\mathbf{X}, \mathbf{\Omega}, E) = \frac{1}{dist(\mathbf{X}, S)} \tag{4.7}$$

and

$$I_{\bar{S}}(\mathbf{X}, \mathbf{\Omega}, E) = dist(\mathbf{X}, S). \tag{4.8}$$

"PATH" importance function

In order to take into account a priori knowledge of preferential pathways, the AMS can be provided with an ordered sequence of spatial points $P_0, \ldots, P_N$, which are used by the code to create a so-called *path*. In that case, the importance for a point X depends on the orthogonal projection $P(X)$ of X on the path. If we denote by $[P_p, P_{p+1}]$ the segment on which $P(X)$ is located, we define the importance at point X as

$$I_S(\mathbf{X}, \mathbf{\Omega}, E) = \sum_{i=0}^{p-1} [dist(P_i, P_{i+1})] + dist(P_p, P(\mathbf{X})) - dist(\mathbf{X}, P(\mathbf{X})), \tag{4.9}$$

so that the importance increases along the path and decreases with the distance to the path.

INIPOND importance map

As discussed in Section 4.1.2, TRIPOLI-4 has a module called INIPOND that pre-computes importance maps for the Exponential Transform variance reduction scheme. As an approximation of the adjoint score of the problem, it gives for a particle with coordinates $(\vec{X}, \vec{\Omega}, E)$ an estimate of its average contribution to the score. It is therefore a good candidate as importance for AMS.

We denote by I_6^+ the six-dimensional importance computed by INIPOND. The INIPOND parameters are defined in the TRIPOLI-4 input file as for regular simulations resorting to variance reduction. This allows the AMS Manager to simply call the INIPOND module during the simulation to get importance values. The default importance returned by the module takes into account the particles positions, directions and energy. However, the spatio-energy and angular parts are calculated separately in the code, so that it is possible to ask the INIPOND module to provide only the non-angular part, which we denote by I_4^+.

The non-angular importance I_4^+ can be seen as an approximation of the *pre-collision* adjoint score. It is indeed computed for any point P, under simplifying assumptions, as an estimation of the average score generated by a particle entering a collision at point P.

This makes I_4^+ an interesting importance function to be used for the pre-collision AMS algorithm (See Section 4.2.2), which precisely needs to classify particle tracks according to their pre-collision importances.

Volume importance weighting

Regardless of the importance function, each region of the geometry is attributed a weighting factor, which is used to weight the importance of any point within the region. This allows the user to increase or decrease the importance region by region, giving more flexibility in the importance construction. This feature can be particularly helpful when using spatial importance functions. All volumes of the geometry have a default importance weight $w_V = 1$, which can be modified in the TRIPOLI-4 input file.

4.3 Validation of AMS in TRIPOLI-4

4.3.1 Bypass geometry

The system chosen to test the AMS implementation in TRIPOLI-4 consists in an extruded box filled with Helium-4 (10^{24} atom per cm^3), with leakage boundary conditions. The dimensions of the box are 10 cm × 10 cm × $+\infty$. A neutron flux is produced from a 2 MeV isotropic neutron source at one corner of the box and detected inside an infinite cylinder of 1 cm in diameter placed at the opposite corner. Between the source and the detector is placed a highly absorbent high density cylinder composed of Boron-10 (10^{25} atoms per cm^3). A top view of the

problem geometry is represented in Figure 4.2.

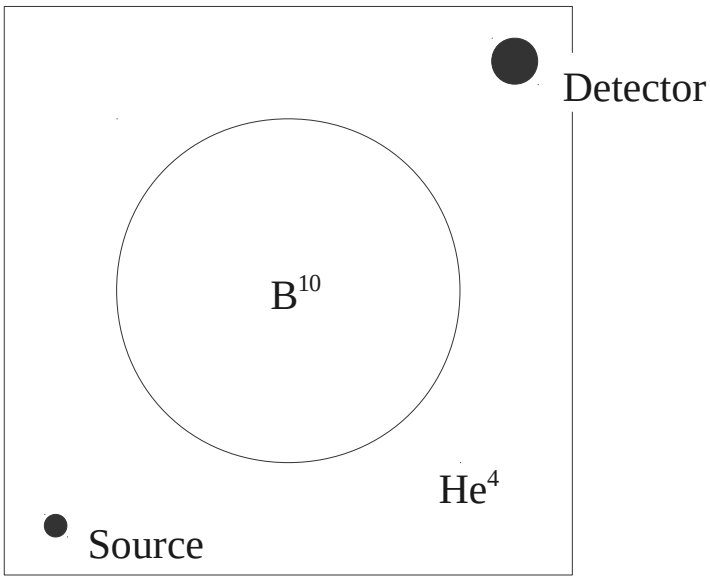

Figure 4.2. Geometry for the bypass problem.

The cross sections used for this simulation are provided by the nuclear data library JEFF-3.1.1, which is the reference evaluation in TRIPOLI-4.

4.3.2 Objectives and setup

The purpose of the bypass problem study is to test the validity of AMS as a variance reduction scheme for TRIPOLI-4. In a first part, we will test the AMS algorithm results and efficiency against analog results. We will then reproduce the sensitivity analysis performed for MENHIR in Section 3.4, in order to test in this new context the impact of the importance function and of the proportion of resampled particles per batch. Finally, we will compare results obtained by TRIPOLI-4 with AMS and with the Exponential Transform.

The challenge for the simulated neutrons in this problem is to successfully bypass the Boron cylinder while staying away from the geometry where they could leak out. To illustrate the high probability of absorption of the high density Boron in the thermal and epithermal energy ranges, we show in Figure 4.3 the total, scattering and absorption cross sections for the Boron element.

In the remainder of this section, three distinct functions will be used as importances for the AMS algorithm:

- the purely spatial importance function I_S, defined for each point as the reciprocal of the distance to the target cylinder (see Section 4.2.3)
- the 6-dimensions importance map I_6^+ computed by the INIPOND module (position, normalized direction, energy)

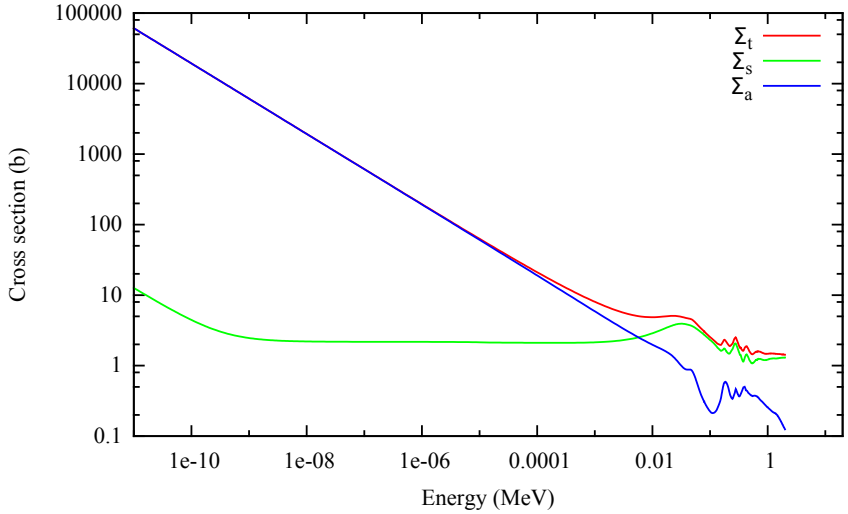

Figure 4.3. Total, scattering and absorption cross sections for the Boron-10 isotope.

- the non-angular 4-dimensions part I_4^+ of the importance map computed by INIPOND (position and energy only) with the pre-collision version of the AMS algorithm (see Section 4.2.3)

The values and gradient of the INIPOND map I_6^+ are represented in Figure 4.4. We can see that the automated module was able to determine the preferential pathways around the Boron cylinder, both in terms of scalar importance and of preferential directions.

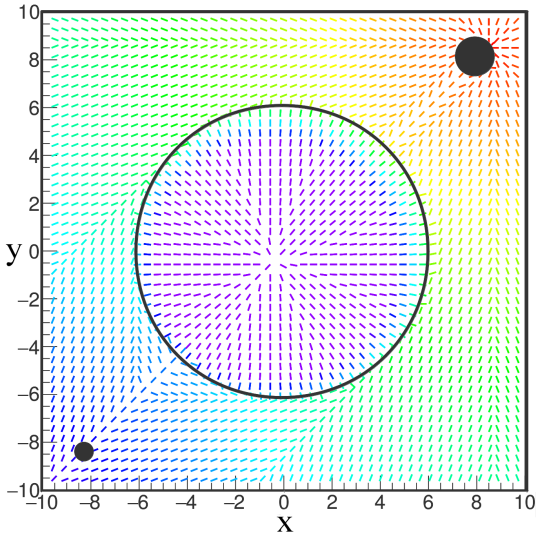

Figure 4.4. Scalar value and gradient of the importance map I_6^+ generated by INIPOND for the bypass problem, restricted to the first energy group.

4.3.3 Neutron tracks in the bypass geometry

We show in Figure 4.5 all the tracks obtained during the AMS iterations. The algorithm was initialized with a set of 20 analog neutron tracks shown in Figure 4.5a. As the neutrons cannot be absorbed by Helium nuclei, all tracks terminate either by leaking out of the geometry or by being absorbed in the Boron cylinder.

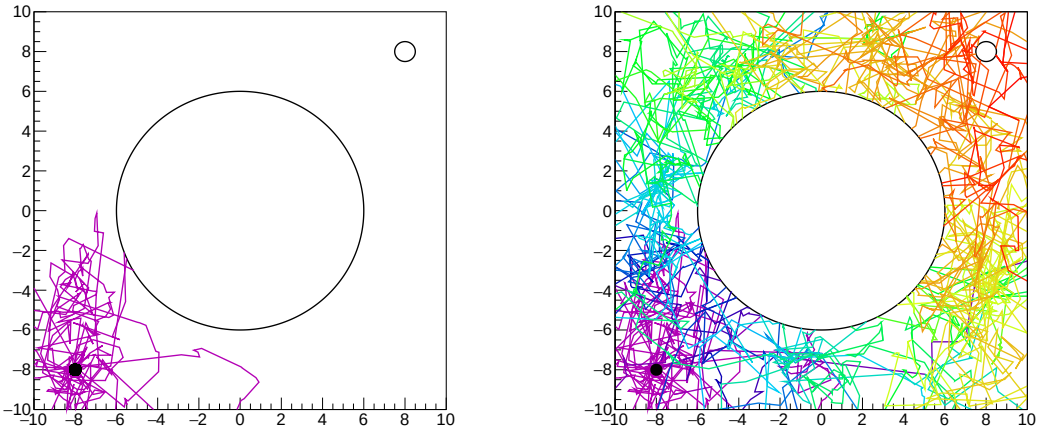

(a) Initial set of analog neutron tracks before the first AMS iteration

(b) Resampled tracks colored by iteration number (0 to 143)

Figure 4.5. Representation of all tracks simulated during an AMS batch in the bypass geometry.

In Figure 4.5b, we show the tracks resampled at each iteration of the AMS algorithm. In this example, $k = 1$ track was resampled per iteration. We can see that as the AMS algorithm iterates, the resampled neutron tracks are getting ever closer to the detector, coming around the Boron massive. After 143 iterations, all the 20 neutron tracks have reached the detector and the algorithm stops.

4.3.4 Impact of the k parameter

All results presented here are issued from simulations of 10^4 batches of 10^4 particles each (meaning $n = 10^4$ particles for each of the 10^4 AMS calculations).

For each of the three AMS importances I_S, I_6^+ and I_4^+, we performed simulations for various k values between $k = 1$ (0.01% of the initial particles) to $k = 9900$ (99% of the initial particles). The results obtained are summed up in Figure 4.6. In this figure, we represent on the upper plot the empirical mean of the estimated fluxes as a function of k with associated 68% confidence intervals. The middle part of the figure shows the relative standard error $\sigma_{\%}$, expressed in

percentage of the mean flux, and the bottom one the Figure Of Merit:

$$FOM = \frac{1}{\sigma_{\%}^2 \times t}. \tag{4.10}$$

We observe that all the confidence intervals obtained with AMS overlap. This is in agreement with the fact that AMS yields an unbiased estimator of the flux for any combination of k and importance function. The estimated fluxes are also in agreement with the analog calculation, for which the standard error is larger for the same number of initially simulated particles. In the middle frame of Figure 4.6, we can see that the standard errors in all AMS simulations with importance I_6^+ are overall smaller than with I_4^+, which are smaller than with I_S. This is in accordance with the expected behaviour of the AMS algorithm, since I_4^+ takes into account both the geometry and the neutron energies and I_6^+ adds a directional dependence.

Concerning the impact of the k parameter, we can see in the bottom part of Figure 4.6 the shapes of the FOM for the three importance functions. Two of the FOM exhibit the same behaviour as previously seen in MENHIR simulations (see Section 3.4). The AMS efficiency increases with k up to a plateau before dropping as k becomes too high. However, the limit at which the FOM becomes stable seems to be $\frac{k}{n} \sim 1\%$. This value is lower than the one obtained in the study performed with MENHIR, which lead to a plateau at $\frac{k}{n} \sim 10\%$. As there is no theoretical explanation for this plateau phenomenon, we can only guess that this difference is either an effect of the AMS implementation or of the considered problem.

Furthermore, we can see that the plateau on the FOM plot in the case of the I_4^+ importance is almost non-existent. Looking closely enough, we observe a plateau even in this case, which is reached for $\frac{k}{n} \sim 2\%$. However the FOM drop for lower k values is far less steep than for other importance maps. This is a side effect of the use of a discretized *and* non-angular importance map. Indeed, every particle located in a given cell of the geometry and in the same energy bin will have the same importance, since their directions are not taken into account. Therefore, many tracks can have the same importance value, so that more than k particles are resampled at each iteration (see Section 2.6.4). In this view, the simulations with the lowest k values do not in practice resample k particles per iteration but actually more than k.

On the FOM plateau however, the efficiency reached for each of the INIPOND importances is very similar. This is an important result, as it shows that the pre-collision AMS algorithm using I_4^+ as importance is as efficient as the regular AMS algorithm with I_6^+. We saw that the variance obtained with I_6^+ was slightly smaller than with the pre-collision algorithm. However, this difference is compensated by the fact that the pre-collision uses a non-angular importance map, so that more than k particles are actually resampled at each iteration of the algorithm.

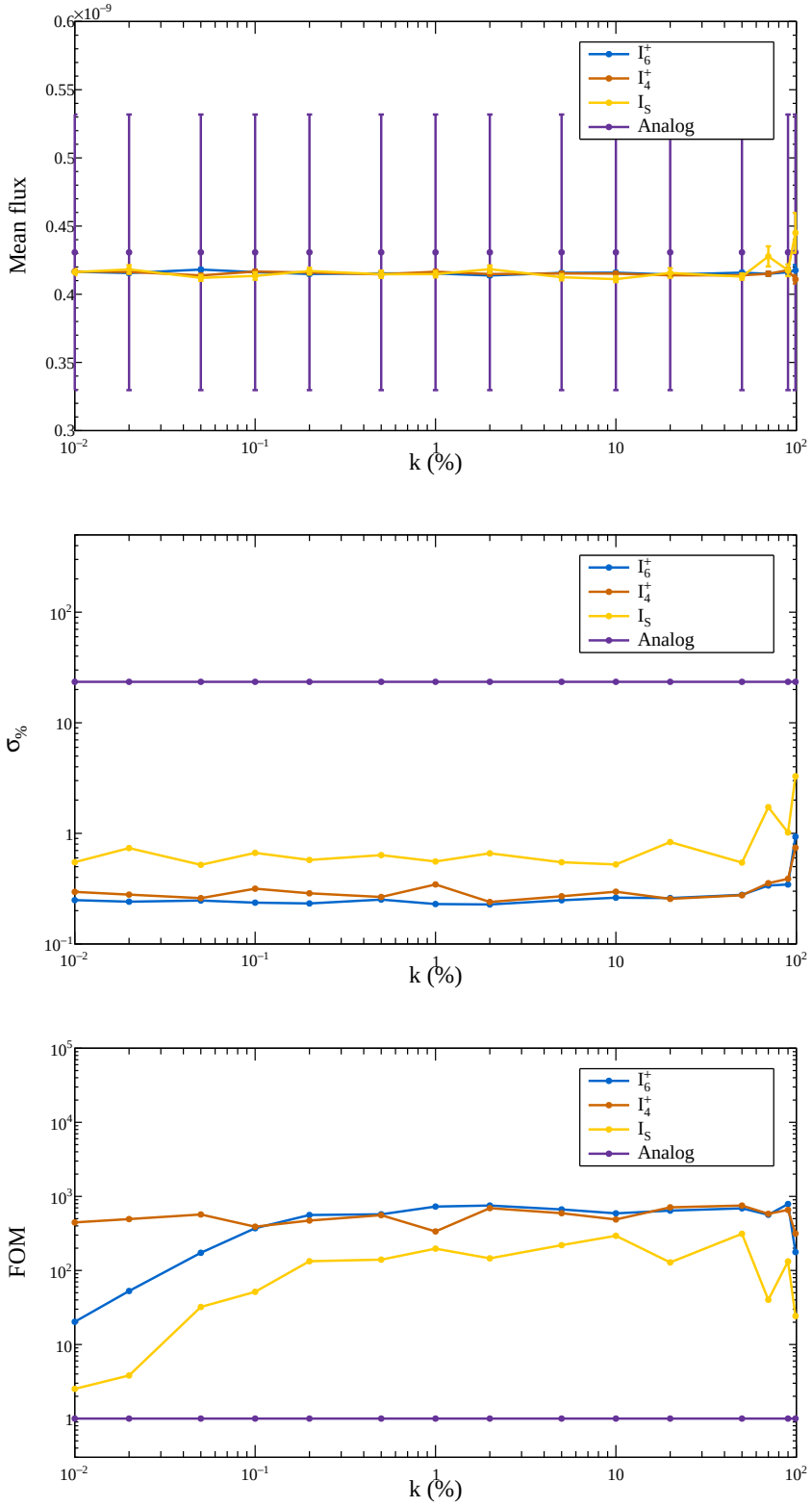

Figure 4.6. Influence of the parameter k on AMS efficiency in TRIPOLI-4 for the bypass problem. Upper to lower: mean flux with 68% confidence intervals, relative standard error, and FOM normalized by the analog FOM.

In order to compare AMS efficiency with regards to the analog calculation, we look at the value of the FOM plateau for each importance function. We can see that the AMS FOM is 200 times larger than the analog FOM with I_S and around 600 times with both I_4^+ and I_6^+. All of the importance functions yield very interesting results in terms of FOM gain, making AMS an interesting variance reduction scheme for TRIPOLI-4. Unlike in the results obtained with MENHIR (see Section 3.4), there is no combination of k and I for which the AMS is less efficient than the analog calculation. As the attenuation is much greater than in the MENHIR's case, the time spent for ordering and resampling is more useful to the simulation. Let us now compare AMS results to other variance reduction techniques in this configuration.

4.3.5 Comparison to the Exponential Transform method

Introducing a new variance reduction method into TRIPOLI-4 raises the concern of comparing its efficiency against pre-existing techniques. The reference variance reduction method in TRIPOLI-4 is the *Exponential Transform* technique, already discussed in Section 2.3, to which the INIPOND module of importance maps pre-calculation is originally dedicated. We launched a simulation using the Exponential Transform method on the bypass problem alongside an analog simulation, two regular AMS simulations (I_6^+, I_S) and a pre-collision AMS (I_4^+). The resampling proportion for the three AMS simulations was set to $k = 1\%$ of the initial number of particles per iteration.

For this comparison, we ran the 5 simulations for the same amount of computational time, recording the flux estimation at regular intervals. We show in Figure 4.7 the convergence of the mean flux estimators, with the relative standard errors and associated Figures Of Merit. In the top plot of the figure, the dotted lines represent the evolution of the mean flux values, while the full lines represent the evolution of the upper and lower bounds of the 68% confidence intervals.

Despite the gain in FOM of AMS over the analog simulation, we observe that the Exponential Transform (E.T.) yields even more interesting results. The best AMS efficiency turns out to be 10 times lower than E.T.

On the middle plot of Figure 4.7, we can see that the AMS estimation of the flux is impaired by several jumps in the standard error. These jumps are a consequence of some realizations of the AMS algorithm that yield a large estimate of the flux. They have an impact on the mean flux estimation but a greater impact on the error estimation.

The AMS simulation using the spatial importance I_S exhibits no jumps, however we can see in the top frame of Figure 4.7 that the mean flux obtained with importance I_S is somewhat underestimated (though it remains in the confidence interval of the other simulations). Therefore, if the simulation ran longer, a large contribution would certainly have arrived and the error would have jumped.

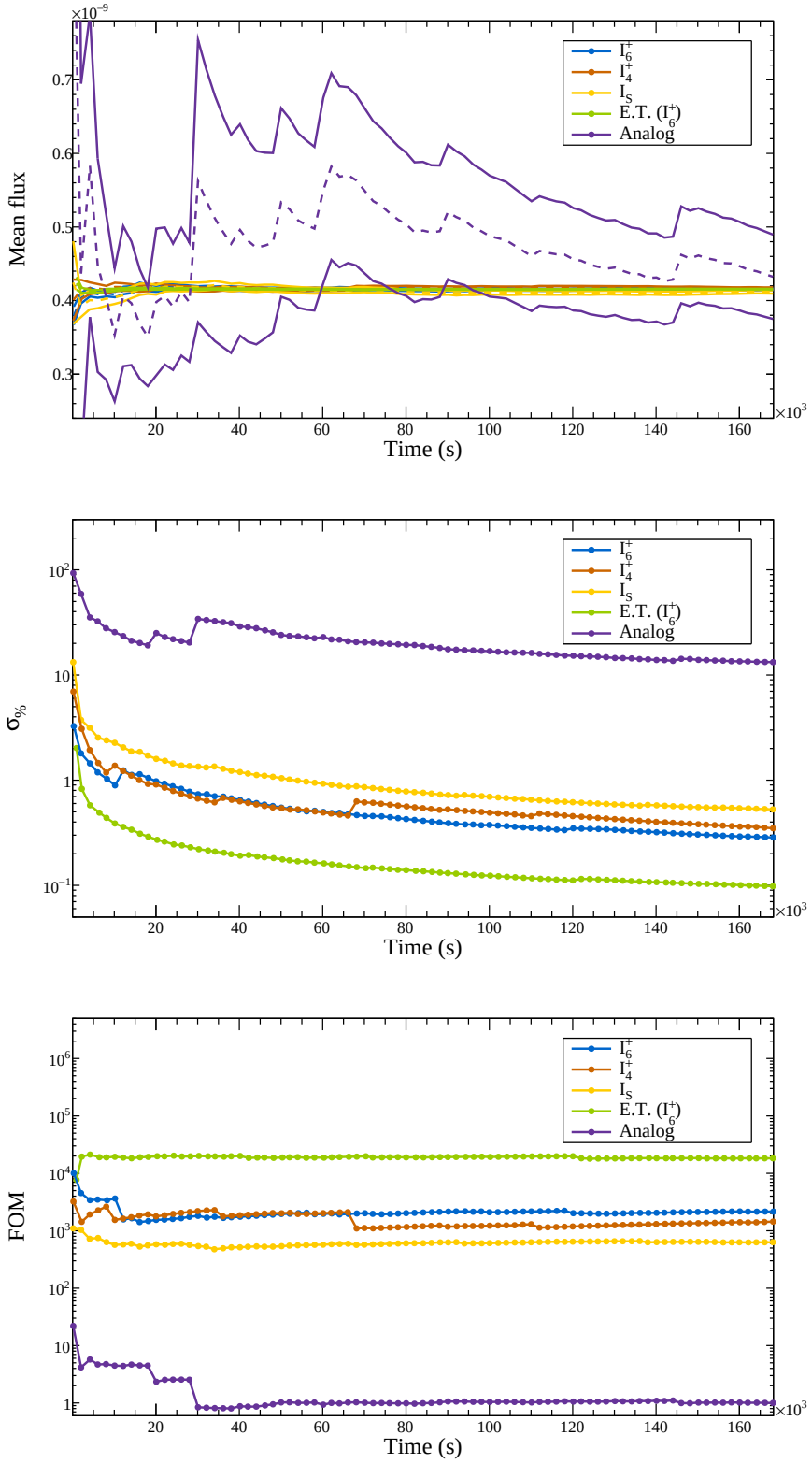

Figure 4.7. Convergence of AMS, analog and Exponential Transform simulations as a function of the computation time for the bypass problem. Upper to lower: mean flux with 68% confidence intervals, relative standard error, and FOM normalized by the final analog FOM.

If a single contribution has a strong impact on the mean value, then the associated rare events are under-represented during the AMS simulations. This happens if the importance function is not able to determine the actual interest of some tracks for the estimation of the flux. The presence of these jumps is consequently a quality indicator of the chosen importance function. This is also true for the Exponential Transform method. In this particular case, the standard error curve obtained with E.T. does not present any jump. We can therefore assume that the INIPOND module was able to provide an importance function that was well suited for E.T. use, but less adapted to AMS.

It should be kept in mind that an absence of variance jump is no insurance that the simulation parametrization is optimal. As it is the case here with AMS and the spatial importance I_S, it is usually impossible to know if the number of performed batches is large enough to have an accurate estimation of the score. The AMS robustness with regards to the importance function provides the possibility of trying multiple importances and ensure that the confidence intervals overlap, thus increasing the reliability of the estimated score.

4.4 Conclusion

The implementation of the Adaptive Multilevel Splitting into TRIPOLI-4 has been performed with a minimal impact on the surrounding code. The implementation of a new class to interface AMS with TRIPOLI-4 and handle the entire AMS processes permitted to limit the intrusions in other classes of the code.

The AMS algorithm implemented in TRIPOLI-4 is controlled through commands in the input file, in the same manner as for other modules of TRIPOLI-4. It allows for an easy use and comparison of various geometric importance functions, as well as the importance maps provided by the INIPOND module, initially designed for the Exponential Transform method.

The study of the Bypass problem presented in the last section of this chapter puts once again into light the robustness of the AMS with regard to the parameter k and the importance, since the obtained result are always unbiased. Furthermore, the AMS results are very interesting in terms of FOM by comparison with the analog results, which makes AMS a legitimate variance reduction scheme for TRIPOLI-4.

The efficiency of this new method has been tested against the reference variance reduction method of TRIPOLI-4, namely the Exponential Transform. For the same computation time, the error on the score estimated using the Exponential Transform method was approximately three times less than the best AMS results. The problem considered here was complicated enough for the variance reduction schemes to have a visible effect on the estimation efficiency. However, this was still a toy model. We will present in the following some results in more realistic configurations.

One of the downside of the AMS algorithm is the computation time overhead due to the simulation of thousands of neutrons between the source and the detector during the iterating process, even though most of those particles do not contribute to the final score. However, they may contribute to responses outside of the target volume, for example fluxes in volumes between the source and the target area. Those quantities could be estimated alongside the target response in *a single* AMS simulation, provided that the AMS algorithm is able to assign the proper weight to each of the contributions. The unbiased estimation of scores outside of the target area is the subject of the following chapter.

Chapter 5

On-the-fly scoring with AMS

The AMS iteration process implies the simulation of many neutrons between the source points and the detector area. In the simple AMS version we have presented before, the only responses that could be estimated with the AMS algorithm had to be associated to the target volume. Therefore, possible contributions to other responses (outside the target area) are not taken into consideration. This could however be performed during the same AMS simulation, provided that the weight given by the algorithm to these contributions is adequately computed.

Taking into account scores outside the target volume could ensure that the AMS simulations use all the information available from the iterating process. However, one could only hope for a variance reduction on the scores that are in areas located on the path of particles going from the source to the AMS target. In other regions, most contributions to the scores will come from the initial particle simulation (iteration zero).

In the AMS theoretical description, there is a straightforward way to take into account scores outside the target volume. This method will be presented in the first part of this chapter. As it will be described in the following, this technique requires to keep in memory the complete histories of all particles, including those of particles that are suppressed at each AMS iteration, and to compute every score at the end of the AMS final step. To circumvent the need of storing all simulated trajectories, we propose an on-the-fly scoring procedure that enables easy and efficient scoring outside of the target volume directly during the iterating process. The last two sections of this chapter are devoted to applications making use of this new functionality to compute flux attenuations in a succession of volumes or through successive surfaces. The first test case presented is the flux attenuation of neutrons in water, and the second one is the flux attenuation in a three-dimensional labyrinth.

5.1 Multiple scoring with AMS

In the theoretical formulation of the AMS algorithm for discrete-time Markov chains described in [3], the scoring process is not limited to scores in the target volume. We present in this section the general scoring process, expressed in terms of particle transport and particles tracks.

5.1.1 Particles genealogy construction

In order to implement the scoring procedure proposed in [3], we need to define the particles "genealogy". The idea behind the genealogy is to store the entire histories of all simulated particles, including the histories that are deleted for resampling, and to associate each of these tracks to a weight value.

In order to build the genealogy, the tracks storage has to be altered: whenever a particle is resampled, its old track has to be kept in memory and a new track created. This new track is a partial copy of the track selected for duplication, from its first point up to the splitting point. When the resampled particle is transported from the splitting point, each of its collision points is appended to the new track.

With those modifications, the genealogy at the end of a given iteration q is composed of n "active" tracks starting from their source points, plus all the tracks that were removed during previous iterations (at least $k \times (q-1)$).

5.1.2 Scoring using the genealogy

Let us consider an observable ψ of the track space (corresponding to any response within the geometry). Using an analog simulation, we can build an unbiased estimator $\hat{\psi}$ of the expected value of ψ as

$$\hat{\psi}_{MC} = \frac{1}{n}\sum_{i=1}^{n}\psi(X_i), \tag{5.1}$$

where $(X_i)_{i\in[1,n]}$ is a set of analog tracks.

In order to define an estimator of $\mathbb{E}(\psi)$ using the particles genealogy, we introduce some notations. For any iteration q of the AMS algorithm, we denote by

- Z_q the splitting level
- K_q the number of particles tracks that have an importance less than Z_q
- T_q^{off} the set of tracks that have an importance less than Z_q, which will be deleted during the iteration

- T_q^{on} the set of tracks having an importance greater than Z_q, which will survive the iteration.

Using these notations, we define $\hat{\psi}_q^{\text{on}}$ and $\hat{\psi}_q^{\text{off}}$ as the contributions to the estimator $\hat{\psi}$ of the histories of iteration q:

$$\hat{\psi}_q^{\text{on}} = \sum_{X \in T_q^{\text{on}}} \psi(X) \qquad \text{and} \qquad \hat{\psi}_q^{\text{off}} = \sum_{X \in T_q^{\text{off}}} \psi(X). \tag{5.2}$$

At the beginning of iteration q of the AMS algorithm, the particles genealogy is composed of all the tracks of iteration q (on and off) and all the tracks deleted at each previous iteration. According to [3], we can construct an unbiased estimator $\hat{\psi}_q$ of the expected value of ψ at each iteration q of the AMS algorithm as

$$\hat{\psi}_q = w_q \hat{\psi}_q^{\text{on}} + \sum_{j=0}^{q} w_j \hat{\psi}_j^{\text{off}}, \tag{5.3}$$

where

$$w_j = \begin{cases} \frac{1}{n} & \text{if } j = 0 \\ \frac{1}{n} \prod_{i=0}^{j-1} \left(1 - \frac{K_i}{n}\right) & \text{if } j > 0 \end{cases}$$

This formula is valid for any response. For a response ϕ estimated in the AMS target area, we should therefore obtain with Equation (5.3) the same expression as the estimator introduced in Section 3.2.3. Let us assume that the algorithm stops iterating after Q iterations. All tracks contributing to the score have necessarily reached the target volume. Therefore, their importance is numerically infinite and they are never resampled. They consequently all belong to the set T_Q^{on}. We have therefore $\hat{\psi}_q^{\text{off}} = 0$ for any $q \leq Q$, which implies

$$\begin{aligned} \hat{\phi}_Q &= w_Q \hat{\phi}_Q^{\text{on}} \\ &= \left[\frac{1}{n} \prod_{q=0}^{Q-1} \left(1 - \frac{K_q}{n}\right)\right] \hat{\phi}_Q^{\text{on}} \\ &= \left[\prod_{q=0}^{Q-1} \left(1 - \frac{K_q}{n}\right)\right] \frac{1}{n} \sum_{X \in T_Q^{\text{on}}} \phi(X), \end{aligned} \tag{5.4}$$

which is identical to the "standard" expression of the AMS estimator of $\mathbb{E}(\phi)$ given in Equation (6.6)).

We can also check that at iteration 0, Equation (5.3) is equivalent to the

expression of the analog estimator for any response ψ:

$$\begin{aligned}\hat{\psi}_0 &= w_0\hat{\psi}_0^{\text{on}} + w_0\hat{\psi}_0^{\text{off}} \\ &= \frac{1}{n}(\hat{\psi}_0^{\text{on}} + \hat{\psi}_0^{\text{off}}) \\ &= \frac{1}{n}\left(\sum_{X\in T_0^{\text{on}}}\psi(X) + \sum_{X\in T_0^{\text{off}}}\psi(X)\right) \\ &= \hat{\psi}_{MC}\end{aligned} \tag{5.5}$$

5.2 On-the-fly scoring procedure

Implementing the genealogy-based scoring method in TRIPOLI-4 would require to keep the partial contributions of particles within the tracks structure, and to be able to duplicate the contributions of particles when they are selected for resampling. Furthermore, we would also need to manage the track weights independently until the score collect at the end of the iterating process.

In order to prevent the algorithm implementation becoming overly complex while still accurately computing all scores, we derive from the genealogy-based scoring a procedure that enables us to collect each score at a specific iteration. Indeed, the estimator introduced in Equation (5.3) is unbiased for any score at any iteration of the AMS algorithm, which means that we can choose a collecting iteration for each score. The choice of the appropriate collecting iteration for each of the scores is the central point of our on-the-fly scoring procedure, and we will show that it allows for an unbiased estimation of any score *without any modification* of the track structure, even out of the target area.

It seems obvious that the score collecting should be delayed as much as possible, in order to take into account contributions from multiple iterations. However, if waiting for too long, the fact that we do not store in the track structures the contributions to scores can induce a loss of information. There are actually two ways in which the contributions can be lost. The first one occurs if a track contributing to the score is deleted, and the second if a track contributing to the score is duplicated without duplicating its contribution.

Those contribution losses can only occur for scores *outside of the target volume*, since particles entering the target area are given a numerical infinite importance. The scoring volumes considered in the following examples are therefore not the target volume of the AMS algorithm, but any other volume of the geometry in which a response is estimated.

5.2.1 Contribution deletion risk

We show in Figure 5.1 an example of potential contribution loss due to the resampling of a particle track that contributed to a score in a volume that is not the AMS target area.

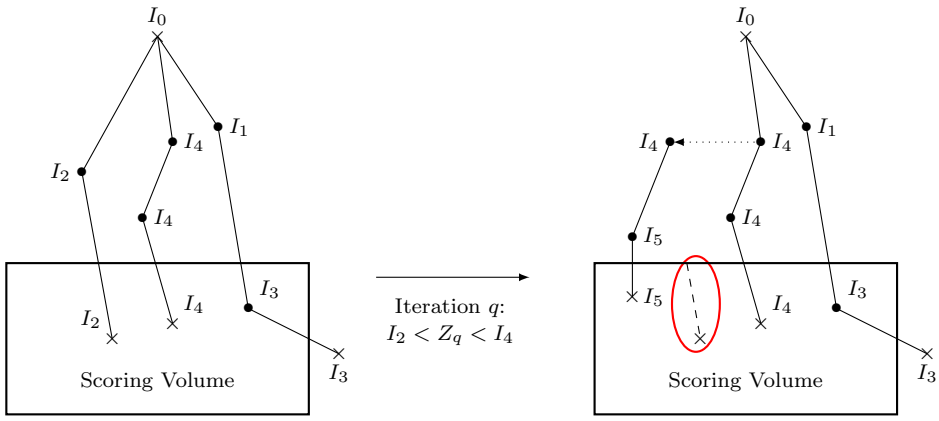

Figure 5.1. Illustration of potential information loss due to the resampling of a contributing track.

In this example, the importances at collision points are such that $I_0 < I_1 < I_2 < I_3 < I_4$. We reach an iteration q for which the splitting level Z_q is greater than I_2 but less than I_4. The left track, having an importance $I_2 < Z_q$, is resampled. The middle track is selected for duplication at its first point of importance greater than Z_q. Since we do not store the particles contributions in the tracks, the contribution of the left track may be lost and lead to a biased result.

We can circumvent this issue by collecting the score ϕ during an iteration q such that no track contributing to the score has ever been deleted from the simulation. We have therefore $\hat{\phi}_j^{off} = 0$ for any $j < q$, so that Equation (5.3) becomes

$$\hat{\phi}_q = W_q \hat{\phi}_q^{\text{on}} + W_q \hat{\phi}_q^{\text{off}}. \tag{5.6}$$

We can see that under the condition that no contributing track is deleted, the weighting factor is unique and equal to the current global AMS weight. Therefore, the collecting iteration for a score has to be such that no contributing track is deleted. Thus, all contributions to the score can be added on the fly during the simulation and without weighting factor. The weighting can be performed on the total score with the AMS global weight at the collecting iteration.

Remark

For any score within the AMS target volume, this collecting criterion is in accordance with the algorithm stopping criterion. Indeed, since the importance of all tracks entering the target is numerically infinite, no tracks contributing to a score within the target can ever be deleted as long as the splitting level is less

than numerical infinity. All contributions to the target score are therefore added during the simulation and the weighting is performed using the final AMS global weight.

5.2.2 Contribution duplication issue

The second issue raised by not storing score contributions in tracks is the inability to copy a track's contributions when it is duplicated. Despite the previous condition imposed on the collecting iteration, situations in which contributions have to be duplicated can still occur.

Let us consider a simple example: a particle is contributing to a score while its track has an importance I_A, and then reaches a zone of greater importance so that the importance of the whole track is $I_B > I_A$. Some iterations later, the splitting level takes a value Z_q so that

$$I_A < Z_q < I_B. \tag{5.7}$$

The track we consider here will not be deleted, since its final importance is greater than Z_q. However, it could be selected for duplication, in which case the splitting point will be a point of the track located *after* the scoring point, since $Z > I_A$. In that case, the computation of the estimator $\hat{\phi}_{q+1}$ would require to duplicate the contribution of the particle and pass it on to the resampled track. An illustration of this situation is shown in Figure 5.2, in which the rightmost particle enters the scoring volume with importance $I_A = I_1$, but has a track of total importance $I_B = I_3$.

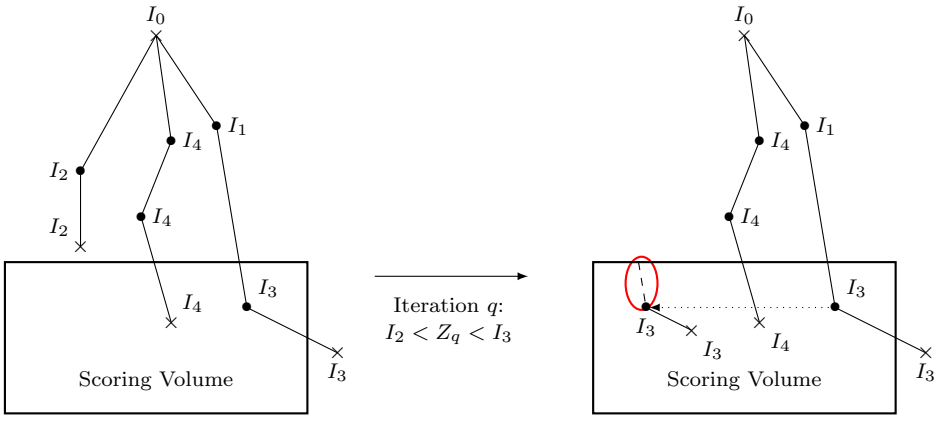

Figure 5.2. Illustration of potential information loss due to the duplication of a contributing track.

For the target scores, we bypassed this problem by adding target entering points to the particles tracks with numerically infinite importance. Since the parts of the tracks that contributes to the target scores are necessarily located after the boundary crossing point, no contribution has ever to be copied. Indeed,

the last point that can be selected as splitting point is the boundary crossing point, since its importance is infinite.

In contrast with target scores, it is impossible to define boundary importances values for intermediate volumes that prevent contributions duplication. That would imply to have boundary importances that are greater than any importance value within the volumes, preventing the AMS algorithm from correctly classifying particle tracks with regard to the target.

In summary, the rule for choosing the optimal collecting iteration has to ensure that no contribution to the score can be deleted, and that no contribution duplication can occur. The on-the-fly scoring procedure we propose in the following is based on the introduction of an importance value for each of the scores. We will show in the following that we can apply a condition on this score importance to trigger the score collect at the appropriate iteration.

5.2.3 Scores importances

In order to accurately choose the optimal collecting iteration for each scores, we attach to each score ϕ a *score importance* I_ϕ. For any track X contributing to the score, the track importance at the moment of the contribution is retrieved. I_ϕ is then computed as the minimum value among these importances.

In TRIPOLI-4, this is handled by the response class (which manages the scores). It attributes an importance value to each score at the beginning of the batch and initializes it to numerical infinity. As soon as a particle contributes to a score, the AMS Manager is called to provide the current importance of the particle's track. This value is compared to the importance of the score and if smaller, the score importance is updated. An example of score importance computation is shown in Figure 5.3.

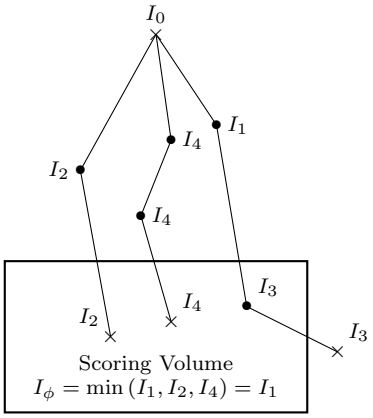

Figure 5.3. Definition of a volumic score importance from the importances of contributing tracks.

In this example, we assume that a track is contributing to the score as soon as it enters the scoring volume. This is for example be the case if the score is the probability of reaching the volume, or the particle current at the volume boundary. The importance of each track *at the moment* of their contribution to the score are therefore left to right I_2, I_4 and I_1. The score importance after the termination of the three trajectories is then

$$\begin{aligned} I_\phi &= min(I_1, I_2, I_4) \\ &= I_1. \end{aligned}$$

5.2.4 On-the-fly scoring process

Let us now express the condition on deleted tracks contributions in terms of score importance. Once per iteration, after the splitting level has been determined but before the resampling process takes place and the AMS global weight is updated, the splitting level is compared to the importance value of each score. If the splitting level is greater than or equal to the score importance, the score is collected and weighted by the current AMS global weight. Each score is collected once per simulation. After a score has been collected, eventual contributions to this score are not taken into account.

This procedure does ensure that no contributing track is ever deleted before the score is collected, since the importance of any track contributing to a score is by definition greater than or equal to the score importance. This technique also allows us to address the problem of duplicated contributions. As described before, this issue arises from situations in which the splitting level is less than the importance of a contributing track but greater than the importance the track had when it contributed to the score, so that if the track is selected for duplication, the splitting point could be located after a contributing part of the track. With the on-the-fly scoring technique however, this situation is solved, since the score will be already collected when the situation arises, so that the duplicated contribution has not to be taken into account.

Not only does this on-the-fly scoring technique define the collecting iterations for every score, but it allows us also to overcome the need of keeping contributions attached to the particle tracks, as all contributions to a score are collected at once using the global AMS weight.

Overall, the only changes made to the previous AMS implementation are

- the addition of an importance value to each score

- the inclusion in the AMS process of a loop on the scores that checks after each splitting level if some of them have to be collected.

5.3 Flux attenuation in a deep-penetration configuration

5.3.1 Problem description

The first problem chosen to test the on-the-fly scoring capacities of the AMS algorithm in TRIPOLI-4 consists in an isotropic neutron point source emitting neutrons according to a Watt spectrum and placed at the bottom of a straight box filled with water. The box is 3 m high and has a base dimension of 60 cm×60 cm. We use this setup to estimate the neutron flux attenuation in water starting from a fission source. This can be seen as an extremely simplified representation of a pool-type reactor, i.e. a nuclear reactor which core is immersed in an open pool of water acting as the neutron moderator, reflector, coolant, and radiation shield. In order to artificially simulate a very large pool, a perfect reflection boundary condition is applied on the side of the pool.

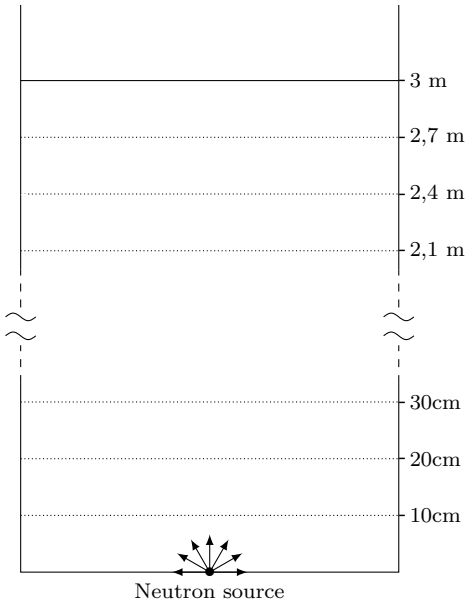

Figure 5.4. Geometry for the deep-penetration study: water pool divided into 10-cm-thick slices.

The probability for a fission neutron to go through 3 m of water without being absorbed is in the order of 10^{-14}. We are going to estimate the volume neutron flux in 10-cm-thick slices from the source to the surface of the pool, in order to test the on-the-fly scoring technique for a succession of volumes.

5.3.2 Results

The same importance functions as in the previous chapter were used to parametrize the AMS algorithm: a purely spatial importance I_S and two INIPOND importance maps: I_4^+ and I_6^+. In this case the importance I_S is defined as the

invert of the depth.

Figure 5.5 shows the estimated neutron flux in the succession of virtual volumes from the source point (0 m) to the water surface (3 m), for the three AMS simulations, an analog run, and a calculation using the Exponential Transform method with importance I_6^+. The results were obtain by running 3000 batches of 1000 initial number of particles each. All AMS simulations were performed with k set to 1% of the number of particles.

The first observation is that all three AMS estimations are in perfect agreement. The confidence intervals around the flux estimation overlap in all volumes from the source to the detector. Furthermore, in the volumes where analog results are available, we can see that the analog and AMS yield the same results. On the other hand, the simulation that used Exponential Transform drastically underestimates the flux in all volumes (around ten times). The smallest discrepancy is to be found near the water surface, which is not surprising since the Exponential Transform is supposed to estimate the flux at the surface.

The bottom plot of Figure 5.5 indicates that in the first 50 cm from the source point, the analog simulation is more efficient than any AMS calculation in estimating the flux. This is a direct consequence of the AMS time overhead, since the algorithm waits for the iterations to end before giving a result, even for scores that have been collected early in the iteration process. The discrepancies in the FOM values obtained with the two importance maps of INIPOND (I_6^+ and I_4^+) are very small, and most likely due to statistical variations.

Despite the fact that the relative standard error obtained with I_S is less than with I_4^+ *for the same number of batches*, we can see that this order is reversed on the FOM plot. This illustrates the capacity of a map that takes into account the particle energies to reduce the AMS computation time even if it increases the uncertainty on the estimation in some energy groups that were deemed less interesting. The results obtained with the spatial map I_S are overall less interesting in terms of FOM, especially in the volumes located between 50 cm and 2 m from the pool bottom, but they remain very close to those obtained with I_4^+ and I_6^+.

We observe that the mean values obtained using the Exponential Transform are well below the values estimated by the other methods, (even the area where analog results are available). It is not unusual for the Exponential Transform to underestimate the flux in locations other than the target area. Indeed, the Exponential Transform alters the transport process in order to convey the particles toward the target, which may result in an apparent underestimation of intermediate scores. In our case however, even the flux estimation at the water surface is barely in agreement with the AMS results. For all Exponential Transform results, it is actually the standard errors that are underestimated. In fact, the simulation is just missing rare events that will eventually cause the estimation to jump and give the same result as the other simulations. There is however no way of pre-

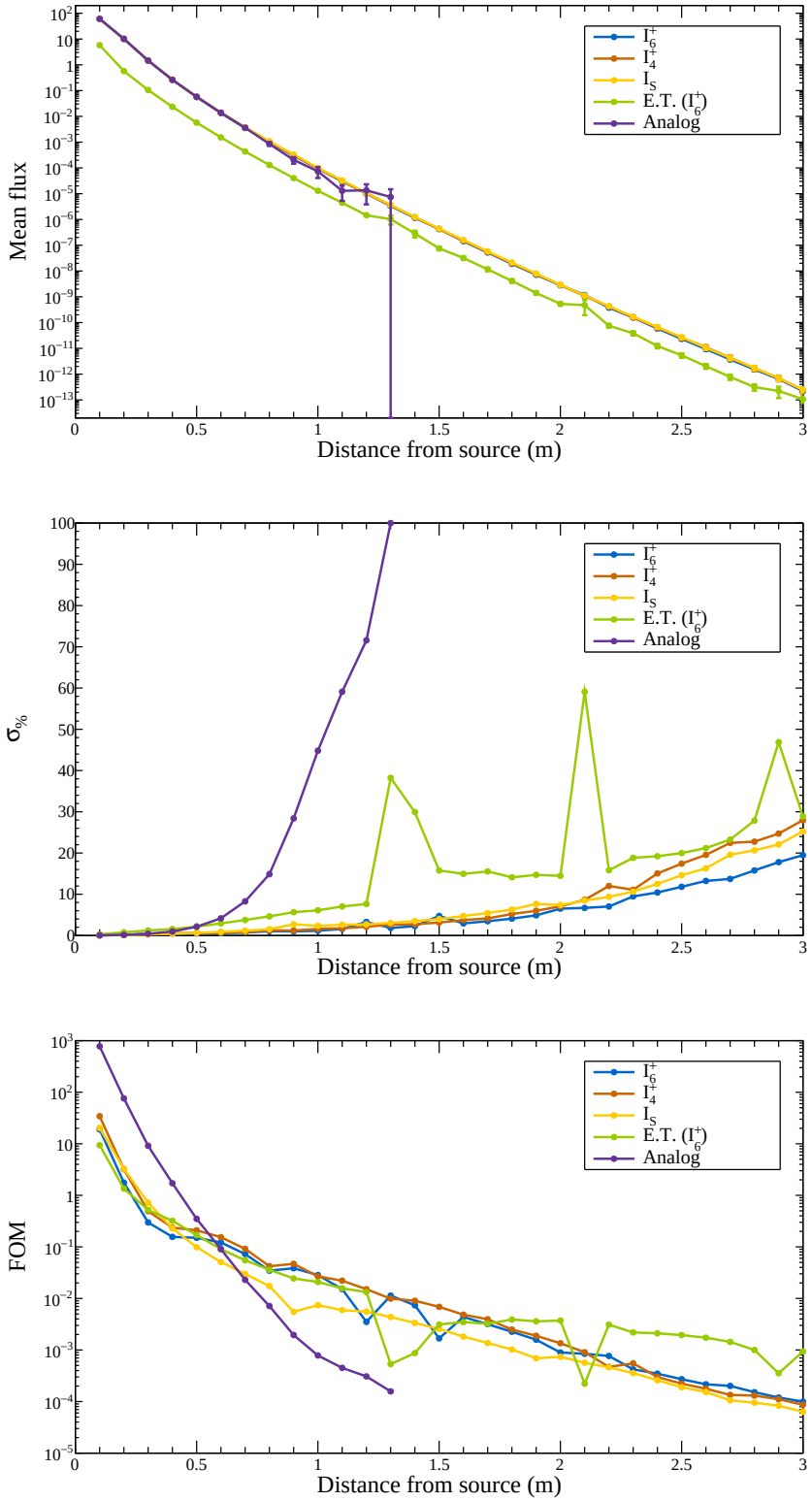

Figure 5.5. Neutron flux attenuation in the water pool problem for AMS and the Exponential Transform method. Upper to lower: mean flux with 68% confidence intervals, relative standard error, and FOM.

dicting when those rare events will be simulated. It is also impossible, without comparison with other results, to know if the estimated values are correct or not.

It should be kept in mind that the computation of all the importance maps used up to this point were constructed by INIPOND while letting the module automatically determining its biasing parameters. It is therefore not surprising to have such a poor convergence for the Exponential Transform method, for which the precision of the importance map has a great impact on efficiency.

The results obtained with Exponential Transform are therefore an indicator that the importance map generated by INIPOND does not accurately represent the problem at hand. The quality of the importance map can however be improved through a manual parametrization of the INIPOND module. Details concerning the INIPOND module as well as its manual parametrization can be found in Appendix B. After multiple studies, we managed to parametrize the INIPOND module so as to obtain an importance map I_6^{++} that would permit the Exponential Transform to accurately estimate the flux. This importance map was also used as importance in new AMS simulations. The results obtained with this optimized importance are shown in Figure 5.6. For the sake of comparison, we added to the figure the best AMS result obtained with the importance map from the automatic mode of INIPOND (i.e. with importance I_4^+).

Although we observe small discrepancies above 2 m due to statistical fluctuations (the relative standard error in this area is most of the time greater than 10%), we can see that the confidence intervals of all the simulations overlap. Near the detector, the optimized importance map allows the Exponential Transform not only to yield the same result as the AMS simulations, but also to be more efficient. The optimization of the INIPOND parameters also allows for an improvement of the AMS FOM in the case of the 6-dimensional map, however not as strong as for the Exponential Transform method.

One should keep in mind that the Exponential Transform method, used with an importance map that is a good approximation of the adjoint solution of the problem, will always be more efficient than the AMS algorithm *in the detector area*. We saw with this example that AMS is an interesting method to reduce the variance of scores located on the path between source and detector. This problem also illustrated how the AMS is much less sensitive to the quality of the importance map than the Exponential Transform method. The automatic parametrization of the INIPOND module allows the AMS algorithm to obtain unbiased results without further parameter optimization.

5.4 Flux attenuation in a 3D streaming configuration

The Exponential Transform aims at reducing the variance by altering the sampled particle flight lengths between collision sites. It is therefore not surprising for it to be really efficient in a deep-penetration problem as seen in the previous

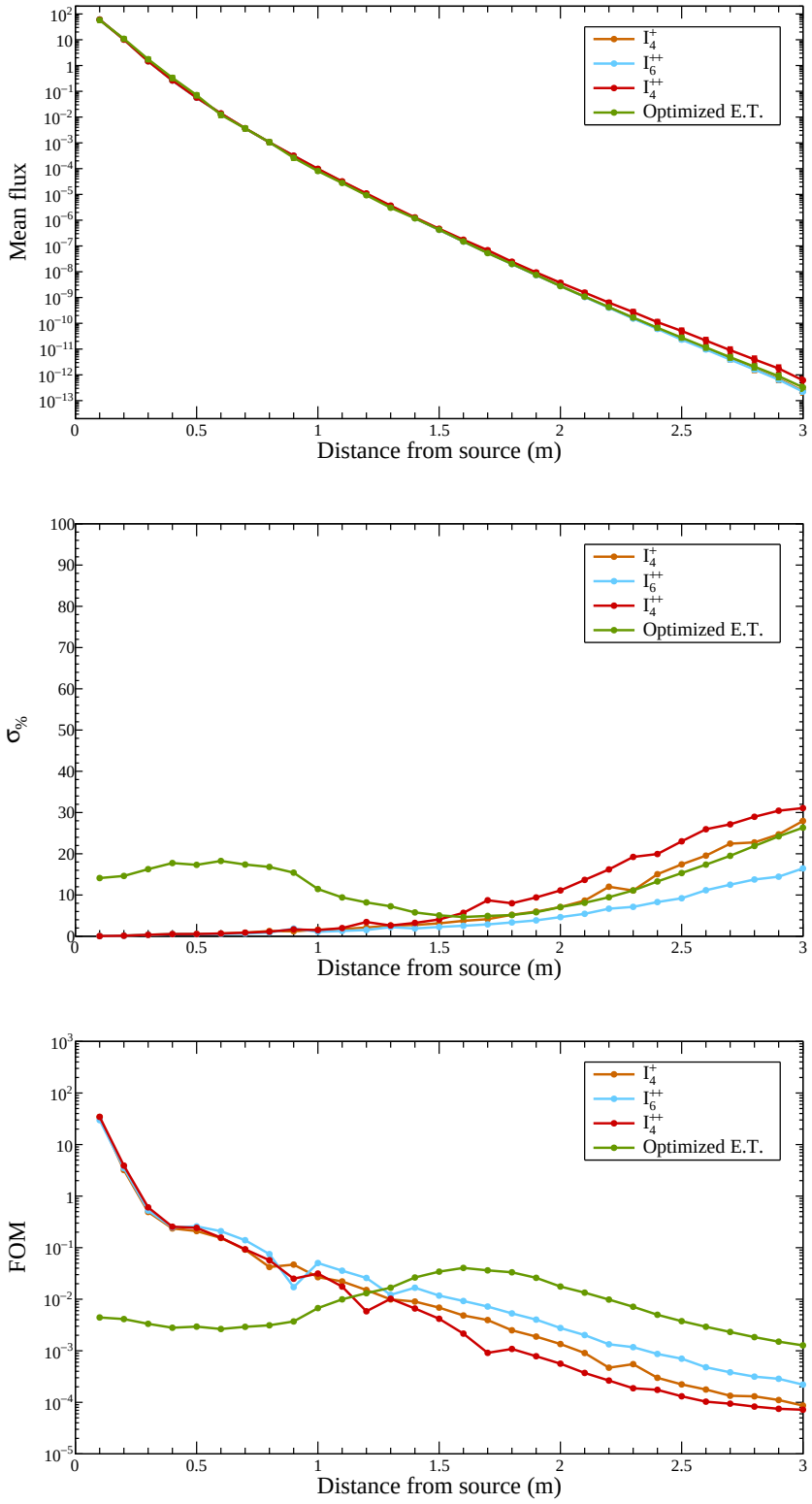

Figure 5.6. Neutron flux attenuation in the water pool problem for AMS and Exponential Transform, using optimized INIPOND maps. Upper to lower: mean flux with 68% confidence intervals, relative standard error, and FOM.

section (provided an adapted importance map is used). However, if we consider a streaming problem, in which the simulated particles have to follow a twisted path to reach the detector area, the shortening or stretching of free flights will most likely not be sufficient for the Exponential Transform to significantly reduce the variance. On the other hand, the AMS algorithm does not seem to have such limitations, and should therefore prove itself most useful for such configurations.

5.4.1 Problem description

The analysis we propose here is the study of neutrons streaming through a three-dimensional labyrinth filled with air and located in a concrete environment. This geometry has already been investigated during in a preliminary study whose results have been presented during this Ph.D. at the International Conference on Mathematics and Computational Methods Applied to Nuclear Science and Engineering (M&C 2017) [22].

In this problem, the air has a density of $0.001\,293\,\mathrm{g/cm^3}$, and the concrete is an ilmenite-limonite concrete of density $2.9\,\mathrm{g/cm^3}$. The labyrinth is shown in Figure 5.7, and the elemental compositions of both air and concrete are detailed in Table 5.1.

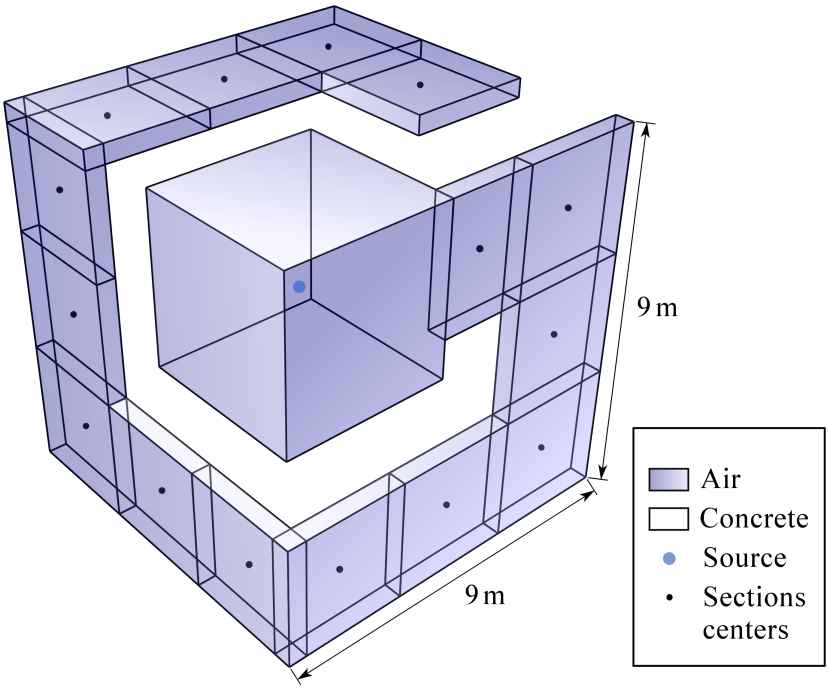

Figure 5.7. Geometry for the labyrinth problem.

Element	Air	Concrete
	$0.001\,293\,\mathrm{g/cm^3}$	$2.9\,\mathrm{g/cm^3}$
Hydrogen	-	00.66
Oxygen	21.00	36.45
Nitrogen	79.00	-
Magnesium	-	00.15
Aluminium	-	00.80
Silicon	-	03.06
Sulfur	-	00.08
Calcium	-	05.83
Titanium	-	16.03
Iron	-	36.93

Table 5.1. Elemental composition of the simulation materials as a percentage by weight.

A 2-MeV isotropic neutron point source is placed at the center of a cubic room of side 4 m. It is represented on Figure 5.7 by a blue point. The entrance of the labyrinth is located at a corner of this room. The labyrinth itself is a 44-meter-long tunnel composed of a section of dimension $2\,\mathrm{m}\times2\,\mathrm{m}\times50\,\mathrm{cm}$ followed by 14 "square" sections of dimensions $3\,\mathrm{m}\times3\,\mathrm{m}\times50\,\mathrm{cm}$. When assembled, those sections compose a tunnel of 7 straight corridors joined by six 90° bends.

This problem has been chosen as a case in which the Exponential Transform can not be of any help to reduce the variance on a score estimated at the end of the labyrinth. Indeed, due to the air concentration, the particle flight lengths within the tunnel will most of the time be large enough for the particle next collision to occur in the concrete walls of the tunnel. Therefore, stretching or shortening the flight length using the Exponential Transform should not have a sufficient impact on the transport behaviour to allow the particles to reach the end of the tunnel, regardless of the importance map quality. In such configurations, the attenuation is induced by abrupt changes of direction in the geometry, which reduces the efficiency of the Exponential Transform method.

In order to validate the AMS variance reduction capacity on other scores than flux in volumes, two types of scores have been defined in this geometry. The first one consists of an estimation of the flux in a mesh covering the entire geometry, and the second one is a surface flux, estimated on surfaces placed at various distances along the tunnel and at the very end of the labyrinth. The chosen surfaces are the interfaces between the square sections composing the labyrinth, and the AMS target is the surface located at the end of the tunnel. We will refer to it as the detector in the remainder of this section.

5.4.2 Construction of importance functions

As for the other cases, we wished to test the AMS efficiency in this context using spatial importance function as well as INIPOND importance maps.

Purely spatial importance function

Given the problem at stake, it seems highly probable that the particles contributing to the flux at the detector are the ones that travel along the tunnel. Therefore, a good purely spatial candidate for the importance function would have the following characteristics:

- For all point within the source room, the importance is inversely proportional to the distance to the labyrinth entrance.
- In the tunnel, the importance increases between the labyrinth entrance and the end of the tunnel.
- In the concrete, the importance is zero.

To build such a function in TRIPOLI-4, we used the *path* spatial importance described in Section 4.2.3, and defined the path as the sequence of source and black points displayed in Figure 5.7. We furthermore forced the importance outside of the labyrinth to zero by setting a null weighting factor to the corresponding volume. The resulting importance function is shown in Figure 5.8.

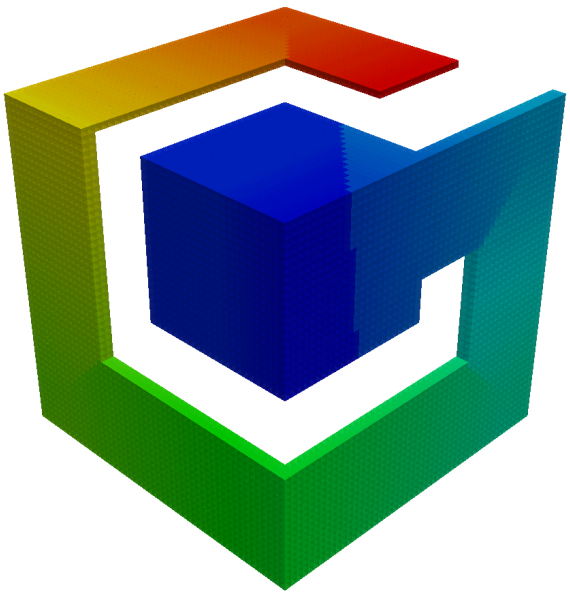

Figure 5.8. Spatial importance I_S for the labyrinth geometry.

INIPOND importance map

The spatial mesh we defined for the INIPOND calculation is composed of $50 \times 50 \times 50$ cells. Their dimensions are approximately $40\,\text{cm} \times 10\,\text{cm} \times 10\,\text{cm}$ in the tunnel, and their size increases progressively with increasing distance from the labyrinth. The energy domain of the simulation (1E−11–20 MeV) has been divided into 6 energy groups, detailed in Table 5.2.

Group	Maximum Energy	Minimum Energy
1	20 MeV	1 MeV
2	1 MeV	100 keV
3	100 keV	5 keV
4	5 keV	0.625 eV
5	0.625 eV	1E−3 eV
6	1E−3 eV	1E−3 eV

Table 5.2. Energy discretization of the importance map.

We used the automatic parametrization of INIPOND to compute the importance I_6^+. The variations of the resulting map being the same in every energy group, we show only in Figure 5.9 the non-angular part I_4^+ of the importance, restricted to a single group.

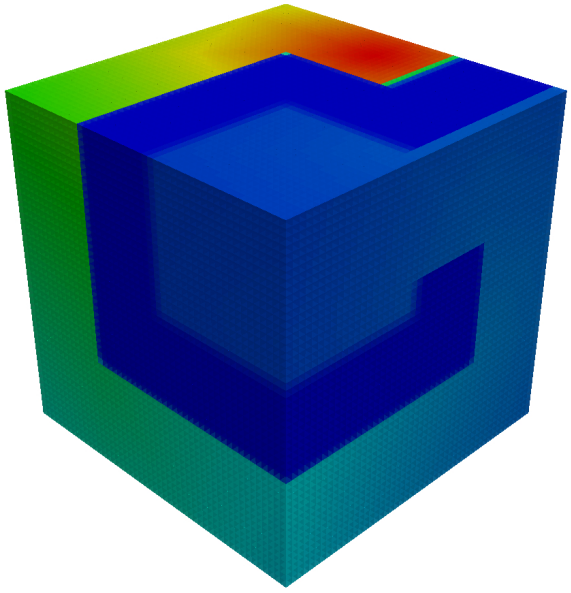

Figure 5.9. Automatically generated importance map I_4^+ for energy group 2.

We can see that the INIPOND module successfully evaluates the importance

map for the entire geometry, also computing an importance for each cell within the concrete. As expected, the preferential path for the neutrons from the source to the detector is indeed through the tunnel.

Mesh score

Figure 5.10 shows the flux obtained in the cells of the mesh covering the labyrinth, with both an analog and AMS simulation with importance I_S. The simulation time was set to 90 minutes for both simulations, which ran on the same computer, each on a single thread. The AMS simulation used 10^4 particles per batch with a k value set to 100.

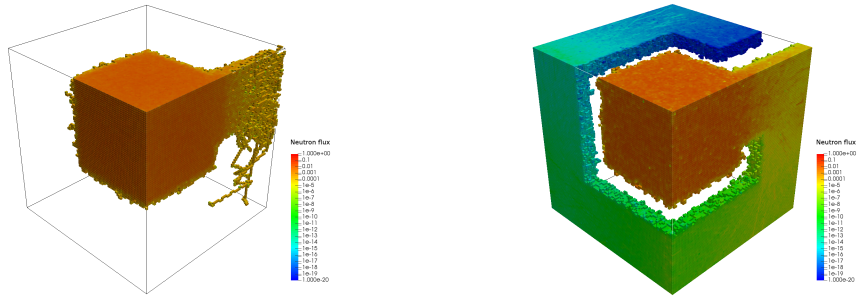

(a) Analog neutron flux **(b)** AMS neutron flux

Figure 5.10. Representation of the mesh neutron flux obtained with an analog simulation (a) and an AMS simulation with I_S (b), for the same computation time.

We can see in Figure 5.10 that the AMS algorithm allows TRIPOLI-4 to estimate a flux in every cell of the mesh inside the labyrinth, despite the 20 orders of magnitude attenuation. Furthermore, we notice that the estimation of the flux outside the tunnel is not impaired by the zero-valued importance of the concrete. This is not surprising, since the AMS algorithm does not modify the transport of particles in the geometry, therefore the collisions in concrete are accounted for in the score estimation, but no track can be duplicated at those points.

Surface Flux Estimations

In order to perform a more quantitative efficiency comparison, we compared the results obtained on the surface flux scores. We performed an analog simulation, an AMS simulation with the purely spatial importance I_S, and two AMS simulations with the importance maps I_6^+ and I_4^+ computed by INIPOND. All the simulations ran simultaneously on the same computer for 67 hours, each of them on a single thread.

The results obtained are shown in Figure 5.11 with respect to the distance between the surfaces and the labyrinth entrance. The dotted vertical lines indi-

cate the locations of the 90° bends in the tunnel.

The comparison of the results obtained for the surface flux tallies puts once again into light the efficiency of the AMS algorithm. Regardless of the importance function, the AMS results are in agreement all along the tunnel, while the analog simulation fails to accurately estimate a flux deeper than 11 meters. Closer to the labyrinth entrance, we can see that the results of the AMS simulation are in very good agreement with the values obtained from the analog simulation.

The relative standard errors for each of the surface flux estimations are reported in the middle frame of Figure 5.11. We can see that for the same computation time, the smallest standard errors are obtained by the AMS using the purely spatial importance map I_S. This indicates that the importance maps computed by INIPOND do not correctly represent the problem. This is most likely the consequence of an incorrect estimation of the spectral effects. Indeed, the INIPOND module does not accurately take into account the particle energy decrease during transport, which in this case leads to an overestimation of the higher energy group importances. This may have little impact on the Exponential Transport behaviour, as particles transported in distinct groups are independently biased, but within the AMS algorithm, those particles are compared to one another. In this case, this leads to illegitimate resampling of low-energy neutrons in favor of high-energy ones, even if they are farther from the end of the tunnel. This has an impact on the AMS efficiency, which spends time performing unnecessary splitting. Every supernumerary AMS iteration lowers the global weight assigned to the particles, eventually leading to underestimated estimations for some batches.

Nevertheless, it must be borne in mind that the INIPOND map did still enable the AMS algorithm to estimate the correct average flux on all considered tallies. Therefore, the use of the INIPOND map for AMS remains a viable option, and may prove itself very efficient in configurations where trivial importance functions are not enough to describe the problem.

It is worth noting that the FOM obtained for the estimations of the first four surface fluxes are greater for the analog simulation than for any AMS simulation. This is a direct consequence of the extra computational time required for the AMS simulation to classify and resample particles, which is penalizing if the score is too easy to estimate.

The use of the Exponential Transform with importance I_6^+ did not yield any results, since the first batch simulation never ended. We tested several other parametrizations of the module but the best results were similar to those of the analog simulation.

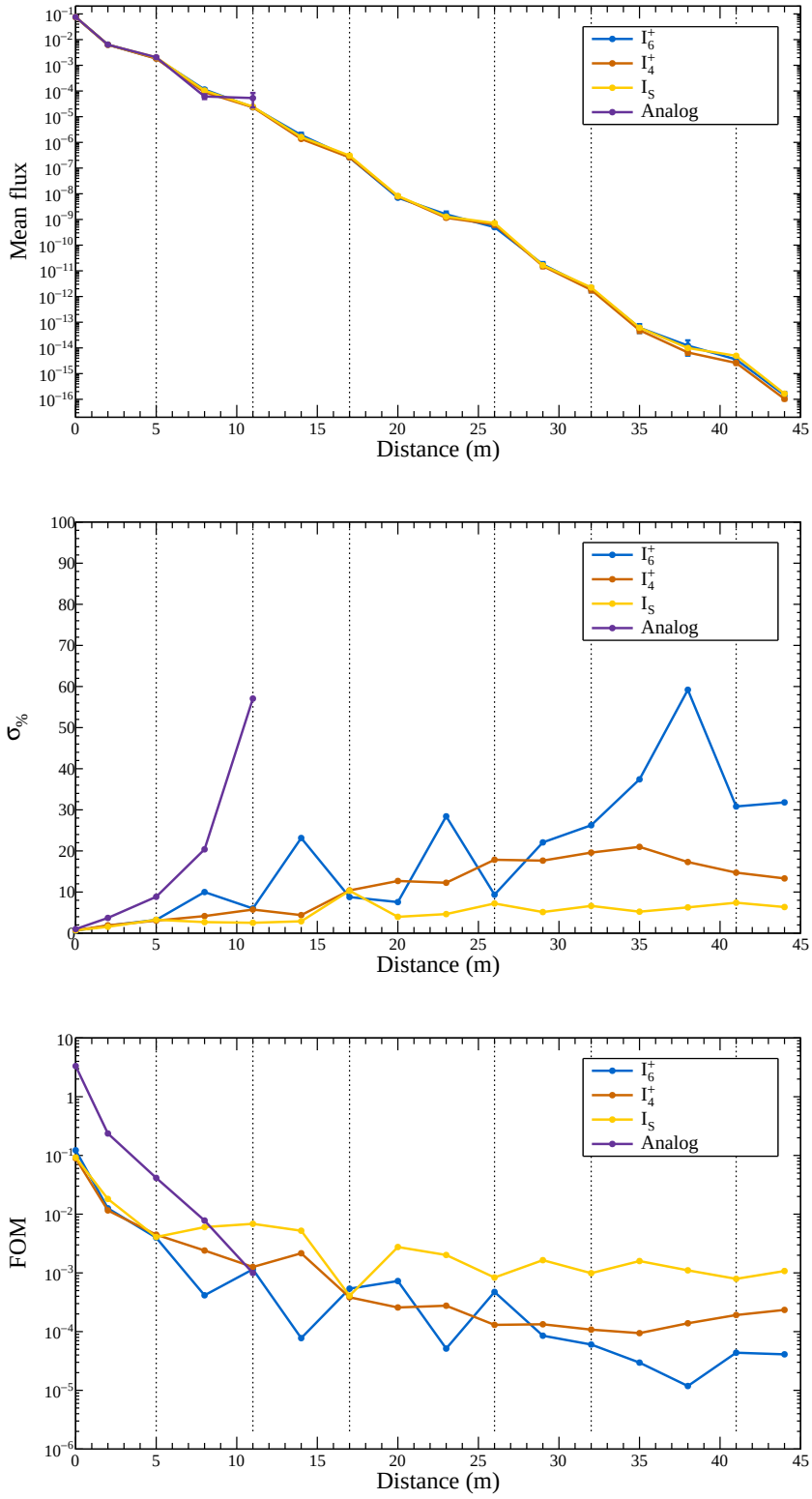

Figure 5.11. Neutron surface flux obtained with AMS and analog simulations with respect to the distance between the surfaces and the tunnel entrance. Upper to lower: mean flux with 68% confidence intervals, relative standard error, and FOM.

5.4.3 Construction of reference values

We wished to compare the AMS results with values obtained using another method. Due to the complexity of the problem however, we were unable to obtain a reference value for the flux using the Exponential Transform variance reduction method. Considering the flux attenuation, it was obviously not reasonable to hope getting analog results all the way to the end of the tunnel.

A deterministic approach was considered, but the size of the geometry and the low concentration of the air inside the tunnel were most likely to lead to difficulties calculating the flux, strong ray effects or other anomalous computational effects [23].

Surface particle restart

The chosen strategy for constructing reference values uses a two-step feature of TRIPOLI-4. It is called surface restart and is based on a two step approach, each step involving a TRIPOLI-4 simulation. In a first simulation, the characteristics of particles crossing the boundary of a given volume are stored and dumped into a file. Then, TRIPOLI-4 uses this file to initialize the source particles for the second simulation, making use of the Markov property of the simulated particle transport. Surface restart can be used in series, each simulation storing particles to be used as source in the next simulation.

In our case, the geometry was divided into eight parts, the first one containing the source room, and each of the successive parts encompassing consecutive pieces of the tunnel. After having restricted the geometry to its first part, 10^6 particles were simulated from the source point (without variance reduction). During the simulation, the particles states at the interface between the first and the second part of the geometry were stored. Then, seven successive simulations were performed, each of them restricted to a single part of the geometry. Each time, 10^6 particles were simulated using the particle states stored during the previous simulation as source and the particles leaving the restricted geometry were stored to be used in the next simulation.

Obviously, less than 10^6 particles were stored at the end of each partial simulation. They have been consequently massively duplicated, and the flux estimation may suffer from correlations. Furthermore, the estimation of the variance on the estimated scores in this multiple-simulation configuration is a complicated matter. We did not estimate the confidence intervals in this study, since our purpose was only to provide a reference value to validate the results obtained with AMS.

Validation of AMS results

Figure 5.12 shows the surface flux estimated with the three AMS simulations as well as the reference values estimated using the surface particle restart strategy presented above, represented as a dashed gray line. We can see that all results

are in accordance, which comfort us in the accuracy of the AMS results.

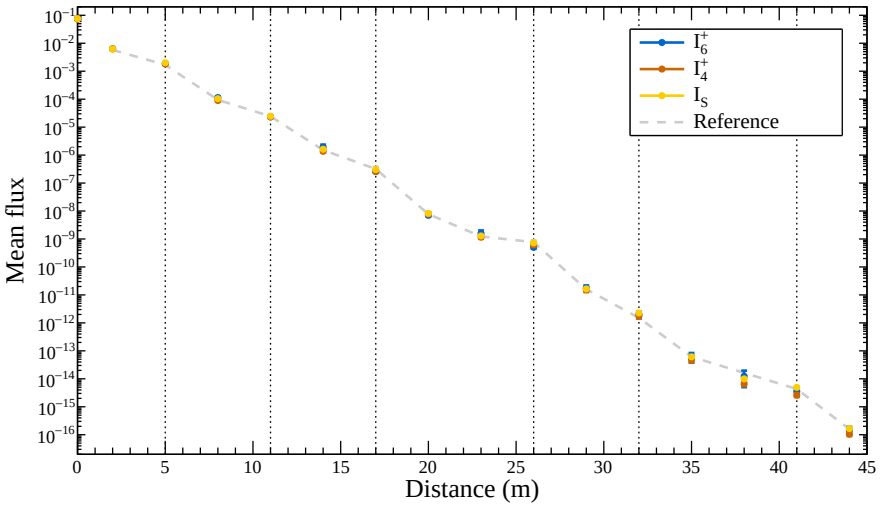

Figure 5.12. Comparison of AMS and reference results along the labyrinth.

5.5 Conclusion

After having adapted the theoretical scoring procedure for scores outside the target volume of the AMS, we showed that any score could be collected at the end of the algorithm iterations, provided that we had access to the whole particle genealogy. However, this genealogy-based scoring would have a strong impact on track storage, and would also require heavy modifications of the scoring process of TRIPOLI-4.

It is however possible to collect scores at any iteration of the AMS algorithm, and this is what is actually done, thereby minimizing the modifications required in TRIPOLI-4. We showed that a wise choice of the scoring iteration allows us to avoid the storing of the whole genealogy to collect scores outside the target volume. We introduced in this chapter an innovative way of determining the best iteration at which to collect scores on the fly during the iterating process, and then showed in two test cases that the resulting implementation was indeed working and efficient, since it permits to estimate unbiased results outside the target volume with a better FOM compared to analog simulation results.

This new feature of AMS in TRIPOLI-4 allows for a wider field of applications, since the AMS estimations are no longer restricted to the target area nor to volume scores. Yet, this implementation of AMS is still not usable in some cases. It is indeed limited to particle tracks that each represents the history of a single particle. In shielding configurations however, the interaction of a particle with a nuclide can result in the emission of one or several secondary particles, and there are cases in which these secondary particles have to be treated explicitly.

In order to have an AMS algorithm that can be used for any shielding simulation, the AMS implementation has therefore to be adapted in order to take branching processes into account. This adaptation is the subject of the next chapter.

Chapter 6

Handling branching tracks with AMS

In Monte Carlo neutron transport simulations, the majority of multiplying reactions can be handled by transporting a single outgoing particle carrying a weight that reflects the particle multiplicity [20]. In analog simulations however, each outgoing particle is treated as an independent particle and transported individually. This is troublesome for the AMS algorithm, since such interactions generate multiple secondary tracks for a single incoming track. We refer to those tracks as "branching tracks".

After describing why we wish the algorithm to be able to deal with branching tracks, we propose a way of defining the importance of branching tracks as well as the associated resampling procedure. In a third part, we address the implementation of this new technique in TRIPOLI-4. The last sections of this chapter are devoted to the study of two cases especially chosen to assess the efficiency of AMS as a variance reduction scheme in simulations where correct handling of branching tracks is required. The first one is a gamma-ray spectrometry case, and the second a coupled neutron-photon calculation.

6.1 Motivation

The AMS algorithm does not provide a direct way of defining importances for branching tracks. The easiest way of bypassing this issue is to let the code assign weights to particles that undergo multiplying reactions so that the resulting track is weighted but not branching.

This workaround can however not be used in every situation. There are simulations in which the weight treatment of particle multiplicities is either not applicable or not sufficient to prevent tracks from branching. In coupled neutron-photon simulations for example, the inelastic scattering of neutrons on a nucleus

leaves the nucleus in an excited state from which it eventually releases radiation in the form of photon(s). In that case, the original neutron carries on its transport while one or several photons are emitted. The emitted photons may very well be represented by a single photon carrying a weight, but the primary neutron and the secondary photon can not be replaced by a single weighted particle due to their distinct nature.

Another example of situation in which the secondary particles have to be simulated one by one are gamma-ray spectrometry simulations. The score in this kind of simulations consists in a spectrum of deposited energy per particle, usually called "pulse-height tally". The related deposited spectrum score of TRIPOLI-4 records the total energy deposited in the detector by a particle from its emission at the source to the termination of all progeny. This implies that all secondary tracks are correlated. If a photon coming from the source point generates two secondary photons of 511 keV energy which are then both absorbed in the detector, deposing all their energy in it, the whole process registers as a *single event* of 1022 keV. Weight-based multiplicity representation is not well suited to handle cases with correlated secondary particles, which can only be accurately represented by an explicit treatment of branching tracks.

Pulse-height tallies are actually non-Boltzmann scores, as they can not be described by the Boltzmann equation due to the fact that they require knowledge of the entire trajectory for a contribution to be computed. Non-Boltzmann scores are a complex matter in terms of variance reduction. The restraint on weight use complicates the application of most variance reduction methods. Most of the time, it is possible to circumvent those problems, but it requires to modify the variance reduction schemes [24]. For the time being, TRIPOLI-4 is not able to use the Exponential Transform method if these kind of scores are requested in the simulation. This gave us one more reason to find a way of handling branching tracks in the AMS algorithm.

6.2 Practical approach

As of today, the problem of applying AMS to branching Markov Chains has never been addressed in the literature. There is however no theoretical impediment to the consideration of branching tracks in AMS, provided that their importances and the associated resampling procedures are correctly defined.

We present in this section a way of defining branching tracks importances and the associated resampling procedures, which looks to fit the framework of [3] and should therefore yield unbiased results. Our approach is extensively tested in the last two sections of this chapter, both to validate the unbiasedness of the estimation and to evaluate its relevance in terms of variance reduction.

6.2.1 Definition of branching track importance

The importance of branching tracks can be simply defined in the same way as non-branching tracks. That is, the importance of the track is the maximum importance of its points. In the case of a branching track, this includes the points of all branches.

An example of importance definition in the case of a branching track is shown in Figure 6.1. The importance in this configuration is assumed to increase when the particle gets closer to the target, so that the importance values displayed on the figure are such that $I_0 < I_1 < \cdots < I_6$.

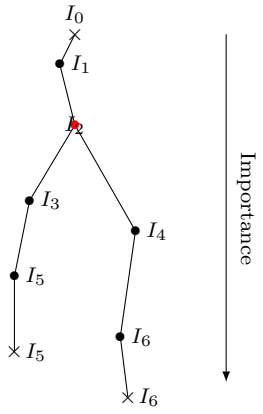

Figure 6.1. Illustration of a branching track. The branching point is drawn in red.

The track displayed in Figure 6.1 branched at its second collision with the medium and resulted in two outgoing particles. Since the point importances are computed *after the collisions*, the importance of the original track at the branching point but prior to the branching event was I_1. Then, each of the secondary particles added its collision points to a secondary track, both secondary tracks being attached to the original track at the branching point. Due to the chosen importance function, the first points of both secondary tracks have the same importance I_2, although their directions differ. One of the secondary tracks reached an importance I_5 while the other culminated at I_6. The overall importance of the entire branching track is therefore $I = \max(I_1, I_5, I_6) = I_6$.

6.2.2 Branching track duplication

Once the importance of branching tracks is defined, the classification process and the selection of the tracks to be resampled remains unchanged. During the resampling of a deleted track however, a branching track can be selected for duplication. In that case, the duplication process is rather more complex than for single-branch tracks.

When a single-branch track is selected for duplication, it is split at the first point of importance greater than the splitting level. In the case of a branching track however, three cases have to be distinguished, depending on the relative position of the splitting level and the branching point:

1. The splitting level crosses the particle track *before* the first branching point, in which case the splitting point is on the primary track.

2. The splitting level crosses the particle track *after* the first branching point and crosses only one secondary track, so that the splitting point is on a single secondary track.

3. The splitting level crosses the particle track *at* or *after* the first branching point and crosses several secondary tracks. Then, multiple secondary tracks should be split.

Primary track splitting

This is the simplest case. As the splitting level crosses the particle track before any branching point, the standard splitting procedure can be implemented and the resampling process remains unchanged. The particle is simply duplicated at the first point of importance greater than the splitting level, and the duplicated particle is then independently simulated.

Let us consider the branching track shown in Figure 6.1. The first two points make up the primary track, which would have to be split for any splitting level Z such that $I_0 < Z < I_1$, as shown in Figure 6.2.

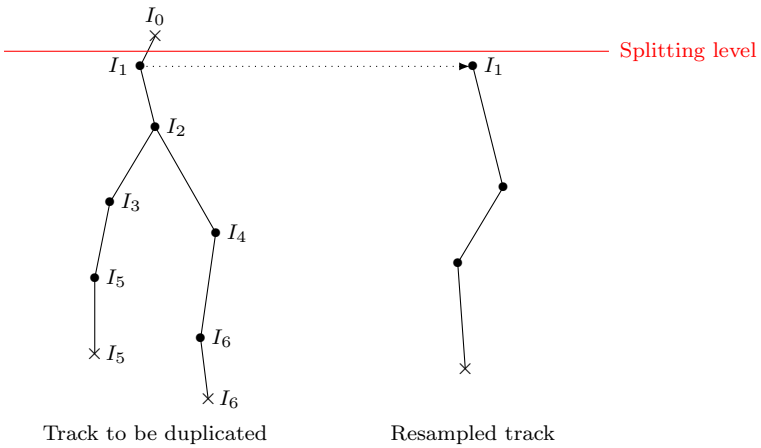

Figure 6.2. Example of a branching track duplication process for a splitting level less than the importance of the branching point

Single secondary branch splitting

The second possible configuration is as follows: one of the secondary tracks has an importance greater than the splitting level, while the importance of the

others are smaller. The duplication of such a branching track is also fairly similar to the standard duplication process. Only the secondary track that reached the level has to be split, which generates a new standard single-branch track.

Using the branching track illustrated in Figure 6.1, we show an example of single secondary track splitting in Figure 6.3, by imposing a splitting level whose value Z is comprised between I_5 and I_6, so that the secondary track on the left has an importance $I_5 < Z$ while the one on the right has an importance $I_6 > Z$.

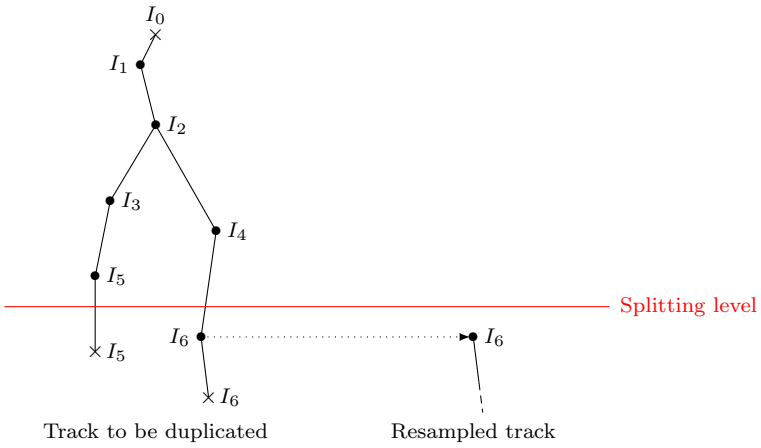

Figure 6.3. Example of a branching track duplication process for a splitting level crossing a single secondary track

Multiple secondary branches splitting

The last possible outcome occurs when the splitting level crosses multiple secondary tracks. In that case, each of those secondary tracks has to be split. However, one should keep in mind that the original duplicating process consists also in copying the track selected for duplication up to the splitting point. In this view, all new tracks resulting from the splitting of multiple secondary tracks have to be considered in the subsequent AMS iterations as secondary tracks of a *virtual single track*. Therefore, they have to be treated together in the rest of the simulation, just as any other branching track.

Once again, we use the branching track of Figure 6.1 to illustrate such a splitting process. It occurs if the track is selected for duplication with any splitting level Z crossing the track after the branching point and such that both secondary tracks have importances greater than Z. An example of such a situation is shown in Figure 6.4.

6.3 Implementation strategy

The implementation in TRIPOLI-4 of the method described above for the treatment of branching tracks within AMS requires a modification of the track structure, so as to be able to take into account secondary tracks after a branching event.

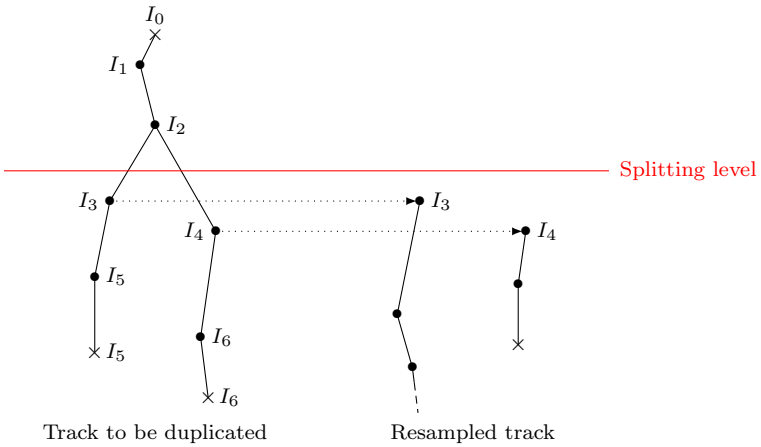

Figure 6.4. Example of a branching track duplication process for a splitting level crossing multiple secondary tracks

6.3.1 Tree-type track structure

The AMS track structure in TRIPOLI-4, as introduced in Section 4.2.1, consists in a points vector and a single importance value for the whole track. It is therefore not well suited to take branching processes into account. We decided to transform these tracks into tree-type structures instead. The new version of the track class holds a vector of *branches*, each of which is actually an instance of the former track structure with an additional "threshold" attribute. We will discuss the value and purpose of this threshold in the following. The data structure of these new tracks is represented in Figure 6.5.

6.3.2 Branching track transport process

The transport of a source particle now begins with the creation of a track holding a single branch to which the particle source point is added. The importance of the branch is set to the importance of its first point, and its threshold is set to zero. The branch is then filled as usual during the particle transport. Note that it is still possible to build the track branches only with points of greater importance than the branch importance so as to reduce the memory load (see Section 3.2.4).

Whenever the particle generates a secondary particle, an empty branch is added to the particle's track. The threshold of this new branch is set to the importance of the "mother" particle immediately prior to the splitting event. Since the importance is only evaluated *after* the collisions or at the boundaries between volumes, the threshold is by construction the importance of the mother track's last point before splitting, which is either the previous collision point, the source point or the last boundary crossing point. The threshold value will play an essential role in the track duplication process. More details will be given in the following.

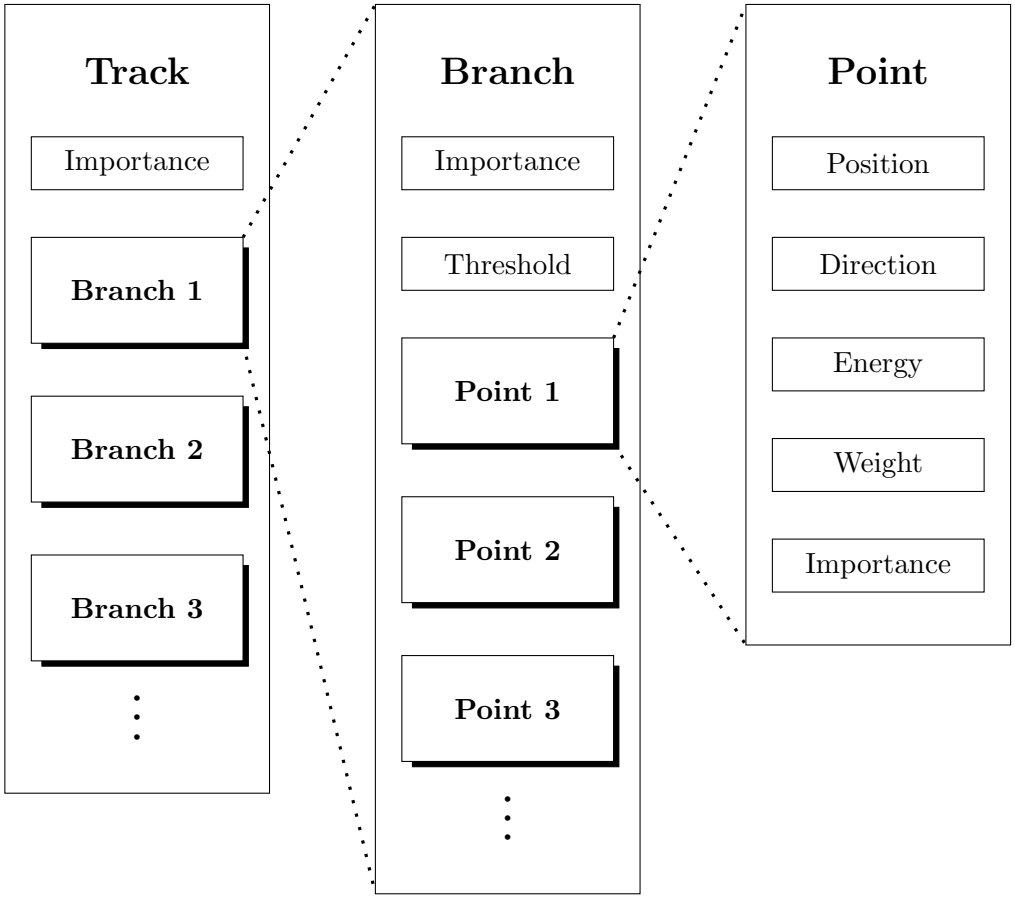

Figure 6.5. Data structure of the tree-type track class.

During the secondary particle transport, its collision points are added to the new branch, following the same process as for a primary particle. If the secondary particle itself generates a tertiary particle, a new branch is created *in the same track* and the tertiary particle is handled as any other secondary particle. Once all progeny is terminated, the importance of the whole track is computed as the maximum importance of all branches within the track. We show in Figure 6.6 an example of branching track history (6.6a) and the corresponding track as stored in the tree-type track structure (6.6b).

6.3.3 Duplicating branches

Once the importance of tracks is defined, the classifying step of the AMS algorithm can be performed as usual. The tracks that have an importance lower than the splitting level are deleted from the simulation (with all their branches), and as many of the remaining tracks are selected for duplication.

Let us consider one of the tracks selected for duplication. The duplication process stipulates that every branch of the track that reached the level should be split. The track importance being greater than the splitting level, at least one of

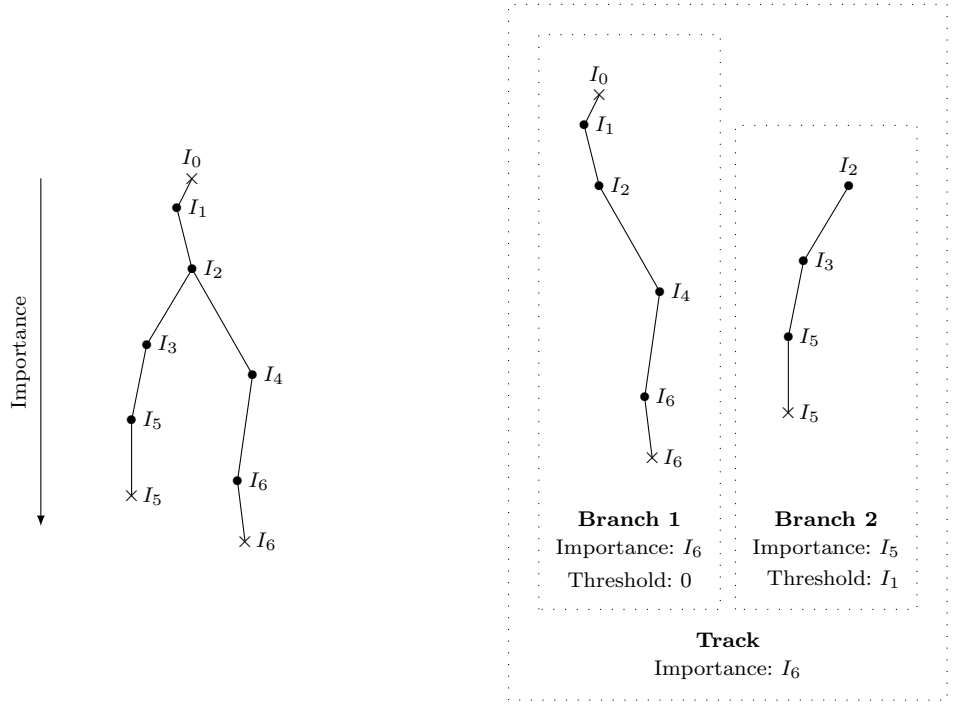

(a) Simulated history **(b)** Stored track

Figure 6.6. Example of branching track storing using the tree-type track structure

its branches will be duplicated. One can determine whether or not a given branch has actually reached the splitting level using only the importance of the branch and its threshold value. Three scenarios are possible:

1. The splitting level is less than the threshold of the branch. This implies that when the corresponding particle was generated, its parent particle had already an importance greater than the level. The branch should therefore not be duplicated. This corresponds to the "Primary track splitting" situation described in the previous section.

2. The splitting level is greater than the branch threshold but less than the branch importance. Either the particle has been produced by a parent which had not yet reached the splitting level, or it is a source particle which reached the level during its transport. The first point of the branch whose importance is above the level is then defined as splitting point.

3. The splitting level is greater than the branch importance. In that case, the particle history has been terminated before reaching the splitting level and the branch is not duplicated.

A new track is instantiated to hold all duplicated branches. Each of those branches is initialized with the corresponding splitting point, and both the branch importance and threshold are set to the value of this point importance. The branch is then filled by transporting a particle from this point until the termina-

tion of its history.

In a configuration without branching events, we can see that the algorithm behaviour is identical to the previous AMS implementation. The only difference is that the points previously stored in the track structure are now contained in branches embedded in the tracks, but with a single branch per track. This has no impact on the simulation, apart from a small change in the storing process. The computational time overhead induced by the tree-type track structure is however negligible with regard to the global AMS cost.

6.4 Gamma-ray spectrometry

The problem considered to validate the use of AMS as a variance reduction method in simulations requiring precise branching tracks handling is the modelling of a measurement station for sodium spectrometry. It is a reproduction of the geometry proposed in [25]. We recall that the score of interest in spectrometry simulation is a pulse-height tally, which is a non-Boltzmann score.

6.4.1 Objective and setup

The geometry is composed of a sodium sample opposite a High-Purity Germanium detector (HPGe). Both are encased in a lead chamber, whose role is to cut off external radiation. The only photon source is therefore the sodium sample. The lead walls of the chamber are coated with a 2-mm-thick copper film. The modelled measurement station is shown in Figure 6.7. The detector is an accurate model of the HPGe Canberra GR2021 detector, and the sodium sample is placed 22 cm away from the detector, so as to maximize the count rate [25]. The photon emission lines of the sodium sample, which will be used as source term for the simulation, are shown in Table 6.1.

Energy (MeV)	Intensity
0.9966	0.000021
1.368626	0.999936
2.754007	0.99855
2.871000	0.0000025
3.866220	0.00074
4.238900	0.0000084

Table 6.1. Simulated photon emission lines of the sodium sample for the spectrometry simulation.

The purpose of the simulation is to reproduce the HPGe detector response. Within the simulation, the corresponding score is a spectrum that registers for each source particle the energy deposited in the germanium crystal by all the secondary particles of its progeny. This can be estimated using a pulse-heigh tally. InFigure 6.7, the germanium crystal is shown in dark cyan. As we aim to

test the AMS algorithm in a realistic case, we decided to explicitly simulate electrons and positrons alongside photons in this problem. In this configuration, each source photon generates on average 17 secondary particles (photons, electrons and positrons combined).

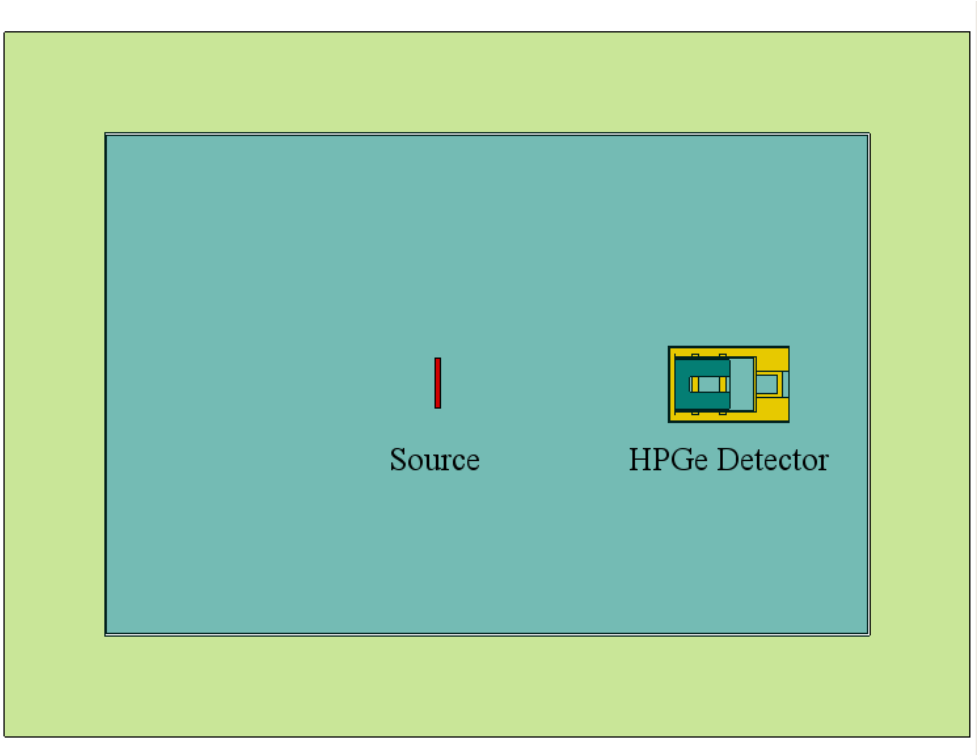

Figure 6.7. Gamma-ray spectrometry setting

6.4.2 AMS results and efficiency

As previously mentioned in Section 6.1, the Exponential Transform method can not be used to reduce the variance on this type of scores. The AMS results presented in the following will therefore be compared only to analog results. The INIPOND module is only able to compute importance maps for neutrons or photons, so the INIPOND photon maps were also used as importance functions for electrons and positrons.

Three AMS simulations (I_6^+, I_4^+ and one with the purely spatial importance I_S) were run alongside an analog simulation. In this case, I_S was defined as the reciprocal of the distance to the center point of the detector (see Section 4.2.3). All simulations used 10^4 source photons per batch, and the AMS k parameter was set to 100. The energy depositions in the germanium crystal were collected during 5 days (CPU time). The energy range between 1E−11 and 8 MeV has been divided into 1600 bins in which the energy depositions were counted. The resulting spectrum, normalized by the number of source photons, is shown in Figure 6.8.

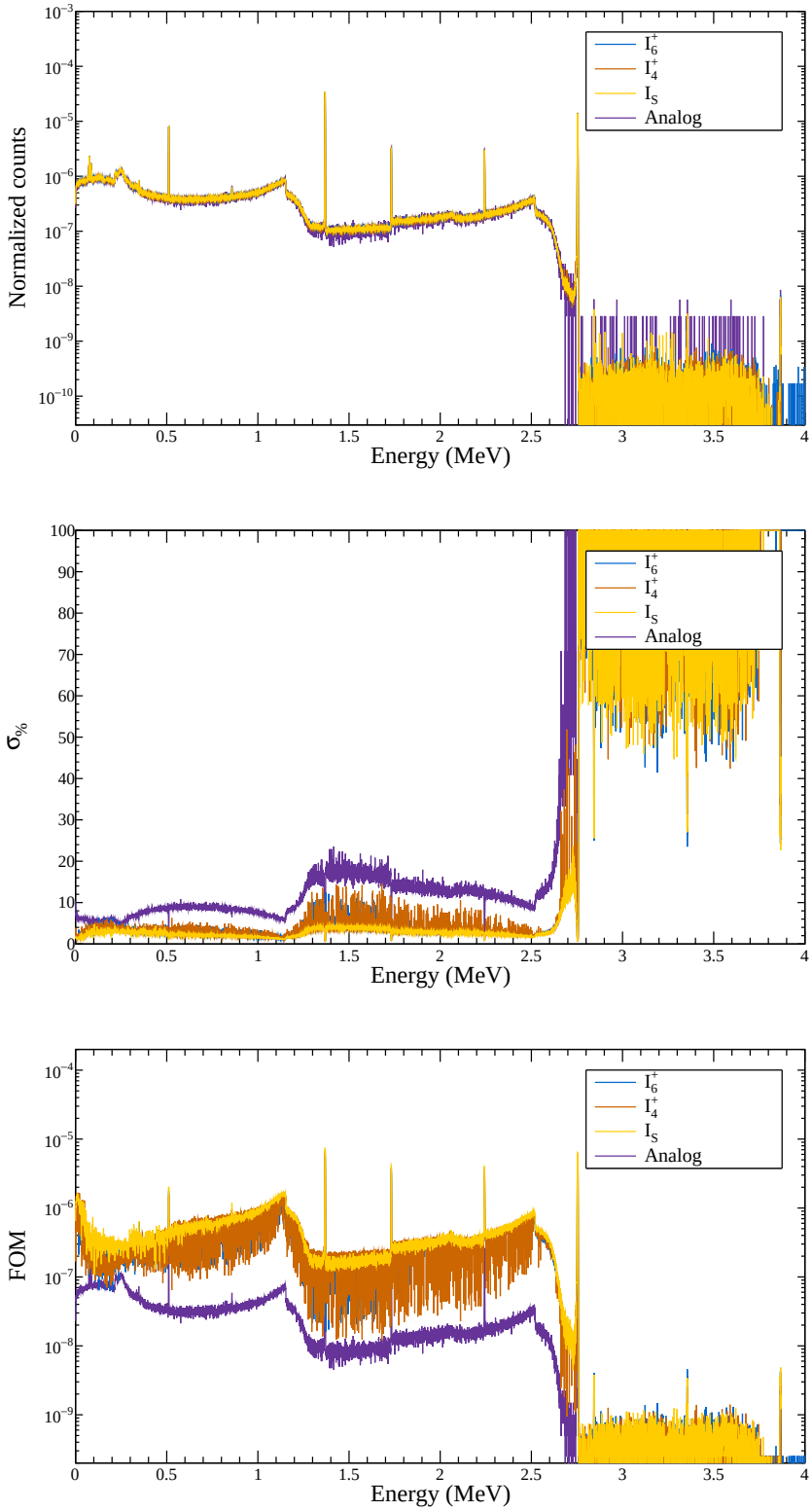

Figure 6.8. Photon spectrum obtained with AMS compared to an analog simulation. Upper to lower: counts normalized by the number of simulated source particles, relative standard error, and FOM.

We can see in the top frame of Figure 6.8 that all four spectra are perfectly superimposed. As they are plotted without confidence intervals, we can observe how the three AMS spectra are far less noisy than the analog spectrum, especially at energies greater than 1 MeV. On the far right side of the spectrum, we observe that all AMS simulations were able to simulate events leading to high-energy depositions that the analog simulation was completely unable to estimate.

The middle frame of the figure shows that the relative standard errors produced by the AMS simulations are smaller than the analog ones in every energy bin for the same computation time, showing that the AMS algorithm is a suitable variance reduction scheme for gamma-ray spectrometry simulations. The resulting FOM gain over the analog simulation is approximately 10 for the AMS calculation using the INIPOND map I_6^+, and up to 30 with the purely spatial importance.

The higher efficiency we managed to reach with the AMS came from the use of a simple spatial importance function. This confirms that the INIPOND importance maps are often not well suited for AMS use. However, the automated generation of an importance map still allows for a great efficiency improvement over the analog simulation.

In order to increase our confidence in the AMS results, we now focus our attention on a specific peak in the photon spectrum, which can only be obtained with a correct treatment of track branching. The 511 keV peak is due to photons of precisely 511 keV being absorbed in the germanium crystal and depositing all their energy therein. Those photons come from positron-electron annihilations. Like all charged particles, a positron continuously loses energy during its transport. At one point, its energy becomes so low that any interaction with an electron of the surrounding medium results in the annihilation of both particles. This process results in the emission of two photons, each with an energy of 511 keV, which are emitted in opposite directions.

Since the particle source of our problem is a photon source, 511 keV photons are necessarily secondary particles emitted by secondary positrons. Therefore, their branches belong to tracks that have branched *at least* twice.

We show in Figure 6.9 the 511 keV peak of the spectra presented in Figure 6.8. The top plot of the figure shows the mean counts of energy around 511 keV with associated 68% confidence intervals. We can observe on this plot that the results obtained by all simulations are in agreement, which illustrates the validity of the method we propose to handle branching tracks in AMS.

This study illustrated the ability of our AMS implementation to yield unbiased results with a reduced variance in situations that require the explicit treatment of branching processes. However, the limitations of the INIPOND module to photons and neutrons prevented us from testing the AMS with distinct importance

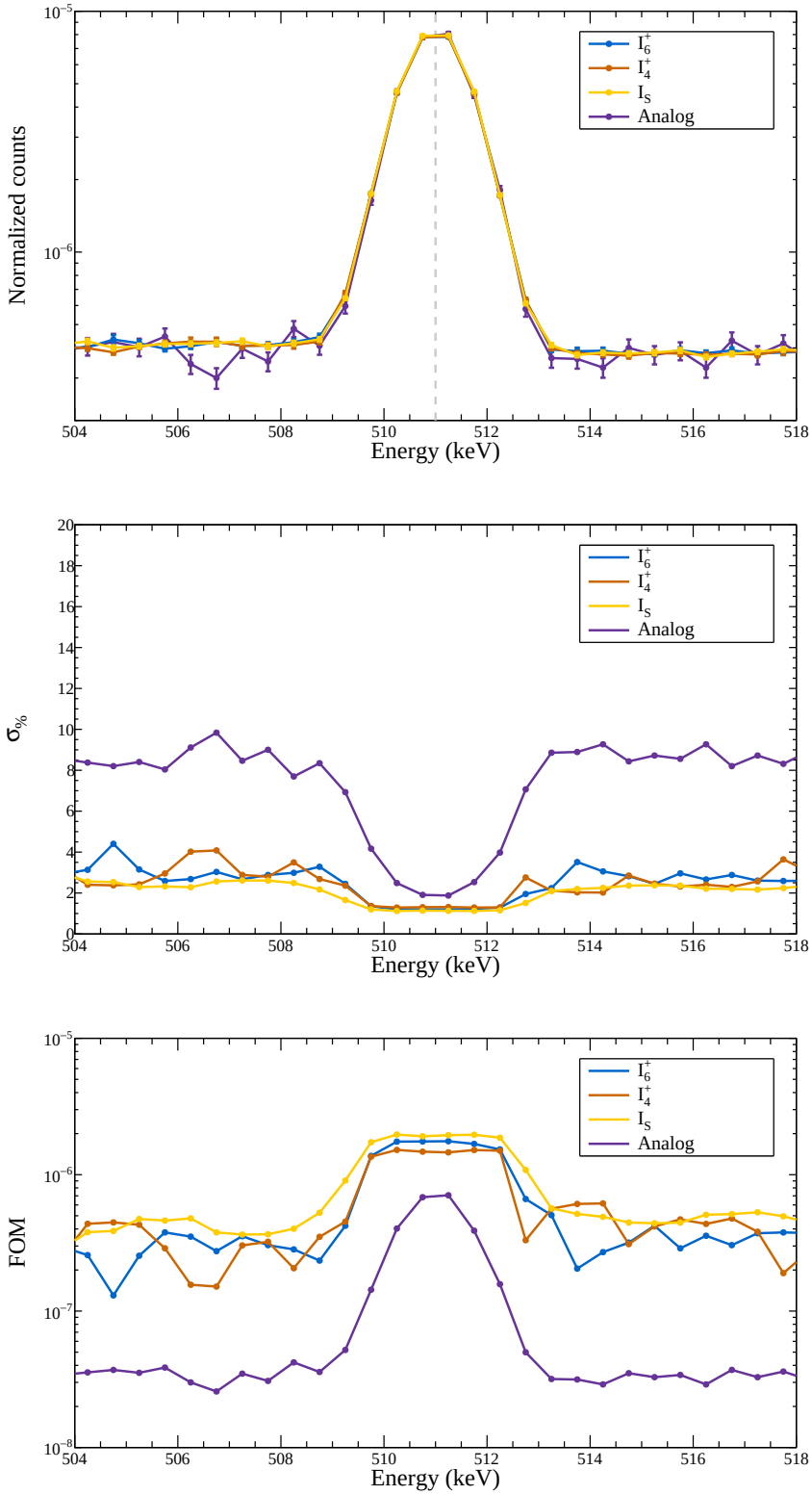

Figure 6.9. 511 keV peak of the photon spectrum for AMS and Analog simulations. Upper to lower: mean flux with 68% confidence intervals, relative standard error, and FOM.

functions for each particle type. Therefore, we decided to test this option on a neutron-photon coupled simulation.

6.5 Neutron/photon coupled calculation

When it comes to branching tracks and variance reduction, one of the situations that is commonly encountered in shielding applications is neutron-photon coupled simulation, in which the purpose is to estimate a photon score in a simulation where the source particles are neutrons.

6.5.1 Variance reduction in coupled simulations

The difficulty with coupled simulations is to find a proper way to implement variance reduction. In the case of neutron-photon simulations, the variance reduction scheme can be applied only to neutrons, only to photons, or to both particle types.

The AMS implementation with tree-type track structures enables multiple ways of dealing with coupled simulations: indeed, it is possible to prevent primary particles from generating new branches in the primary particle track. Thus, in the case of a neutron-photon simulations, the secondary photons would be left out of the track structure, and the algorithm applied only to neutrons. The eventual contributions scored by the secondary photons can then be considered as contributions attached to the neutron collision that generated the photons. It is also possible to perform an analog neutron simulation, and to build new AMS tracks only for secondary photons before launching the AMS iterations. In that case, AMS would only apply to photons.

Another possibility is to add both neutrons and photons to the track structures, but use different importance functions depending on the particle type. This last possibility should be the most efficient, but the difficulty lies in defining a good importance function for neutrons, since the most important neutrons in a coupled neutron-photon simulation are those that are most likely to produce interesting photons. The optimal neutron importance in this case should therefore take into account the photon production in all modelled materials.

This issue has already been studied in TRIPOLI-4, which was provided with a tool to compute a neutron importance map as the product of the photon importance with the photon production probability [26]. This coupled importance map could be a good candidate as neutron importance function to optimize the AMS for coupled neutron-photon simulations.

6.5.2 Coupled problem description

In this section, we test the new AMS implementation abilities in reducing the variance for a given coupled neutron-photon problem. The considered problem is the same as was used in [26] to investigate the variance reduction efficiency of

TRIPOLI-4 for coupled neutron-photon simulations. That study found an optimized biasing scheme for TRIPOLI-4 that allowed for a variance reduction using the Exponential Transform method. The AMS results presented in this section will therefore be compared to the optimized configuration.

The problem consists of an isotropic neutron source with a Watt emission spectrum, placed in a paraffin collimator which is separated from a detector by 10 slabs composed of either polyethylene or stainless steel. The slabs are disposed alternately, except for two successive slabs of polyethylene, as shown in Figure 6.10. The whole system is enclosed in an air-filled box with leakage boundary conditions. The score we are interested in is a photon dose in the detector region.

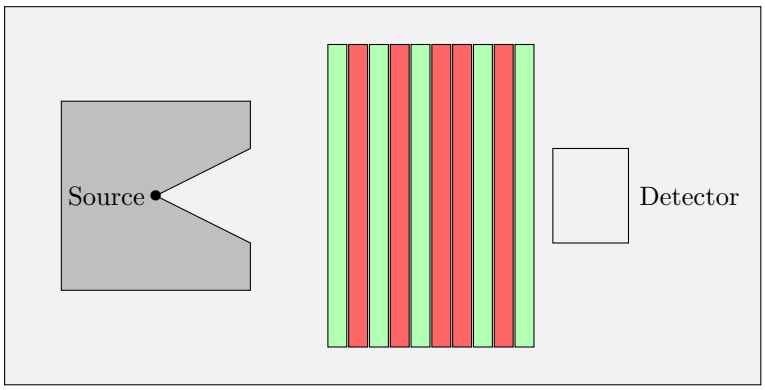

Figure 6.10. Geometry for the coupled neutron-gamma problem. The stainless steel slabs are shown in green and the polyethylene slabs in red.

6.5.3 Importance functions

For this problem, seven distinct importance functions were used:

- the purely spatial importance function I_S, defined for each point as the reciprocal of the distance to the center of the detector

- the neutron importance maps I_6^n and I_4^n computed by the INIPOND module (with and without angular dependency)

- the photon importance map I_6^p and I_4^p computed by the INIPOND module (with and without angular dependency)

- the coupled importance map I_6^c and I_4^c computed by the INIPOND module (with and without angular dependency)

The photon importance maps I_6^p and I_4^p are built by INIPOND using the same algorithm as for neutrons importance maps, but with photon cross sections. The

coupled importance maps I_6^c and I_4^c are actually neutron importance functions, which are computed for any point $(\vec{X}, \vec{\Omega})$ of the energy group g as:

$$I_6^c(\vec{X}, \vec{\Omega}, g) = \sum_{g'} \left[\Gamma_{g'}\big(\vec{X}, g\big) \times I_6^p\big(\vec{X}, \vec{\Omega}, g'\big) \right] \tag{6.1}$$

and

$$I_4^c(\vec{X}, \vec{\Omega}, g) = \sum_{g'} \left[\Gamma_{g'}\big(\vec{X}, g\big) \times I_4^p\big(\vec{X}, \vec{\Omega}, g'\big) \right], \tag{6.2}$$

where $\Gamma_{g'}(\vec{X}, g)$ is the production probability of group-g' photons for a neutron at point $\vec{X}$ and within energy group g. The photon production probabilities are related to the photon multiplicities, which are tabulated values available in the nuclear data libraries alongside cross sections.

6.5.4 Results

Using those seven functions, we ran 9 AMS simulations with $k = 1\%$ and various importance parametrizations, which we denote by pairs $(I_1 - I_2)$, where I_1 the importance function used for neutrons and I_2 the importance used for photons. The parametrizations $(. - I_2)$ correspond to AMS applied on photons only with importance I_2, after an analog neutron transport.

Two simulations were performed using the Exponential Transform method. One of them used importance I_6^p to bias the photon transport, leaving the neutron transport unaltered. The other was a reproduction of the most efficient parametrization found by Petit et al. in [26]. It consists of using I_6^p to bias the photon transport while increasing by a factor 10 the photon production in the stainless steel slabs.

All simulations ran simultaneously for 15 h, and the obtained results are gathered in Table 6.2, in which the best parametrization of the Exponential transform is denoted $\Gamma \times 10$.

We can see that all estimated results are in perfect agreement. Furthermore, the AMS algorithm efficiently reduces the variance for every parametrization (the FOM gain over the analog simulation is always greater than one). The AMS parametrization that yielded the most interesting results in terms of variance reduction is (I_S - I_S), where the purely spatial importance is used for both neutrons and photons. In this case, the FOM is almost 80 times greater than the analog simulation and more than 20 times greater than the best Exponential Transform result.

A comparison of the results obtained with parametrizations (I_S - .), (. - I_S) and (I_S - I_S) exhibits the difficulty in applying a reduction variance scheme

Type	Parametrization	Dose Rate	Relative Error (%)	FOM Gain
Analog	N/A	1.06e+03	6.31	1.00
E.T.	$\Gamma \times 10$	1.03e+03	3.37	3.50
	I_6^p	1.07e+03	5.91	1.14
AMS	I_S - I_S	1.04e+03	0.71	79.51
	I_6^n - I_6^p	1.02e+03	2.02	9.73
	. - I_S	1.01e+03	2.06	9.39
	I_6^p - I_6^p	1.03e+03	2.24	7.97
	. - I_6^p	1.04e+03	2.64	5.70
	I_4^p - I_4^p	1.05e+03	3.10	4.14
	I_4^n - I_4^p	1.10e+03	2.91	4.70
	. - I_4^p	1.04e+03	3.46	3.33
	I_S - .	1.01e+03	3.61	3.05
	I_4^c - I_4^p	1.06e+03	3.72	2.88
	I_6^c - I_6^p	1.08e+03	5.67	1.24

Table 6.2. Estimated photon dose rate (in µSv/h) for the coupled neutron-photon problem.

to a coupled problem. The (I_S - .) parametrization is 3 times more efficient in estimating the photon dose rate than the analog simulation, although it does not resample the secondary photons simulated during the neutron iterations. On the other hand, keeping the neutron tracks unchanged and resampling the photons improves the estimation efficiency over the analog simulation by a factor 9. By applying a variance reduction scheme on both particle types (I_S - I_S), we are able to obtain a FOM gain 10 times greater than that.

Once again, the most efficient estimation is given by an AMS simulation that uses purely spatial importance functions. This seems to indicate a poor energy treatment in the importance map generated by the INIPOND module. In order to investigate this more thoroughly, we present in Table 6.3 the dose rate estimations restricted to several energy ranges for some of the simulations presented above.

Our first observation is that all results are in agreement regardless of the energy range. We can see that the most energetic group accounts for most of the integrated dose rate (around 84%). It is therefore not surprising that the FOM gains computed in this group are close to those obtained for the total dose rate. However, there is some information to derive from the results in the lower energy ranges.

If we focus on comparing the FOM gain evolution with regards to the energy group for each of the simulations, we can see that when using a purely spatial importance function, the AMS efficiency is greater in the lowest energies. This makes sense, since the use of a spatial importance favours the particles that are

Energy Range	Simulation	Dose Rate	Error (%)	FOM Gain
	Analog	8.97e+02	7.27	1.00
	E.T.($\Gamma \times 10$)	8.81e+02	3.56	4.16
E >1 MeV	AMS ($I_S - I_S$)	8.73e+02	0.81	80.38
	AMS (I_6^n - I_6^p)	8.46e+02	2.24	10.52
	AMS (I_S - .)	8.74e+02	3.96	3.36
	Analog	1.65e+02	8.01	1.00
	E.T.($\Gamma \times 10$)	1.51e+02	8.49	0.89
$E \in$[100 keV,1 MeV]	AMS ($I_S - I_S$)	1.68e+02	0.46	309.8
	AMS (I_6^n - I_6^p)	1.75e+02	4.26	3.55
	AMS (I_S - .)	1.74e+02	6.03	1.77
	Analog	6.95e-01	100	1.00
	E.T.($\Gamma \times 10$)	2.02e-01	25.74	15.11
E <100 keV	AMS ($I_S - I_S$)	2.22e-01	2.74	1334
	AMS (I_6^n - I_6^p)	1.19e-01	21.37	21.93
	AMS (I_S - .)	1.88e-01	44.4	5.07

Table 6.3. Energy repartition of the photon dose rate (in µSv/h) for the coupled neutron-photon problem.

the closest to the detector area, which are most likely those that have the lowest energies, since they are farther from the source point. This illustrates how the AMS could be even more efficient, if it were to optimize the simulation efficiency in groups that matter the most. On the other hand, focusing on the results obtained with the INIPOND importance maps, we can see that the FOM gain drops in the intermediate energy range regardless of the variance reduction method. For the Exponential Transform simulation, it is even lower than 1 in that group. This clearly indicates a bad treatment of the energy dependency of the problem by the INIPOND module.

It is worth noting that the discrepancies in the FOM gains between energy groups is only a *symptom* of a bad energy representation in the importance map, and it does not give enough information to design a better importance function. Indeed, if the estimate in a given energy group has a greater variance than the other estimates within the detector area, it is not necessarily the importance values in that group that are incorrect. The error most likely originates from wrong importances in a higher energy range and in an area outside of the detector.

In addition to the photon results, we also show in Table 6.4 the neutron dose rate estimated in the detector during the same simulations. Even if the purpose of the problem was to reduce the variance on the photon dose rate, it is still interesting to see that most AMS simulations were able to correctly estimate the neutron dose rate in the same simulation. What is more, some of the AMS simulations even managed to reduce quite effectively the variance of

Type	Parametrization	Dose Rate	Relative Error (%)	FOM Gain
Analog	N/A	2.96e+03	13.66	1.00
E.T.	$\Gamma \times 10$	3.04e+03	15.89	0.74
	I_6^p	2.12e+03	17.67	0.60
AMS	I_S - .	2.90e+03	1.25	119.12
	I_S - I_S	2.98e+03	1.27	116.39
	I_6^n - I_6^p	3.04e+03	6.62	4.27
	I_6^p - I_6^p	3.28e+03	15.86	0.74
	I_4^n - I_4^p	3.14e+03	13.72	0.99
	I_4^p - I_4^p	3.27e+03	11.86	1.33
	I_6^c - I_6^p	2.24e+03	25.17	0.30
	. - I_4^p	2.64e+03	20.03	0.47
	I_4^c - I_4^p	4.16e+03	26.15	0.27
	. - I_6^p	3.30e+03	15.26	0.80
	. - I_S	3.35e+03	17.53	0.61

Table 6.4. Estimated neutron dose rate (in µSv/h) for the coupled neutron-photon problem.

the neutron score as well as the photon score. It should be kept in mind that the Exponential Transform results presented in Table 6.4 come from simulations that were parametrized to optimize the photon score, which probably explains the low FOM that were obtained.

The study of this problem confirmed the ability of the AMS algorithm to reduce the variance in simulations presenting branching processes. We showed that the AMS can use a distinct importance function for each particle type, and illustrated once again how a simple spatial importance function allows for an efficient estimation of the result. However, we also highlighted the need for an importance-generating tool more suited to the use of the AMS algorithm than the INIPOND module.

6.6 Conclusion

In this section we proposed a method that allows the AMS to be applied on branching processes and presented the necessary modifications to be implemented in TRIPOLI-4 for the AMS algorithm to handle branching tracks.

This new ability of the AMS in TRIPOLI-4 was at first validated using a photon-electron-positron spectrometry simulation. Not only did we show that our AMS algorithm yielded an unbiased estimation of the score over the entire energy range, but we showed that the estimation of a non-Boltzmann score did not damage the AMS performance as a variance reduction technique, and we observed a drastic increase of the FOM for both INIPOND and purely spatial importances (up to 30 times greater than the analog FOM over the entire spectrum).

After validating the AMS efficiency in simulations containing branching particle trajectories, we decided to use the AMS algorithm in a common challenging configuration for variance reduction methods in radiation shielding simulations, and tested the AMS efficiency in a coupled photon-neutron simulation. The results of this study showed that the algorithm was a suitable variance reduction method for such configurations. We demonstrated the robustness of the AMS with regard to the importance function as well as the new possibility of using distinct importances for primary and secondary particles in the presence of branching events.

In its current state, the AMS algorithm can now be used in TRIPOLI-4 for any fixed-source particle transport simulation, without limitations on the type of scores nor on the geometry.

Conclusion and perspectives

The purpose of this Ph.D. was to study the applicability of the Adaptive Multilevel Splitting algorithm as a variance reduction scheme for Monte Carlo particle transport.

To that end, the algorithm was first reformulated to fit the frame of particle transport. In order to validate this adapted version of the algorithm, a Monte Carlo transport prototype able to use the AMS algorithm was developed (See Chapter 3). The MENHIR prototype was designed to estimate a particle flux in a very specific geometry, with enough simplifications to allow for an analytical computation of the result. The comparison of results obtained with AMS relative to the analytical reference flux showed that the AMS was able to give unbiased estimations of the flux regardless of the algorithm parametrization, just as predicted by the theory. Using MENHIR in both AMS and analog transport modes, we were able to assess the abilities of the AMS algorithm as a variance reduction scheme for Monte Carlo particle transport. The comparison of the Figures Of Merit demonstrated that the AMS algorithm could indeed be a viable variance reduction method for Monte Carlo particle transport in configurations in which rare event simulation is required to have a precise estimation of the score.

These preliminary results paved the way for the implementation of the AMS algorithm in a production Monte Carlo transport code. The method was therefore implemented in the transport code TRIPOLI-4® (See Chapter 4). A bypass geometry was used as a first test case to validate the implementation of AMS in this new context, which showed that the use of AMS could improve the efficiency of the score estimation by a factor 600 compared to an analog simulation. In this case however, the Exponential Transform method, which is the current reference variance reduction scheme of TRIPOLI-4, turned out to be more efficient in reducing the variance than the AMS algorithm.

The bypass geometry was a configuration that enabled us to confirm that the AMS algorithm was indeed an interesting variance reduction scheme. However, the first implementation of AMS in TRIPOLI-4 did not take full advantage of the algorithm possibilities, among which is the ability to estimate scores outside the

AMS target area. We derived from the applied mathematics theoretical formulation of the AMS estimator an on-the-fly scoring method that enabled multi-zone scoring during the AMS iterations (Chapter 5). We illustrated this new feature through the study of two typical shielding problems: a deep-penetration configuration and a streaming simulation. In both cases, the AMS turned out to be an efficient way of reducing the variance on score estimations both inside and outside of the target area. The deep-penetration problem demonstrated the robustness of the AMS algorithm with regard to the importance function, while the 3D-streaming configuration showed the AMS variance reduction capabilities in a problem for which the use of the Exponential Transform method was of no help.

This improved implementation of the AMS in TRIPOLI-4 allowed for unbiased scoring of multiple scores in multiple locations of the geometry. The algorithm could however not be used in every situation, as it was unable to handle branching trajectories, which are common in Monte Carlo particle transport simulations. Branching particle trajectories can result for example from particles travelling in a multiplying medium, or in coupled simulations in which particles of multiple types are simulated. As the problem of branching processes in the AMS algorithm is not addressed in the literature, we proposed in Chapter 6 an innovative method that enables the AMS algorithm to deal with branching trajectories.

After adequately modifying the AMS implementation in TRIPOLI-4 so as to handle branching trajectories, the upgraded AMS algorithm was used to reduce the variance for a gamma-spectrometry simulation, which is a situation in which most weight-based variance reduction schemes are either not usable or require heavy modifications. The final AMS implementation in TRIPOLI-4 is however directly applicable in those configurations. Thus, we validated our branching track handling procedure, and we illustrated the ability of the AMS in reducing the variance even on such non-Boltzmann scores. Last, we considered a coupled neutron-photon simulation, in which we were interested in a photon score with a neutron-source simulation. The results presented in the last section of this thesis showed that the AMS was able to efficiently reduce the variance in this new context, and even allowed for the use of various importances for distinct particle types.

The studies presented in this thesis, alongside all the tests performed during this Ph.D., show that regardless of the importance function, either purely spatial or provided by an INIPOND calculation, the AMS algorithm is always able to estimate the score of interest with increased efficiency as compared to an analog simulation. However, we saw that the additional knowledge supposedly brought by INIPOND-generated maps did not always improve the AMS efficiency. It should be kept in mind that the INIPOND module is a tool designed for use by the Exponential Transform method. The importance maps it provides are based on assumptions that are not always suited to other importance-based variance reduction methods. For example, the INIPOND maps do not take into account the slowing down of particles during transport, which often leads to mistreatment

of the energy-dependence in the importance maps by assigning too great an importance to higher energy groups. Within the AMS algorithm, this issue can lead to illegitimate resampling of low-energy particles in favor of high-energy particles, even in configurations in which the particles need to lose energy in order to reach the detector.

As of today, there is no proof that the optimal importance map for AMS in a given particle transport problem is the adjoint score. Our guess is that it is most likely a function related to the adjoint problem, either the adjoint score or the adjoint probability of reaching the detector area. Further theoretical work around the AMS algorithm could provide clues to answer this question. In the meantime, it would be of great interest to study the AMS efficiency using high-quality importance functions, even if it requires the use of a third-party software to be computed (i.e. a software developed outside of the TRIPOLI-4 project). Once the optimal importance function is found, it should be possible to implement a specific module to compute an estimation of this importance function especially designed for AMS use.

Another possibility is to use the many tracks simulated during the AMS iterations in order to improve the quality of the importance map at the end of each batch. The AMS can indeed be used to build a genealogy of particle histories going from the source to the detector, with associated occurrence probabilities. One can then derive an estimation of the adjoint score for every point of the genealogy, as the average score generated by particles that have passed by those points, and use this knowledge to correct errors in the importance map. This step-by-step importance map improvement could for example be performed through machine learning algorithms.

Résumé

Contexte de l'étude

Le comportement des particules neutres qui se déplacent dans de la matière peut être décrit physiquement par un processus stochastique. C'est ce processus qui est reproduit dans les simulations de transport de particules utilisant la méthode Monte-Carlo. Les codes utilisés pour simuler le transport Monte-Carlo de particules ont deux modes de fonctionnement : criticité ou source fixe. Les simulations de criticité reproduisent la réaction en chaîne de la fission nucléaire et s'appuient sur des itérations sur la puissance pour étudier la physique du cœur, tandis que les calculs à source fixe sont utilisées pour traiter des problèmes de radioprotection, de vieillissement et de démantèlement.

L'objectif des simulations de radioprotection est l'estimation d'un flux de particules dans une zone d'intérêt, ou bien de quantités dérivées de flux telles que des taux de réactions ou des dépôts d'énergie. Dans une simulation donnée, la quantité estimée est souvent appelée "score" ou "tally". Les configurations étudiées dans les simulations de radioprotection sont souvent associées à l'étude de problèmes à forte atténuation, auquel cas les particules simulées ont une probabilité très faible de contribuer au score. Le nombre de particules qu'il est nécessaire de simuler devient alors trop grand pour espérer avoir une estimation précise du score en un temps de calcul raisonnable. Dans ce contexte, les méthodes de réduction de variance se proposent de modifier le processus de transport des particules afin d'augmenter la probabilité d'occurrence des évènements rares, tout en conservant une estimation non biaisé du score. Ainsi, elles permettent de réduire la variance sur l'estimation du flux pour un temps de calcul donné.

Dans cette optique, les méthodes dites de *multilevel splitting* furent introduites par Kahn et Harris [1]. Leur principe est d'augmenter le nombre de particules simulées à proximité des zones d'intérêts de la simulation. En pratique, l'espace de la simulation est divisé en régions d'importance, délimitées par des frontières virtuelles appelées *niveaux de splitting*. Lorsqu'une particule simulée passe d'une région de moindre importance à une région d'importance plus élevée, elle est dupliquée. Chacune des particules résultante de la duplication se voit attribuer la

moitié du poids statistique de la particule initiale, afin que la simulation reste non-biaisée. En utilisant ces techniques, le temps de calcul est alloué à la simulation de particules dont les trajectoires semblent intéressantes, c'est-à-dire susceptibles de contribuer au flux, plutôt qu'à la simulation de particules générées à la source. Un des avantages de ces méthodes, par comparaison aux autres techniques existantes, est qu'elles permettent de ne pas altérer le transport des particules entre les évènements de splitting. En effet, le transport de particules entre les régions d'importance reste analogue, ce qui permet de garder la physique sous-jacente intacte. Le problème inhérent à ces méthodes de splitting est qu'elles nécessitent une connaissance précise du problème afin de définir les régions d'importance de manière efficace. Il faut s'assurer que suffisamment de particules changent de région pour avoir un effet perceptible sur la variance du flux estimé, mais un découpage du problème en régions trop petites entraînerait une explosion de la population de particules à simuler.

Ce problème a été contourné dans le domaine des mathématiques appliquées, où une méthode appelée Adaptive Multilevel Splitting (AMS) a été proposée par Cérou et Guyader [2], puis étudiée dans une configuration plus générale par Bréhier et al. [3]. Cette méthode, qui a également pour objectif de dupliquer les particules ayant des trajectoires intéressantes, s'affranchit de la définition de régions d'importance en amont de la simulation. À la place, les niveaux de splitting sont déterminés à la volée durant le processus de simulation, suivant un mécanisme de sélection basé sur la classification des trajectoires de particules déjà simulées. Cependant, cet algorithme n'a jamais été appliqué à la simulation du transport de particules. Elle pourrait pourtant s'avérer utile pour les configurations nécessitant une simulation précise d'évènements rares.

La méthode AMS

L'algorithme AMS présenté par la suite est une version condensée de l'algorithme adapté au transport Monte-Carlo de particules mis en place durant cette thèse. Dans ce contexte, le processus itératif de l'AMS s'enclenche après une phase d'initialisation constituée d'une simulation analogue de n particules, c'est-à-dire une simulation n'utilisant pas de méthode de réduction de variance. Puis, chaque itération de l'algorithme contient deux phases : une de classement et une de rééchantillonnage. L'AMS dépend de deux paramètres : la *fonction d'importance* servant au classement des particules, et le nombre entier k utilisé pour définir le nombre de rééchantillonnage à effectuer à chaque itération. Le numéro de l'itération courante est notée q.

La phase de classement

Durant cette phase, la fonction d'importance est utilisée pour classer les trajectoires des particules simulées précédemment. À l'itération 1, les trajectoires prises en compte sont celles des particules analogues simulées durant l'initialisation. Lors des itérations suivantes, les trajectoires à classer seront celles provenant de

la phase de rééchantillonnage de l'itération précédente. La fonction d'importance associe à chaque point de l'espace des phases une valeur d'importance reliée à la probabilité pour une particule émise en ce point de contribuer au score final. L'importance d'une trajectoire de particule est alors définie comme l'importance maximale parmi celles des points la composant. Une fois l'importance de chaque trajectoire calculée, ces traces sont classées par ordre d'importance croissant.

Nombre de méthodes de réduction de variance reposent sur l'utilisation de fonctions d'importance. Néanmoins, l'AMS utilise l'importance de façon particulière, puisque l'importance n'est pas utilisée lors de la simulation, mais uniquement pour comparer les trajectoires les unes aux autres après que la simulation des particules les générant soit terminée. Ainsi, il n'est pas nécessaire que la valeur numérique de la fonction d'importance à un point donné ait un sens par elle-même. Cette propriété est l'une des forces de la méthode AMS, puisqu'elle permet l'utilisation de fonctions triviales comme importances, telles que l'inverse de la distance au point cible de la simulation.

Une fois les trajectoires des particules classées, un *niveau de splitting* est défini pour l'itération en cours. Il s'agit d'une valeur d'importance limite en deçà de laquelle les trajectoires seront rééchantillonnées durant la deuxième phase de l'itération. Le niveau de splitting est défini comme l'importance de la $k$ième trajectoire la moins bien classée. Les trajectoires des particules ayant une importance inférieure au niveau de splitting sont supprimées. Le nombre de trajectoires supprimées est nécessairement supérieur ou égal à k. À l'itération q, ce nombre est noté K_q.

La phase de rééchantillonnage

Durant cette phase, K_q nouvelles trajectoires de particules sont échantillonnées afin de remplacer celles supprimées à l'issue de la phase de classement. Ainsi, le nombre n de traces disponibles au début de l'itération $q+1$ reste inchangé.

Pour chacune des trajectoires à rééchantillonner, l'une des $n-K_q$ traces ayant survécu à la phase de classement est sélectionnée au hasard pour être dupliquée. La distribution de probabilité pour la sélection de la trajectoire à dupliquer est uniforme et avec remise. Le *point de splitting*, point d'émission de la nouvelle trajectoire, est défini comme le premier point le long de la trajectoire sélectionnée pour duplication dont l'importance est supérieure au niveau de splitting. La particule rééchantillonnée est ensuite simulée de manière analogue comme si elle avait été émise depuis ce point.

Le processus de rééchantillonnage duplique K_q particules parmi un ensemble de $n - K_q$ traces. De façon à conserver un résultat non-biaisé à l'issue de la simulation, tous les poids des particules doivent être pondérées à la fin de l'itération q par un facteur [2, 3] :

$$W_q = 1 - \frac{K_q}{n}$$

En pratique, le poids cumulé par les particules durant les itérations successives est le même pour toutes les particules, et est enregistré comme un poids global

$$\begin{aligned} w_q &= \prod_{i=1}^{q} W_i \\ &= \prod_{i=1}^{q} (1 - \frac{K_i}{n}). \end{aligned} \tag{6.3}$$

Fin des itérations

L'algorithme AMS s'arrête d'itérer à la fin de l'itération q si $n - K_q + 1$ particules ont atteint la zone d'intérêt. Pour n'importe quel score ϕ dans la zone d'intérêt, un estimateur AMS peut être construit. Si l'on dénote $\hat{\phi}_{MC}$ la valeur estimée utilisant un estimateur Monte-Carlo standard, alors

$$\hat{\phi}_{AMS} = w_q \times \hat{\phi}_{MC}$$

est un estimateur non biaisé de la quantité $\mathbb{E}(\phi(X))$ [3].

Application novatrice

Après avoir adapté la formulation de l'AMS aux spécificités du transport Monte-Carlo de particules, comme reproduit ci-dessus, un prototype de code de transport Monte-Carlo mettant en œuvre l'AMS a été développé (voir Chapitre 3) afin d'étudier l'applicabilité de cette méthode à un code de transport de particules. Le prototype MENHIR a été conçu pour estimer un flux de particules dans une géométrie très spécifique, avec un processus de transport suffisamment simplifié pour permettre un calcul analytique du flux. La comparaison des résultats de référence et de ceux obtenus par simulation AMS montre que la méthode de réduction de variance donne effectivement une estimation non biaisée du flux, et ce quelle que soit la paramétrisation de l'algorithme. MENHIR est également capable d'effectuer des simulations Monte-Carlo "analogues", c'est-à-dire sans appliquer de méthode de réduction de variance. En utilisant MENHIR à la fois en mode analogue et en mode AMS, nous avons également testé les capacités de l'AMS à réduire la variance sur le flux estimé. La comparaison de résultats obtenus par des simulations dans les deux modes pour un temps de calcul donné a démontré que l'AMS pouvait être une méthode de réduction de variance viable pour le transport Monte-Carlo de particules en présence d'évènements rares.

Ces résultats encourageants ont ouvert la voie à l'implémentation de l'AMS dans un vrai code Monte-Carlo de transport de particules. La méthode a donc été implémentée dans le code TRIPOLI-4® (voir Chapitre 4). Une première configuration test a été utilisée pour valider l'implémentation dans ce nouveau contexte.

Dans le cas considéré, l'atténuation provient de la nécessité par les particules de contourner un massif très absorbant pour atteindre la zone d'encaissement. L'étude de ce problème démontra que l'AMS implémenté dans TRIPOLI-4 permet d'augmenter l'efficacité d'estimation du score d'un facteur 600 par rapport à une simulation analogue.

L'étude du cas de contournement a permis de confirmer l'intérêt d'utiliser l'AMS dans des simulations de transport de particules à fortes atténuations. Cependant, la première version de son implémentation dans TRIPOLI-4 n'utilisait pas toutes les capacités de l'algorithme, parmi lesquelles la possibilité d'estimer des scores hors de la zone cible de l'algorithme. Depuis la formulation théorique de l'estimateur AMS, telle qu'introduite dans la littérature de mathématiques appliquées, nous avons mis en œuvre une méthode d'encaissement à la volée permettant l'estimation de scores dans plusieurs zones de la géométrie en une seule simulation AMS (Chapitre 5). Nous avons ensuite illustré les capacités de cette nouvelle implémentation par l'étude de deux problèmes typiques du domaine de radioprotection: un calcul d'atténuation du flux de neutrons dans une grande profondeur d'eau ("deep penetration"), et une configuration dite de "streaming", c'est-à-dire dans laquelle l'atténuation du flux provient de contraintes géométriques et non de la capacité d'absorption du milieu. Dans les deux études, l'AMS s'est montré efficace en tant que méthode de réduction de variance, à la fois pour les scores estimés à l'intérieur et à l'extérieur de la zone cible. La première configuration a été utilisée pour illustrer la robustesse de l'AMS vis-à-vis de la fonction d'importance, et la seconde a montré les capacités de réduction de variance de l'AMS dans un cas dans lequel la méthode de réduction de variance actuelle de TRIPOLI-4 est inutilisable.

Cette implémentation améliorée de l'AMS dans TRIPOLI-4 ne permettait pas encore l'utilisation de l'algorithme dans tout type de configurations, car la méthode était encore dans l'incapacité de traiter les trajectoires branchantes. Dans le contexte étudié, une trajectoire branchante peut par exemple résulter du transport d'une particule dans un milieu multiplicateur, ou encore d'une simulation couplée dans laquelle plusieurs types de particules sont simulées (neutrons, photons, etc.). La prise en compte des trajectoires branchantes par l'AMS est un sujet qui n'a jamais été abordé dans la littérature avant cette thèse. Nous avons donc mis en place une méthode innovante permettant à l'algorithme de manipuler ce type de trajectoires (Chapitre 6).

Après avoir modifié l'implémentation de l'AMS dans TRIPOLI-4 afin d'étendre le champ d'application de l'AMS aux trajectoires branchantes, l'AMS a été utilisé pour réduire la variance dans une simulation de spectrométrie gamma, qui est une situation dans laquelle les méthodes de réduction de variance usuelles sont soit indisponibles soit difficilement applicables. La version définitive de l'AMS dans TRIPOLI-4 est par contre utilisable directement dans cette configuration. Ainsi, nous avons validé notre procédure de prise en compte des trajectoires branchantes dans l'AMS, et avons également illustré la capacité de l'AMS à réduire

dans ce type de cas. Enfin, nous avons considéré une simulation couplée neutrons/photons, dans laquelle la quantité d'intérêt est un score photon alors que la source de particules émet exclusivement des neutrons. Les résultats obtenus montrent que l'AMS est capable de réduire efficacement la variance dans ce nouveau contexte, et permet même l'utilisation de fonctions d'importances dépendant du type de particules tout en restant non-biaisé.

L'ensemble des études de cas effectuées durant cette thèse ont montré que l'AMS est une méthode de réduction de variance efficace, et innovante par rapport aux méthodes classiques. Le travail effectué a abouti à une implémentation opérationnelle de la méthode AMS dans le code Monte-Carlo de transport de particules TRIPOLI-4®, dans lequel elle est appelée à devenir une alternative puissante à la méthode actuelle de la transformation exponentielle. Bien qu'ayant mis en avant certains cas dans lesquels la méthode de la transformée exponentielle est plus efficace que l'Adaptive Multilevel Splitting, nous avons démontré la simplicité de mise œuvre de l'AMS, ainsi que sa capacité à traiter des configurations extrêmement sévères ou de natures complexes dans lesquelles l'utilisation de la méthode actuelle est simplement impossible.

References

[1] Kahn, H. & Harris, T. E. "Estimation of particle transmission by random sampling." *National Bureau of Standards applied mathematics series*, 12:27–30 (1951).

[2] Cérou, F. & Guyader, A. "Adaptive multilevel splitting for rare event analysis." *Stochastic Analysis and Applications*, 25(2):417–443 (2007).

[3] Bréhier, C.-E., Gazeau, M., Goudenège, L., *et al.* "Unbiasedness of some generalized Adaptive Multilevel Splitting algorithms." *The Annals of Applied Probability*, 26(6):3559–3601 (2016).

[4] Reuss, P. *Précis de Neutronique* (EDP Sciences, Les Ulis, France, 2003).

[5] Bell, G. I. & Glasstone, S. *Nuclear reactor theory*, volume 252 (Van Nostrand Reinhold New York, 1970).

[6] Santamarina, A., Bernard, D., Blaise, P., *et al.* "The JEFF-3.1. 1 nuclear data library." *JEFF report*, 22(10.2):2 (2009).

[7] Chadwick, M., Obložinskỳ, P., Herman, M., *et al.* "ENDF/B-VII. 0: next generation evaluated nuclear data library for nuclear science and technology." *Nuclear data sheets*, 107(12):2931–3060 (2006).

[8] Reuss, P. & Bussac, J. "Traité de neutronique." *Hermann, Paris* (1985).

[9] Abramowitz, M. & Stegun, I. A. "Handbook of mathematical functions Dover Publications." *New York*, (361) (1972).

[10] Spanier, J. & Gelbard, E. *Monte Carlo Principles and Neutron Transport Problems* (Addison-Wesley Publishing Company, 1969).

[11] Woodcock, E., Murphy, T., Hemmings, P., *et al.* "Techniques used in the GEM code for Monte Carlo neutronics calculations in reactors and other systems of complex geometry." In: *Proc. Conf. Applications of Computing Methods to Reactor Problems*, volume 557, (2) (1965).

[12] Clark, F. H. "The Exponential Transform as an Importance-Sampling Device. A Review." Technical report, Oak Ridge National Lab., Tenn. (1966).

[13] Diop, C., Petit, O., Dumonteil, E., *et al.* "TRIPOLI-4: a 3D continuous-energy Monte Carlo transport code." *TRANSACTIONS-AMERICAN NUCLEAR SOCIETY*, 95:661 (2006).

[14] Both, J., Nimal, J., & Vergnaud, T. "Automated importance generation and biasing techniques for Monte Carlo shielding techniques by the TRIPOLI-3 code." *Progress in Nuclear Energy*, 24(1-3):273–281 (1990).

[15] Dieudonné, C. "Accélération de la simulation Monte Carlo du transport des neutrons dans un milieu évoluant par la méthode des échantillons corrélés." Ph.D. thesis, Université Paris Sud-Paris XI (2013).

[16] James, B. "Variance reduction techniques." *Journal of the Operational Research Society*, 36(6):525–530 (1985).

[17] Louvin, H., Dumonteil, E., Lelièvre, T., *et al.* "Adaptive Multilevel Splitting for Monte Carlo particle transport." *EPJ-N* (to be published).

[18] ISO, I. "IEC 14882: 2011 Information technology—Programming languages—C++." *International Organization for Standardization, Geneva, Switzerland*, 27:59 (2012).

[19] Glasserman, P., Heidelberger, P., Shahabuddin, P., *et al.* "A large deviations perspective on the efficiency of multilevel splitting." *IEEE Transactions on Automatic Control*, 43(12):1666–1679 (1998).

[20] Brun, E., Damian, F., Diop, C., *et al.* "Tripoli-4®, CEA, EDF and AREVA reference Monte Carlo code." *Annals of Nuclear Energy*, 82:151–160 (2015).

[21] Brun, E., Damian, F., Dumonteil, E., *et al.* "TRIPOLI-4 R Version 8 User Guide." Technical report, CEA Saclay (2013).

[22] Louvin, H., Dumonteil, E., & Lelièvre, T. "Three-dimensional neutron streaming calculations using Adaptive Multilevel Splitting." In: *International Conference on Mathematics and Computational Methods Applied to Nuclear Science and Engineering (M&C 2017), Jeju, Korea* (2017).

[23] Lathrop, K. "Ray effects in discrete ordinates equations." *Nuclear Science and Engineering*, 32:357–369 (1968).

[24] Booth, T. E. "Pulse-height tally variance reduction in MCNP." *Los Alamos Report LA-13955* (2002).

[25] Rohée, E. "Détection des ruptures de gaines sur RNR-Na par spectrométrie gamma hauts taux de comptage." Ph.D. thesis, Université de Caen Normandie (2016).

[26] Petit, O., Lee, Y.-K., & Diop, C. M. "Variance reduction adjustment in Monte Carlo TRIPOLI-4® neutron gamma coupled calculations." *Progress in Nuclear Science and Technology*, 4:408–412 (2014).

[27] Case, K. M., Placzek, G., & Hoffmann, F. "Introduction to the theory of neutron diffusion, v. 1." (1953).

APPENDIX AAPPENDIX A:

ANALYTICAL SOLUTION FOR MENHIR

The construction of an analytical solution for the problem simulated in MENHIR described in this appendix is derived from the works presented in [5] and [27], where the authors propose methods for computing the neutron density in uniform infinite medium with isotropic scattering and isotropic point source.

In MENHIR, an isotropic point source of monokinetic particles is located at point $(0, 0, 0)$, the medium is infinite and homogeneous with constant cross sections. The total cross section value is considered to be 1, and the only available reactions are isotropic scattering with probability σ_s and capture with probability $1 - \sigma_s$.

The source term Q can then be written

$$Q(\vec{r}, \vec{\Omega}) = Q(\vec{r}) = \frac{1}{4\pi}\delta(|\vec{r}|) \tag{A.1}$$

where δ is the Dirac delta function. The collision kernel $\mathcal{C}$ is reduced to

$$\mathcal{C}(\vec{X}, \vec{\Omega}' \to \vec{\Omega}, E' \to E\big) = \frac{\sigma_s}{4\pi} \tag{A.2}$$

Under those assumptions, we can derive from Equation (1.3) and expression for the particle flux at point $\vec{r}$:

$$\phi(\vec{r}) = \int e^{-|\vec{r}-\vec{r'}|}\frac{1}{4\pi|\vec{r}-\vec{r'}|^2}\delta(|\vec{r'}|)d\vec{r'} + \int e^{-|\vec{r}-\vec{r'}|}\frac{\sigma_s}{4\pi|\vec{r}-\vec{r'}|^2}\phi(\vec{r'})d\vec{r'}, \tag{A.3}$$

or equivalently

$$\phi(\vec{r}) = \int \left[\delta(|\vec{r'}|) + \sigma_s\phi(\vec{r'})\right]\frac{e^{-|\vec{r}-\vec{r'}|}}{4\pi|\vec{r}-\vec{r'}|^2}d\vec{r'}. \tag{A.4}$$

This last expression can be put in integrable form by the use of Fourier transforms. If we denote by $\psi(\vec{k})$ the Fourier transform of $\phi(\vec{r})$, such that

$$\psi(\vec{k}) = \int e^{i\vec{k}.\vec{r}}\phi(\vec{r})d\vec{r}, \tag{A.5}$$

then the Fourier transform of Equation (A.4) yields

$$\psi(k) = [1 + \sigma_s\psi(k)]\frac{\arctan k}{k},$$

so that

$$\psi(k) = \frac{1}{\frac{k}{\arctan k} - \sigma_s}. \tag{A.6}$$

Using the inversion formula, we obtain for the scalar flux

$$\phi(r) = \int_0^\infty r^{\frac{3}{2}} k^{-\frac{1}{2}} J_{\frac{1}{2}} \psi(k) dk, \tag{A.7}$$

where $J_{\frac{1}{2}}$ is the first kind Bessel function of order $\frac{1}{2}$.

The flux in a shell of inner radius r_1 and outer radius r_2 is therefore

$$\phi = \frac{3}{4\pi(r_2^3 - r_1^3)} \int_{r_1}^{r_2} \phi(r) dr, \tag{A.8}$$

which can be numerically computed using a mathematical symbolic computation program (Mathematica®in our case).

APPENDIX BAPPENDIX B:

THE INIPOND MODULE OF TRIPOLI-4

The INIPOND module of TRIPOLI-4 is designed to build importance maps for any problem, on a discretized phase space. The formula used to compute the importance in each cell of the mesh covering the geometry is derived from the expression of the importance in an infinite slab geometry.

B.1 IMPORTANCE FUNCTION FOR MONOKINETIC PARTICLES IN AN INFINITE SLAB GEOMETRY

Let us try and compute an importance value for a homogeneous infinite slab geometry. Let us assume that monokinetic particles are transported in this geometry, and that the score of interest is the probability to reach an infinite detector surface, defined as the plane of equation $x = 0$. The position of a particle is given by the coordinates $(\vec{X}, \vec{\Omega})$, where $\vec{X} = (x, y, z)$. In this configuration, the importance at a given point depends only on the distance between the point and the detector. We illustrate in Figure B.1 the relative position of a particle to the plane detector before and after a displacement of length s.

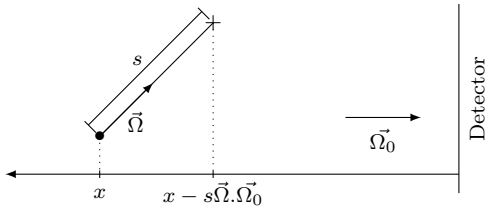

Figure B.1. Relative position of a particle to the detector area before and after displacement in the infinite slab geometry.

Let us denote by $I_b(\vec{X}, \vec{\Omega})$ the importance *before collision*, which is the importance of a particle entering a collision at spatial point $\vec{X}$ with direction $\vec{\Omega}$. We similarly define $I_a(\vec{X}, \vec{\Omega})$ as the importance *after collision*, referring to the importance of a particle having undergone a collision at spatial point $\vec{X}$ and coming out of this collision with direction $\vec{\Omega}$.

In order for the functions I_b and I_a to be consistent, we must ensure that the importance of a particle entering a collision is equal to the sum of the importances of all particles that could come out of it, and that the importance of a particle starting a flight at a given point is equal to the sum of the importances over all possible locations of the next collision point. Formally, we have:

$$I_b(\vec{X}, \vec{\Omega}) = \int C(\vec{X}, \vec{\Omega} \to \vec{\Omega}') I_a(\vec{X}, \vec{\Omega}') d\vec{\Omega}' \tag{B.1}$$

and

$$I_a(\vec{X},\vec{\Omega}) = \int D(\vec{X} \to \vec{X}',\vec{\Omega}) I_b(\vec{X}',\vec{\Omega}) d\vec{X}'. \tag{B.2}$$

Under the assumption of isotropic reactions, the importance before collision does not depend on $\vec{\Omega}$. Furthermore, the considered problem being symmetrical with regards to the y and z coordinates, the importance before collision is only dependent on the x coordinate. We place the origin of the coordinate system on the volume of interest, so that x increases with the distance to the detector, $x = 0$ being the detector frontier. Let us assume that the importance before collision at a given point $(\vec{X},\vec{\Omega})$ takes the form

$$I_b(\vec{X},\vec{\Omega}) = I_b(x) = e^{-\kappa x}, \tag{B.3}$$

where κ is a constant parameter of the medium, which will be determined in the following.

If we express requirement (B.2) in terms of flight length, we obtain for the importance after collision:

$$\begin{aligned} I_a(\vec{X},\vec{\Omega}) &= \int D(\vec{X} \to \vec{X} + s\vec{\Omega},\vec{\Omega}) I_b(\vec{X} + s\vec{\Omega},\vec{\Omega}) ds \\ &= \int_0^\infty \Sigma_t e^{-\Sigma_t s} I_b(x - s\vec{\Omega}.\vec{\Omega}_0) ds \end{aligned}$$

in which the vector $\vec{\Omega}_0$ is the direction vector $(-1, 0, 0)$.

We can now derive an expression for I_a:

$$\begin{aligned} I_a(\vec{X},\vec{\Omega}) &= \int_0^\infty \Sigma_t e^{-\Sigma_t s} e^{-\kappa(x - s\vec{\Omega}.\vec{\Omega}_0)} ds \\ &= \Sigma_t e^{-\kappa x} \int_0^\infty e^{-(\Sigma_t - \kappa\vec{\Omega}.\vec{\Omega}_0)s} ds \\ &= \frac{\Sigma_t}{\Sigma_t - \kappa\vec{\Omega}.\vec{\Omega}_0} e^{-\kappa x}. \end{aligned}$$

We replace this expression in Equation (B.1) in order to get a condition on the parameter κ that will ensure consistency between the definition of the two importances I_a and I_b.

$$I_b(\vec{X},\vec{\Omega}) = \int C(\vec{X},\vec{\Omega} \to \vec{\Omega}') I_a(\vec{X},\vec{\Omega}') d\vec{\Omega}' \tag{B.4}$$

$$= e^{-\kappa x} \int C(\vec{X},\vec{\Omega} \to \vec{\Omega}') \frac{\Sigma_t}{\Sigma_t - \kappa\vec{\Omega}'.\vec{\Omega}_0} d\vec{\Omega}' \tag{B.5}$$

In this simplified case, the collision kernel C is reduced to a scattering kernel. The homogeneity of the medium implies that all cross sections are independent

on $\vec{X}$, and due to the isotropy of the scattering events, the scattering cross section $\Sigma_s(\vec{\Omega} \to \vec{\Omega}')$ does not depend on the direction. The probability of passing from a direction $\vec{\Omega}$ to any direction $\vec{\Omega}'$ is then $1/4\pi$, so that

$$\begin{aligned} I_b(\vec{X}, \vec{\Omega}) &= e^{-\kappa x} \int \frac{1}{4\pi} \frac{\Sigma_s}{\Sigma_t} \frac{\Sigma_t}{\Sigma_t - \kappa \vec{\Omega}'.\vec{\Omega}_0} d\vec{\Omega}' \\ &= \frac{\Sigma_s}{2\kappa} \ln\left(\frac{\Sigma_t + \kappa}{\Sigma_t - \kappa}\right) e^{-\kappa x}. \end{aligned}$$

Consequently, in order for the assumption (B.3) to hold true, we must ensure that

$$\frac{\Sigma_s}{2\kappa} \ln\left(\frac{\Sigma_t + \kappa}{\Sigma_t - \kappa}\right) = 1, \tag{B.6}$$

which is a Placzek equation on κ. κ is therefore often referred to as *Placzek* coefficient.

B.2 EXTENSION TO MULTI-KINETIC CASE

Let us now extend the previous formula for energy-dependent cross sections. The simulated energy range is supposed to be divided into energy groups such that inside every group g, the cross section $\Sigma_t(g)$ is constant. Any point of the phase space is therefore defined by the coordinates $(\vec{X}, \vec{\Omega}, g)$. Assuming now that we can compute a Placzek coefficient κ_g for each group and that the expression for I_b is

$$I_b(\vec{X}, \vec{\Omega}, g) = I_b(x, g) = e^{-\kappa_g x}, \tag{B.7}$$

and the expression computed for I_a becomes

$$I_a(\vec{X}, \vec{\Omega}, g) = \frac{\Sigma_t(g)}{\Sigma_t(g) - \kappa_g \vec{\Omega}.\vec{\Omega}_0} e^{-\kappa_g x}. \tag{B.8}$$

The energy aspect has an impact on the collision kernel C. It is still a scattering kernel, but now takes into account the probability for a particle at point $\vec{X}$ in energy group g to come out of the scatter event in a lower group g':

$$C(\vec{X}, \vec{\Omega} \to \vec{\Omega}', g \to g') = \frac{\Sigma_s(g \to g')}{\Sigma_t(g)}. \tag{B.9}$$

We have for the importance before collision:

$$\begin{aligned} I_b(\vec{X},\vec{\Omega}) &= \iint C(\vec{X},\vec{\Omega}\to\vec{\Omega}',g\to g')I_a(\vec{X},\vec{\Omega}',g')d\vec{\Omega}'dg' \\ &= \sum_{g'\leq g}\left[\int C(\vec{X},\vec{\Omega}\to\vec{\Omega}',g\to g')I_a(\vec{X},\vec{\Omega}',g')d\vec{\Omega}'\right] \\ &= \sum_{g'\leq g}\left[\int C(\vec{X},\vec{\Omega}\to\vec{\Omega}',g\to g')\frac{I_a(\vec{X},\vec{\Omega}',g')}{I_a(\vec{X},\vec{\Omega}',g)}I_a(\vec{X},\vec{\Omega}',g)d\vec{\Omega}'\right] \\ &= \sum_{g'\leq g}\left[e^{-\kappa_g x}\int\frac{1}{4\pi}\frac{I_a(\vec{X},\vec{\Omega}',g')}{I_a(\vec{X},\vec{\Omega}',g)}\frac{\Sigma_s(g\to g')}{\Sigma_t(g)}\frac{\Sigma_t(g)}{\Sigma_t(g)-\kappa_g\vec{\Omega}'.\vec{\Omega}_0}d\vec{\Omega}'\right]. \end{aligned}$$

If we now assume that the energetic profile of the importance function does not depend on the position $\vec{X}$ nor on the direction $\vec{\Omega}$, so that

$$\frac{I_a(\vec{X},\vec{\Omega}',g')}{I_a(\vec{X},\vec{\Omega}',g)} = \frac{I_a(g')}{I_a(g)} \tag{B.10}$$

we can now compute the integral, which leads to

$$I_b(\vec{X},\vec{\Omega}) = \sum_{g'\leq g}\left[\frac{I_a(g')}{I_a(g)}\frac{\Sigma_s(g\to g')}{2\kappa_g}\ln\left(\frac{\Sigma_t(g)+\kappa_g}{\Sigma_t(g)-\kappa_g}\right)e^{-\kappa_g x}\right]. \tag{B.11}$$

Combining Equation (B.11) with Equation (B.7) yields

$$\frac{\sum_{g'\leq g}\left[\Sigma_s(g\to g')\frac{I_a(g')}{I_a(g)}\right]}{2\kappa_g}\ln\left(\frac{\Sigma_t(g)+\kappa_g}{\Sigma_t(g)-\kappa_g}\right) = 1. \tag{B.12}$$

The INIPOND module is initiated with a parameter β that is used to define the energetic profile of the importance map. It computes $I_a(g)$ for any group g as:

$$\frac{1}{\beta+1}\frac{(E_g^+)^{\beta+1}-(E_g^-)^{\beta+1}}{E_g^+-E_g^-}, \tag{B.13}$$

where E_g^- and E_g^+ are the inferior and superior energies of group g, respectively. Then, it solves the Placzek equation Equation (B.12) to find the value of κ_g for each group.

B.3 MESH IMPORTANCE COMPUTATION

The importance maps computed by INIPOND are discretized both spatially and energetically. The bins of the spatial discretization are referred to as *cells*, while the energy bins are called *groups*. In addition to the spatial and energetic meshes, the INIPOND module is provided with the position of one or several detectors D_i, each of them associated to a biasing parameter β_i. **Each energy**

group g is then given a weight $W_{i,g}$ such that:

$$W_{i,g} = \frac{1}{\beta_i + 1} \frac{(E_g^+)^{\beta_i+1} - (E_g^-)^{\beta_i+1}}{E_g^+ - E_g^-} \tag{B.14}$$

where E_g^- and E_g^+ are the inferior and superior energies of group g, respectively.

To compute the importance map, INIPOND starts by calculating for each volume of the geometry a Placzek coefficient per energy group. For each group g the Placzek coefficient κ_g is computed. In order to minimize discrepancies between energy groups, which could be troublesome for the Exponential Transform method, the Placzek coefficient is replaced by a value k_g such that

- If $\kappa_g < 0$, $k_g = 0$
- If $g > 1$ and $\kappa_g < k_{g-1} - 0.05$, $k_g = k_{g-1} - 0.05$
- If $g > 1$ and $\kappa_g > k_{g-1} + 0.05$, $k_g = k_{g-1} + 0.05$
- If $\kappa_g > 0.9 \times \Sigma_t(g)$, $k_g = 0.9 \times \Sigma_t(g)$

Then, starting from the center of the detector cell, the module uses a Dijkstra algorithm to compute the shortest path between each cell and the detector cell. In this process, the distance between two adjacent cells takes into account the Placzek coefficients. For two cells c_1 and c_2, it is defined as

$$d_g(c_1, c_2) = k_g \times dist(c_1, c_2), \tag{B.15}$$

where $dist(c_j, c_k)$ is the geometric distance between the centers of cells 1 and 2, and k_g the smoothed Placzek coefficient of group g.

For each combination of cell, detector and energy group, the Dijkstra algorithm is used to compute the shortest path length from the center of the cell to the detector in group g, passing by the centers of other cells. The paths lengths are computed using the inter-cell distances defined previously. We denote these values $l_g(c_j, D_i)$, and define the non-angular importance of any cell c_j in group g as

$$I_g(c_j) = \sum_i W_{i,g} e^{-l_g(c_j, D_i)}. \tag{B.16}$$

B.4 POINT IMPORTANCE

When the importance of a point $(\vec{X}, \vec{\Omega}, E)$ is asked to the INIPOND module, the cell c corresponding to the point $\vec{X}$ is retrieved as well as the energy group g containing E. The non-angular importance is then

$$I_4(\vec{X}, \vec{\Omega}, E) = I_g(c), \tag{B.17}$$

while the angular importance is computed as

$$I_6(\vec{X},\vec{\Omega},E) = I_4(\vec{X},\vec{\Omega},E)\frac{\Sigma_t(\vec{X},E)}{\Sigma^\star(\vec{X},E)} \tag{B.18}$$

where

$$\Sigma^\star(\vec{X},E) = \Sigma_t(\vec{X},E) - k_g\vec{\Omega}.\vec{\Omega}_c. \tag{B.19}$$

In order to prevent abrupt variations of the importance, $\Sigma^\star$ is set to $0.2 \times \Sigma_t$ whenever $\Sigma_t(\vec{X},E) - k_g\vec{\Omega}.\vec{\Omega}_c < 0.2\Sigma_t$.

B.5 MANUAL INIPOND PARAMETRIZATION

Due to the approximations made in the automatic computation of Placzek coefficient (in particular the assumption of Equation (B.10)), the obtained values may very well be inadequate to compute an accurate importance map in some configurations. This could result in the Exponential Transform being stuck in the first batch simulation, or in an under-estimation of the score.

To solve those problems, one can manually parametrize the INIPOND module, that is, giving values to be used as Placzek coefficients *at hand* in TRIPOLI-4 input file. This requires a lot of work and expertise, since each material have to be given a Placzek coefficient per energy group.

The common way to adjust Placzek coefficient is to perform a short Exponential Transform simulation (only a few batches) while storing the particle collision sites. The user can then use a tool to visualize collision points in the geometry for each energy group, and adjust the Placzek coefficient so as to balance the particle population between volumes and energy groups on the path between the source and the detector.

In the case of a single-detector importance map, it follows from the Exponential Transform method and the INIPOND module importance definition that a variation Δk in a Placzek coefficient value yields an increase or decrease of the particle population in the corresponding energy group at a distance l from the detector by a factor

$$R = e^{\Delta k.l}. \tag{B.20}$$

This method requires most of the time multiple test simulations and subsequent Placzek coefficients modifications to eventually reach the expected behaviour. Furthermore, some experience is needed to correctly relate the collision points distribution to the particle population, as well as to decide which coefficients to adjust.

APPENDIX CAPPENDIX C:
AMS INPUT FILE SYNTAX FOR TRIPOLI-4

C.1 OVERVIEW

```
AMS
      TARGET <target_definition>
      IMPORTANCE <PARTICLE_TYPE1 >
            Description of importance function
      END_IMPORTANCE
      IMPORTANCE <PARTICLE_TYPE2 >
            Description of importance function
      END_IMPORTANCE
      ...
      RESAMPLE_COLLISIONS <flag>
      CROSS_SPLIT <flag>
      SPLIT proportion
END_AMS
```

Within the `AMS` block, the mandatory keywords are `TARGET` and `IMPORTANCE`. The default values for other parameters are specified in the following sections.

C.2 TARGET DEFINITION

The keyword `TARGET` is used to define the volume of interest for the simulation (typically a detector). It is the responsibility of the user to ensure that the defined target is in accordance with the importance function used during the simulation. There are two ways to define the target of the simulation:

C.2.1 SINGLE TARGET

The syntax is the following:

```
TARGET num(vol)
```

where *volume_id* is either the volume number or name.

C.2.2 MULTIPLE TARGETS

```
TARGET LIST nb(vol)
      num(vol1) ... num(voln)
```

AMS can handle a list of volumes as target, enabling the user to divide the target in multiple volumes. It should be kept in mind that the smallest variance for a given volume will be achieved with an AMS simulation using this particular volume as single target.

C.2.3 SCORING OUTSIDE TARGETS

AMS is capable of returning an **unbiased** estimator of any score within the geometry. However a variance reduction can only be expected for scores which are estimated either around the target(s) or on the path of the particles between their emission point(s) and the target(s).

C.3 SPLITTING PROPORTION

The keyword `SPLIT` allows the user to change the proportion of particles to be splitted at each AMS iteration. According to experiment, this parameter has no noticeable influence on efficiency as long as it remains greater than 0.5%. On the other hand, it seems unreasonable in terms of correlations to split more than half of the particles per iteration, which is why it is recommended to keep this proportion below 50%.

If `SPLIT` is not specified, a value of 1% is assumed. The syntax is as follows:

SPLIT proportion

where *proportion* is expressed in percent.

C.4 AMS OPTIONS

C.4.1 CROSSING POINTS SPLITTING

In order to have a more precise estimation of the importance of a particle during its transport through the geometry, the AMS algorithm can evaluate its importance when it crosses frontiers between volumes. This allows the method to classify and split particles at crossing points, which are treated in the exact same way as collision points. This functionality is controlled by a flag which can take the values 1 (activated) or 0 (disabled):

CROSS_SPLIT <flag>

The default value for this flag is 1, but it can be useful to disable crossing points if the geometry is composed of many volumes, which can significantly increase computation time.

C.4.2 COLLISION RESAMPLING

There is two ways of performing particle splitting with AMS: Either the particles importances are evaluated just after collision points, in which case the particles are duplicated by coying the particles characteristics outgoing a collision. In some cases, such as simulations with highly absorbing materials or importance functions with poor or no account of the particles direction, it may be interesting to evaluate importance *before* collisions, and to duplicate particles at collision sites while resampling collisions. The syntax for enabling/disabling collision resampling is

RESAMPLE_COLLISIONS <flag>

C.5 IMPORTANCE FUNCTIONS

The AMS algorithm uses an importance function to determine which particle tracks are the most interesting. The keyword `IMPORTANCE` *has* to be followed by the type of particle type (`NEUTRON`, `PHOTON`, `ELECTRON` or `POSITRON`). The corresponding particles will be taken into account by the AMS algorithm with the importance defined inside the block.

Obviously, the AMS can not perform variance reduction on particles that are not in the simulation. If a single particle type is present in the simulation, this type should be given after `IMPORTANCE`. If multiple particle types are simulated, an `IMPORTANCE` block has to be given for each particle type that the AMS should take into account. The particles that do not have a corresponding importance will be left out of the AMS reduction variance algorithm.

To apply the same importance function to all particle types present in the simulation, one can use `ALL_PARTICLE` as particle type.

C.5.1 IMPORTANCE MAPS

When parametrized with `MAP`, AMS uses an importance map computed by the INIPOND module Therefore, it **requires** the `VARIANCE_REDUCTION` block in the same data file. AMS takes into account every option available to other variance reduction techniques, such as the manual modification of the bias parameters $k_{placzek}$ or the importance monitoring. The keyword `MAP` *has* to be followed by the type of particle type (either `NEUTRON` or `PHOTON`) corresponding to one of the types specified in the `VARIANCE_REDUCTION` block. This allows for example to use a photon importance while performing AMS on neutrons. The syntax is as follows:

IMPORTANCE <PARTICLE_TYPE>
MAP <REDVAR_TYPE>
END_IMPORTANCE

NOTE: There are no evidence that importance monitoring improves the efficiency of AMS. Its use forces the first batches of the simulation to run without AMS, which may lead the simulation to freeze the same way it would if another variance reduction technique was used. This is why I recommend to disable importance monitoring by adding the line `MONITORING 0` to the `SIMULATION` block.

C.5.2 SPATIAL IMPORTANCE FUNCTIONS

The keywords `FROM`, `TOWARDS` and `PATH` allow the user to set a spatial importance. The importance of a point is in this case computed regarding to a `POINT`, `LINE`, `PLANE`, `SPHERE`, `CYLINDER`, `RING` or `PATH`.

POINT

IMPORTANCE <PARTICLE_TYPE>
<MODE> POINT X Y Z
END_IMPORTANCE

The importance of a given point is defined according to the distance d between this point and the point (X, Y, Z). <MODE> is either `FROM` or `TOWARDS`. Using `FROM`, the importance is d, which causes the particles to be pushed away from the point (X, Y, Z), regardless of the geometry. With `TOWARDS`, the importance is $\frac{1}{d}$, which causes the particles to be attracted to (X, Y, Z).

LINE

IMPORTANCE <PARTICLE_TYPE>
<MODE> LINE
POINT X Y Z
VECTOR V_X V_Y V_Z
END_IMPORTANCE

The importance of a given point is defined according to the shorter distance d_L between this point and the line passing through point (X, Y, Z) and parallel to direction vector (V_X, V_Y, V_Z). <MODE> is either `FROM` or `TOWARDS`. Using `FROM`, the importance is d_L, which causes the particles to be pushed away from the line. With `TOWARDS`, the importance is $\frac{1}{d_L}$, which causes the particles to be attracted to the line.

PLANE

```
IMPORTANCE <PARTICLE_TYPE>
    <MODE> PLANE
        POINT X Y Z
        VECTOR V_X V_Y V_Z
END_IMPORTANCE
```

The importance of a given point is defined according to the shorter distance d_P between this point and the plane passing through point (X, Y, Z) with normal vector (V_X, V_Y, V_Z). <MODE> is either `FROM` or `TOWARDS` . Using `FROM`, the importance is d_P, which causes the particles to be pushed away from the plane. With `TOWARDS`, the importance is $\frac{1}{d_P}$, which causes the particles to be attracted to the plane.

SPHERE

```
IMPORTANCE <PARTICLE_TYPE>
    <MODE> SPHERE R
        POINT X Y Z
END_IMPORTANCE
```

The importance of a given point is defined according to the distance d_S between this point and the sphere of radius R and center (X, Y, Z). <MODE> is either `FROM` or `TOWARDS`. Using `FROM`, the importance is d_S, which causes the particles to be pushed away from the sphere surface regardless of the geometry. With `TOWARDS`, the importance is $\frac{1}{d_S}$, which causes the particles to be attracted towards the sphere surface.

CYLINDER

```
IMPORTANCE <PARTICLE_TYPE>
    <MODE> CYLINDER R
        POINT X Y Z
        VECTOR V_X V_Y V_Z
END_IMPORTANCE
```

The importance of a given point is defined according to the distance d_C between this point and the surface of the infinite cylinder with radius R which axis passes through point (X, Y, Z) and is directed by vector (V_X, V_Y, V_Z). <MODE> is either `FROM` or `TOWARDS`. Using `FROM`, the importance is d_C, which causes the particles to be pushed away from the cylinder surface. With `TOWARDS`, the importance is $\frac{1}{d_C}$, which causes the particles to be attracted towards the cylinder.

RING

```
IMPORTANCE <PARTICLE_TYPE>
    <MODE> RING R
        POINT X Y Z
        VECTOR V_X V_Y V_Z
END_IMPORTANCE
```

The importance of a given point is defined according to the distance d_R between this point and the ring of radius R and center (X, Y, Z), which axis is directed by vector (V_X, V_Y, V_Z). <MODE> is either `FROM` or `TOWARDS`. Using `FROM`, the importance is d_R, which causes the particles to be pushed away from the ring. With `TOWARDS`, the importance is $\frac{1}{d_R}$, which causes the particles to be attracted towards the ring.

PATH

```
IMPORTANCE <PARTICLE_TYPE>
    PATH
        STRENGTH s
        POINT LIST nb(points)
            X_1 Y_1 Z_1
            ...
            X_n Y_n Z_n
    END_PATH
END_IMPORTANCE
```

A path is defined as an ordered sequence of points. The importance of a point outside the path is defined using the minimal distance from the point to the path $d_\perp$, and the distance along the path from the first point of the path to the orthogonal projection of the point on the path $d_\parallel$. The importance is defined as

$$I = d_\parallel - s.d_\perp, \tag{C.1}$$

so that it increases with the distance along the path and decreases with the distance to the path. The parameter s represents the attraction strength of the path, which influences the slope of the importance function around the path.

Volume importance weighting

In addition to the importance function, each volume of the geometry carries an importance factor that weights the importance of any point within its boundaries. By default, this value is set to 1. The user can change the weight of any number of volumes using the following syntax:

```
VOLU num(vol1)...num(voln) WEIGHT w
```

IMPORTANCE <PARTICLE_TYPE>
...
VOLU num(vol1)...num(voln) WEIGHT w
END_IMPORTANCE

université PARIS-SACLAY | ÉCOLE DOCTORALE PHENIICS

Titre : Développement d'une méthode de réduction de variance adaptative pour le transport Monte-Carlo de particules

Mots clefs : Simulation Monte-Carlo, transport de particules, réduction de variance, Adaptive Multilevel Splitting, AMS, TRIPOLI-4

Résumé : L'algorithme *Adaptive Multilevel Splitting* (AMS) a récemment fait son apparition dans la littérature de mathématiques appliquées, en tant que méthode de réduction de variance pour la simulation Monte Carlo de chaînes de Markov. Ce travail de thèse se propose d'implémenter cette méthode de réduction de variance adaptative dans le code Monte-Carlo de transport de particules TRIPOLI-4®, dédié entre autres aux études de radioprotection et d'instrumentation nucléaire. Caractérisées par de fortes atténuations des rayonnements dans la matière, ces études entrent dans la problématique du traitement d'évènements rares.

Outre son implémentation inédite dans ce domaine d'application, deux nouvelles fonctionnalités ont été développées pour l'AMS, testées puis validées. La première est une procédure d'encaissement au vol permettant d'optimiser plusieurs scores en une seule simulation AMS. La seconde est une extension de l'AMS aux processus branchants, courants dans les simulations de radioprotection, par exemple lors du transport couplé de neutrons et des photons induits par ces derniers.

L'efficacité et la robustesse de l'AMS dans ce nouveau cadre applicatif ont été démontrées dans des configurations physiquement très sévères (atténuations du flux de particules de plus de 10 ordres de grandeur), mettant ainsi en évidence les avantages prometteurs de l'AMS par rapport aux méthodes de réduction de variance existantes.

Title : Development of an adaptive variance reduction technique for Monte Carlo particle transport

Keywords : Monte Carlo simulation, particle transport, variance reduction, Adaptive Multilevel Splitting, AMS, TRIPOLI-4

Abstract : The *Adaptive Multilevel Splitting* algorithm (AMS) has recently been introduced to the field of applied mathematics as a variance reduction scheme for Monte Carlo Markov chains simulation. This Ph.D. work intends to implement this adaptative variance reduction method in the particle transport Monte Carlo code TRIPOLI-4®, dedicated among others to radiation shielding and nuclear instrumentation studies. Those studies are characterized by strong radiation attenuation in matter, so that they fall within the scope of rare events analysis.

In addition to its unprecedented implementation in the field of particle transport, two new features were developped for the AMS. The first is an on-the-fly scoring procedure, designed to optimize the estimation of multiple scores in a single AMS simulation. The second is an extension of the AMS to branching processes, which are common in radiation shielding simulations. For example, in coupled neutron-photon simulations, the neutrons have to be transported alongside the photons they produce.

The efficiency and robustness of AMS in this new framework have been demonstrated in physically challenging configurations (particle flux attenuations larger than 10 orders of magnitude), which highlights the promising advantages of the AMS algorithm over existing variance reduction techniques.

Université Paris-Saclay
Espace Technologique / Immeuble Discovery
Route de l'Orme aux Merisiers RD 128 / 91190 Saint-Aubin, France